

NASA TECHNICAL NOTE



NASA TN D-5974

C. I

LOAN COPY: RETUR  
AFWL (WLOL)  
KIRTLAND AFB, N

0129715



TECH LIBRARY KAFB, NM

NASA TN D-5974

WIND-TUNNEL STUDIES OF EFFECTS OF  
CONSTRUCTION METHODS, DESIGN DETAILS,  
AND CANOPY SLOTS ON THE AERODYNAMIC  
CHARACTERISTICS OF SMALL-SCALE  
ALL-FLEXIBLE PARAWINGS

by Paul G. Fournier and William C. Sleeman, Jr.

Langley Research Center  
Hampton, Va. 23365

NATIONAL AERONAUTICS AND SPACE ADMINISTRATION • WASHINGTON, D. C. • OCTOBER 1970



0132715

1. Report No. NASA TN D-5974	2. Government Accession No.	3. Recipient's Catalog No.	
4. Title and Subtitle     WIND-TUNNEL STUDIES OF EFFECTS OF CONSTRUCTION METHODS, DESIGN DETAILS, AND CANOPY SLOTS ON THE AERODYNAMIC CHARACTERISTICS OF SMALL-SCALE ALL-FLEXIBLE PARAWINGS			
7. Author(s)  Paul G. Fournier and William C. Sleeman, Jr.	5. Report Date October 1970		
9. Performing Organization Name and Address  NASA Langley Research Center Hampton, Va. 23365	6. Performing Organization Code		
12. Sponsoring Agency Name and Address  National Aeronautics and Space Administration Washington, D.C. 20546	8. Performing Organization Report No. L-7013		
15. Supplementary Notes	10. Work Unit No. 126-13-10-03		
16. Abstract  A low-speed wind-tunnel investigation was conducted to determine the effects of canopy construction methods, design details, and canopy slots on the static longitudinal aerodynamic characteristics of all-flexible parawings. Construction details such as type of nonporous canopy fabric, glued or sewed seams, tape reinforcement, or cloth-weave orientation had little effect on maximum lift-drag ratios and resultant-force coefficients. The maximum lift-drag ratios varied from 2.2 to 2.5 for the various single-keel unslotted parawings, and from 2.2 to 2.4 for the slotted canopy parawings. Incremental reductions in the lengths of all the suspension lines caused corresponding reductions in the resultant-force coefficients and maximum lift-drag ratios. The available range for modulation of resultant-force coefficient and lift-drag ratio by shortening the control lines was very limited.	11. Contract or Grant No.		
17. Key Words (Suggested by Author(s))  All-flexible parawings Single keel Canopy slots Construction methods Low-speed aerodynamics	18. Distribution Statement  Unclassified - Unlimited		
19. Security Classif. (of this report) Unclassified	20. Security Classif. (of this page) Unclassified	21. No. of Pages 91	22. Price* \$3.00

WIND-TUNNEL STUDIES OF EFFECTS OF CONSTRUCTION METHODS,  
DESIGN DETAILS, AND CANOPY SLOTS ON THE AERODYNAMIC  
CHARACTERISTICS OF SMALL-SCALE  
ALL-FLEXIBLE PARAWINGS

By Paul G. Fournier and William C. Sleeman, Jr.  
Langley Research Center

SUMMARY

A low-speed wind-tunnel investigation of single-keel, all-flexible parawing configurations was conducted to assess aerodynamic effects of variations in canopy materials and construction techniques on a basic  $45^{\circ}$  swept parawing and to study briefly several detailed modifications to the basic configuration. Some slotted parawings were also investigated with different arrangements of slots in the canopy.

Maximum lift-drag ratios obtained ranged from approximately 2.2 to 2.5 on the different unslotted parawings, and from about 2.2 to 2.4 on the slotted parawings. A maximum resultant-force coefficient of at least 1.3 was obtained on both the slotted and unslotted configurations when only the rear keel line was shortened. The aerodynamic characteristics were not greatly dependent upon the canopy material used in this investigation or the construction details investigated. In addition, the various modifications to the basic wing had little effect on the overall results obtained. Incremental reductions in the lengths of all of the suspension lines, however, caused corresponding reductions in both the resultant-force coefficients and maximum lift-drag ratios. The available range for modulation of resultant-force coefficient and lift-drag ratio by shortening the control lines was very limited.

INTRODUCTION

Research investigations of parawings conducted by the National Aeronautics and Space Administration in the past several years have been concerned with several different types of parawing configurations with widely varying geometric, structural, and aerodynamic characteristics. (See refs. 1 to 4.) Recent parawing research has concentrated on all-fabric lifting surfaces having no structural members or stiffness. These all-flexible parawings are capable of providing gliding, controllable flight by proper rigging of multiple suspension lines which connect the wing to the payload. Parawings of this type show

considerable promise for use in applications where compact storage and weight requirements dictate the use of a parachute-like tension structure and where significant glide capability is necessary.

A fairly broad survey of wing planforms and nose details was made in the investigation of reference 5 to establish a basic parawing configuration for continuing research. The configuration selected had  $45^{\circ}$  sweep of the canopy flat planform, leading edges and keel of equal length, and the nose cut off 0.125 of the keel length at the apex. Several configuration details not covered in the tests of reference 5 were pertinent for subsequent investigation, and many of these details were studied in the present investigation. The effects of various construction details such as fabric-weave orientation, number and placement of line attachments, method of joining fabric seams, use of cloth tape for edging and load transfer across the canopy, and model size were investigated. The basic questions concerning effects of construction details needed resolution because many models were to be constructed for performance evaluation. It was necessary, therefore, to select methods of construction that would not obscure the performance potential or comparative results for the different configuration. In addition to the studies of construction details, investigations were made of slotted canopies, multiple-keel wings, and effects of control line shortening.

Tests were conducted in the 17-foot (5.18-meter) test section of the Langley 300-MPH 7- by 10-foot tunnel at dynamic pressures of  $1.0 \text{ lb}/\text{ft}^2$  ( $47.9 \text{ N}/\text{m}^2$ ) and  $2.0 \text{ lb}/\text{ft}^2$  ( $95.8 \text{ N}/\text{m}^2$ ). A tethered test technique was used in which the suspension lines from the wing were attached to a special rigging mount which was on a sting-mounted strain-gage balance. The wing was rigged to fly in tethered flight at  $0^{\circ}$  sting angle of attack, and then the sting angle of attack was varied over a range from about  $-4^{\circ}$  to  $21^{\circ}$ . The type of tests made provided a range of wing angle of attack in order to assess the potential of each wing with regard to maximum lift-drag ratio and to define the variation of lift-drag ratio with resultant-force coefficient.

## SYMBOLS

The data presented are referred to the stability axes. The positive directions of forces, pitching moment, and wing angle of attack are shown in figure 1. The moment reference location was at the confluence of lines and is shown in figure 2. There was no well-defined reference line on the wing for use in determining wing angle of attack; therefore, the angle of the seventh line back on the keel with respect to the vertical was usually taken as the angle of attack for most of the wings. The reference area used in determining the coefficients was the area of the actual wing-canopy flat planform, and the reference length was the theoretical keel length  $l_k$  minus the length of the nose cutoff. For the

data presentation, all measured lengths were nondimensionalized by the theoretical keel length.

$b_0$	span of wing-canopy flat planform, ft (m)
$c$	reference length, $l_k$ minus nose cutoff, ft (m)
$C_D$	drag coefficient, Drag/qS
$C_L$	lift coefficient, Lift/qS
$C_m$	pitching-moment coefficient, Pitching moment/qSc
$C_R$	resultant-force coefficient, $\sqrt{C_L^2 + C_D^2}$
$d_1, d_2$	longitudinal distances from moment reference to control-line attachments on rigging mount (see fig. 2 and table I)
$h_1, h_2$	vertical distances from moment reference to control-line attachments on rigging mount (see fig. 2 and table I)
L/D	lift-drag ratio, $C_L/C_D$
$l_k$	keel length of theoretical wing-canopy flat planform, measured from theoretical apex to the trailing edge at the plane of symmetry, ft (m)
$l_{le}$	leading-edge length, ft (m)
$l/l_k$	nondimensional length of suspension lines measured from wing attachment to top of clamping block
q	free-stream dynamic pressure, lb/ft <sup>2</sup> (N/m <sup>2</sup> )
S	area of actual wing-canopy flat planform, ft <sup>2</sup> (m <sup>2</sup> )
$x_k$	distance along keel, ft (m)
$x_{le}$	distance along leading edge, ft (m)

$x/l_k$	line attachment point along wing leading edge, midspan, or keel
$y, y_1$	spanwise distances from moment reference to control line attachments on rigging mount (see fig. 2 and table I)
$\alpha$	sting angle of attack, deg
$\alpha_w$	angle of keel line number 7 measured from the vertical when viewed from the side, positive for rearward displacement of the line, deg (for some models a keel line other than the seventh had to be used and is so indicated on the geometric drawing accompanying the specific model data)
$\Delta l/l_k$	incremental nondimensional change in length of suspension line
$\Lambda_0$	angle of sweepback of leading edge of wing-canopy flat planform, deg

#### DESCRIPTION OF MODELS

Several planforms of all-flexible parawings were tested in this investigation and included configurations having two and four canopy lobes. The basic two-lobe configuration had a flat-planform sweep of 45°, leading edges and keel of equal length for the theoretical planform, and the forward 0.125 of the keel length removed by cutting the nose perpendicular to the keel. Effects of construction techniques, fabric orientation, type of fabric, and wing size were investigated on the basic wing planform. Effects of various modifications to the basic wing canopy and wing-to-confluence separation distance were also investigated. Canopy configurations investigated are shown in figure 3, and photographs of the different models in the tunnel are given in figure 4.

A sketch showing the construction details of a glued canopy is presented in figure 5(a). The construction of the sewed canopies was similar to that of the glued model except that all joints and line attachment loops were sewn. (See fig. 5(b).) The weave of the fabric was oriented so that the warp was parallel to the trailing edge, except where noted. No seams or reinforcements were made to the leading and trailing edges, except where cloth tape was used as indicated. Fraying of the fabric edges was avoided by cutting the material with a hot iron.

The suspension lines for the models were, in most cases, 130-lb-test (578-N) dacron cord with a diameter of about 1/32 inch (0.8 mm). Nylon cord having a rated strength of 100 lb (445 N) test and a diameter of about 1/16 inch (1.6 mm) was used on two models and 85-lb-test (378-N) braided nylon cord was used on three models.

The canopy material, type of construction, and type of lines used are summarized in table II for each wing tested.

#### Basic-Planform Models

The basic  $\Lambda_0 = 45^\circ$  planform with three different keel lengths was tested: 5 ft (1.524 m), 8 ft (2.438 m), and 6.56 ft (2.0 m), and the planform is shown in figures 3, 5, and 6. The small 5-ft models included glued and sewed types of construction. Most of the models were made of 1.1 oz/yd<sup>2</sup> (37.3 g/m<sup>2</sup>) acrylic-coated nylon; however, there was one sewed model made of 2.2 oz/yd<sup>2</sup> (74.6 g/m<sup>2</sup>) calendered nylon. The porosity of the calendered nylon was approximately  $\frac{5 \text{ ft}^3/\text{min}}{\text{ft}^2} \left( \frac{1.524 \text{ m}^3/\text{min}}{\text{m}^2} \right)$  for a pressure difference of 1/2 inch (1.27 cm) of water. The large 8-ft basic model was a sewed 1.1 oz/yd<sup>2</sup> acrylic-coated nylon, and the 6.56-ft wing was made of nonporous 0.75 oz/yd<sup>2</sup> (25.3 g/m<sup>2</sup>) resin-impregnated nylon. All these models were made so that the fabric was oriented with the warp parallel to the wing trailing edge, except for the bias-constructed wing, which had the warp of the fabric running perpendicular to the keel.

#### Modifications to Basic Configuration

There were several models having the same planform as the basic model, but with alterations in design and construction. The material used for the canopies and lines of each model is given in table II.

Tape reinforcement.- The 8-ft (2.438-m) tape-reinforced wing had the same planform and line attachments as the basic wing. The reinforcement tape on this model was  $0.004 l_k$ -wide and cotton tape located along the leading edges, keel, and over the canopy as shown in the sketches of figures 3 and 14. This type of construction was used in an attempt to simulate that used in the fabrication of parachutes, where part of the load in the suspension lines is carried by the tapes extending over the canopy.

Revised number of line attachments.- A 5-ft (1.524-m) model having 22 line attachments instead of the basic 23 attachments was made. This model, which was a sewed wing, had eight line attachments on the keel and seven line attachments on each leading edge. (See figs. 3 and 16.)

Cambered keel.- The cambered-keel model was made by taking darts in the fabric along the keel of a basic wing as shown in figures 3 and 18. This modification was an attempt to remove some of the wrinkles in the fabric near the keel of the basic wing. A photograph of the cambered-keel wing is presented in figure 4(b). The location and amount of fabric removed were determined from observation of a basic wing in the tunnel. This 5-ft (1.524-m) sewed model had  $0.008 l_k$ -wide cotton tape on the perimeter and keel.

The cambered-keel model was also tested with a cloth-dam attached (see fig. 18) to the undersurface of the wing and extended across from the second leading-edge-line attachments to the second keel-line attachment.

Curved leading edge.- The curved-leading-edge model was derived from the basic-planform wing, but the leading edges were arcs with a radius of  $1.25l_k$ . This wing had the suspension-line attachments evenly spaced along the leading edge and keel. There were seven line attachments on each leading edge and eight attachments on the keel. A sketch of this model is presented in figures 3 and 20, and a photograph of the model in the wind tunnel is given in figure 4(b).

### Slotted Wings

Wing with multiple slots.- The 5-ft (1.524-m) sewed wing with multiple slots had the same planform as the basic wing but had eight evenly spaced line attachments on the keel and six evenly spaced line attachments on each leading edge. The model had six rows of slots, a total of 52 individual slots, and  $0.008l_k$ -wide cotton tape on the trailing edge of the model and on the leading edge of each panel. The location of the slots and tape is shown in figures 3 and 24, and a photograph of the model in the tunnel is presented in figure 4(c).

Tests were also made with the trailing edges of the last two rows of slots scalloped by removing a  $0.047l_k$ -radius portion of the panel. The photograph (fig. 4(c)) of the model shows these scalloped panels.

Rear-slot wing.- The 5-ft (1.524-m) sewed wing with two rows of slots near the rear portion of the canopy had the same planform as the basic wing but had a different number of suspension-line attachments. There were nine line attachments on the keel and seven line attachments evenly spaced on each leading edge. The model had  $0.008l_k$ -wide cotton tape attached as indicated in the sketches on figures 3 and 27; however, the slot panels did not have tape on their trailing edges, as can be seen in the photograph of the model in figure 4(c).

Wing with multiple slots and radial tapes.- The 8-ft (2.438-m) wing with multiple slots and radial tapes had six suspension line attachments on the keel and each of the leading edges. The leading-edge sweep of the canopy flat pattern was  $45^\circ$ . There were two sizes of cotton tape on the model:  $0.005l_k$ -wide tape on the leading edge, keel, and on the leading edge and trailing edge of each main panel; and  $0.004l_k$ -wide tape extending radially along the canopy, except for the leading edges.

Each of the five main panels was slightly different. The individual panels of a given main panel were the same, but the amount of fullness in the trailing edge of the individual panels varied with radial position. At radial position 1 (see fig. 29), the trailing edge of

panel 1 had 1 percent excess length; panel 2 had 2 percent; panel 3 had 3 percent; panel 4 had 4 percent; and panel 5 had 0 percent. A sketch of the model, showing the location of the attachment points is shown in figures 3 and 29, and a photograph of the model in the tunnel is presented in figure 4(c).

#### Four-Lobe Models

Composite wing.- The 5-ft (1.524-m) four-lobe sewed wing was made by joining two basic two-lobe  $\Lambda_0 = 45^\circ$  wings at their leading edges; the left leading edge of one was attached by sewing to the right leading edge of the other. The model had a flat-planform sweep of  $0^\circ$ ; the leading edges, midspan keels, and center keel were of equal length when extended to the theoretical apex and had 40 suspension line attachments. The location of the line attachments and the planform of the model are presented in figures 3 and 31.

A photograph of the model in the tunnel is presented in figure 4(d).

35° swept wing.- The 4-ft (1.219-m) four-lobe sewed wing had a flat-planform leading-edge sweep of  $35^\circ$ , a center keel, and two midspan keels. Some tests were made with the pointed wing-tips, and then the tips were removed and additional lines were added to provide lines for both the leading edge and trailing edge of the tip. The suspension-line attachments along the leading edges and the keels were evenly spaced, as shown in the sketches of figures 3 and 33. The nose apex of the model was cut off as shown in figure 3 to alleviate the problem of nose collapse which was encountered during preliminary testing. A photograph of the model in the tunnel is presented in figure 4(d).

Rectangular unswept wing.- The 2.125-ft (0.648-m) rectangular four-lobe wing had a flat-planform leading-edge sweep of  $0^\circ$ , a center keel, and two midspan keels. The suspension-line attachments along the keels and wing tips were evenly spaced as shown in the sketches of figures 3 and 35.

In order to make this model inflate properly and assume a steady-flight condition, a boltrope was put in the leading edge and in a portion of the trailing edge of the wing. Then the boltrope was shortened. The amount by which the boltrope is shorter than the fabric is called boltrope shortening and is expressed as a percentage of the fabric length for the portion containing the boltrope. The amount of boltrope shortening in each portion of the wing was as follows: 10 percent in the leading edge of the outer panels, 9 percent in the trailing edge of the outer panel, and 1 percent in the leading edge of the inner panels. The effect of boltrope shortening on the canopy shape may be seen in the photograph of the model in figure 4(d).

## TESTS AND CORRECTIONS

Static wind-tunnel tests were conducted in the 17-foot (5.18-meter) test section of the Langley 300-MPH 7- by 10-foot tunnel. Most of the results were obtained at dynamic pressures of 1.0 and 2.0 lb/ft<sup>2</sup> (47.9 and 95.8 N/m<sup>2</sup>). The test Reynolds number based on a model keel length of 5 ft (1.524 m) was  $1.2 \times 10^6$  at  $q = 2.0 \text{ lb/ft}^2$  (95.8 N/m<sup>2</sup>).

### Tethered Method of Testing

The tests were made by the tethered technique in which the model is flown in the tunnel and the suspension lines are attached to a rigging mount which is attached to a six-component strain-gage balance. The strain-gage balance was mounted to a variable-angle sting positioned near the floor of the test section. The suspension lines for all of the models were held at the confluence point in a clamp as shown in figure 2. Dimensions pertinent to the location of the line attachments in figure 2 are given in table I for each data figure. The model could not be tested in the wind tunnel with the one-point suspension system normally used in free-glide flight tests because the model diverged in roll when tethered to a single point. In order to stabilize the model so that data could be obtained, the attachment points of the rear keel and tip lines were moved rearward, and the tip line attachments moved outward by means of the special rigging mount shown in figure 2.

### Test Procedure

The wings were rigged in tethered flight with the sting angle of attack set at 0° by adjusting the length of each suspension line to obtain the most forward flight position in the tunnel (maximum lift-drag ratio). The sting angle of attack was then varied over as wide a range as possible. The sting-angle range generally varied from the angle for nose collapse to the angle at which the wing stalled or large lateral oscillations occurred. Measurements of wing angle of attack were made visually by sighting the reference suspension line through a window-mounted protractor.

Most of the test results presented herein were obtained with the wing rigged for maximum lift-drag ratio at a sting angle of attack of 0°, and the sting angle was then varied in taking data. Increasing the sting angle of attack provided a control input that was similar to shortening the three rear lines. In order to obtain a more direct indication of the effects of control-line shortening, a few tests were made with different combinations of control-line shortening.

### Corrections to Data

Jet-boundary corrections to angle of attack and drag coefficients, as determined from reference 6, and blockage corrections to the dynamic pressure, as determined from reference 7, have been applied to the measured data.

## PRESENTATION OF DATA

The present test results were obtained in an investigation of a number of similar models, and in order to avoid possible confusion in matching results with configurations, a drawing of the model precedes the data obtained for each set of similar models. Details of the line attachment points on the mounting fixture to balance are given in figure 2 and table I. The data consist of longitudinal aerodynamic characteristics through a range of sting angle of attack and figures showing line lengths and rigging variations.

The drawings of the models and the test results are presented in the following figures:

	Figure
<b>Basic planform; <math>\Lambda_0 = 45^\circ</math>; <math>l_k = 5</math> ft (1.524 m):</b>	
1.1 oz/yd <sup>2</sup> (37.3 g/m <sup>2</sup> ) nylon, glued construction . . . . .	5(a), 6, 7
2.2 oz/yd <sup>2</sup> (74.6 g/m <sup>2</sup> ) nylon, glued construction . . . . .	5(a), 6, 8
1.1 oz/yd <sup>2</sup> nylon, sewed construction . . . . .	5(b), 6, 9
1.1 oz/yd <sup>2</sup> nylon, bias-sewed construction . . . . .	6, 10
1.1 oz/yd <sup>2</sup> nylon, glued construction, control-line shortening . . . . .	5(a), 6, 11
<b>Basic planform; <math>\Lambda_0 = 45^\circ</math>; <math>l_k = 8</math> ft (2.438 m); 1.1 oz/yd<sup>2</sup> nylon:</b>	
Sewed construction . . . . .	12, 13
Sewed construction, tape reinforcement . . . . .	14, 15
<b>Modified basic; <math>\Lambda_0 = 45^\circ</math>; <math>l_k = 5</math> ft (1.524 m);</b>	
1.1 oz/yd <sup>2</sup> nylon; sewed construction:	
Revised line attachment (eight keel and seven leading-edge lines) . . . . .	16, 17
Cambered keel . . . . .	18, 19
Curved leading edges . . . . .	20, 21
Effect of varying wing-to-confluence separation distance . . . . .	22, 23
<b>Slotted wings; 1.1 oz/yd<sup>2</sup> nylon; sewed construction:</b>	
Multiple slots . . . . .	24, 25
Multiple slots, scalloped trailing edge . . . . .	24, 26
Rear slots . . . . .	27, 28
Multiple slots, radial tapes . . . . .	29, 30
<b>Four-lobe wings:</b>	
Composite wing . . . . .	31, 32
35° swept wing . . . . .	33, 34
Rectangular unswept wing . . . . .	35, 36
<b>Summary figures</b> . . . . .	<b>37-42</b>

## DISCUSSION

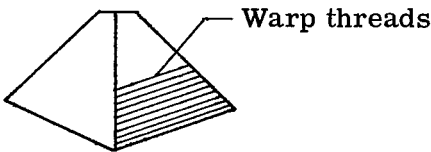
A simple evaluation and selection procedure was followed in arriving at an all-flexible parawing configuration for use in early wind-tunnel and flight tests. This procedure consisted of indoor glide tests of several different hand-launched wing planforms which had 2-ft (0.6096-m) keel lengths. On the basis of these tests, a planform was selected that had the leading edges and keel of equal length, 45° sweep of the flat-planform leading edge, and a  $0.125l_k$  nose cut that removed a triangular portion at the apex. Effects of leading-edge sweep and many configuration details were studied in the investigation reported in reference 5, and in general, none of the configuration details studied, with the exception of keel stiffening, offered significant performance gains over the simple basic wing. The present investigation was undertaken to explore effects of several configuration details on the basic planform of reference 5 and to investigate slotted and four-lobe wing designs.

### Effects of Construction Technique and Material

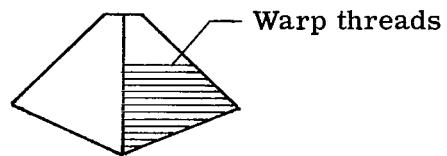
Canopy material.- Figures 7 and 8 present results for 5-ft (1.524-m) wings that were identical except for the materials used for the canopy and lines. The aerodynamic characteristics obtained for the wing having a lightweight, acrylic-coated-nylon canopy and nylon lines (fig. 7) were not greatly different from the characteristics obtained for the relatively heavy calendered-nylon canopy and smaller, less-elastic dacron lines (fig. 8). The maximum lift-drag ratio obtained for both wings was 2.3 and the maximum lift coefficient was approximately 1.045. A slightly higher maximum resultant-force coefficient was obtained for the coated canopy.

Glued and sewed construction.- Results obtained with a glued and a sewed construction may be found by comparing data in figures 7 and 9 and the summary comparison in figure 37. The data show a slightly higher maximum lift-drag ratio and higher maximum resultant-force coefficient for the sewed canopy than for the glued canopy. Each wing was individually rigged for its maximum performance before taking data, and there were differences in rigging, as shown by the line lengths in figures 7 and 9, for the glued and sewed canopies. It is believed that the differences in results for the sewed and glued canopies can be attributed more to effects of the differences in rigging rather than to effects of construction techniques.

Fabric-weave orientation.- General practice in the construction of wing canopies for wind-tunnel and flight models has been to orient the fabric with the warp parallel to the trailing edge as shown in sketch A. In order to determine whether fabric orientation had any significant effects on aerodynamic characteristics, a canopy was constructed with the trailing edge cut on the cloth bias as shown in sketch B.



Sketch A



Sketch B

Test results obtained with the bias-cut trailing edge are presented in figure 10, and these basic data can be compared with results for the sewed wing of figure 9 and the glued wing of figure 8. A summary of the effects of construction methods and materials is presented in figure 37. When consideration is given to the differences in results obtained for the glued, the sewed, and the bias-construction wing for the two dynamic pressures, it can be concluded that the use of a bias orientation of the trailing edge had no significant aerodynamic effects.

#### Effects of Modifications to the Basic Configuration

Tape reinforcement.- Test results obtained on the wing having tape reinforcement around the edges and across the canopy are presented in figure 15 and compared with data for a similar wing without tapes in figure 39. The use of fabric tape to transfer load across the canopy from the leading-edge lines to the keel lines is similar in concept to parachute construction, and canopy deformations caused by the loaded tapes could affect the aerodynamic characteristics of the wing. The comparison of data presented in figure 39 for the 8-ft (2.438-m) wings indicates that the use of tapes across the canopy had very little effect on the maximum lift-drag ratio or the variation of lift-drag ratio with resultant-force coefficient.

Revised line attachments.- The line arrangement used on the basic wing was developed in free-glide tests of small hand-launched models and was retained because it appeared to work very well for wings having keel lengths up to 60 ft (18.288 m). Inasmuch as the shape of the inflated canopy is dependent upon the number, location, and lengths of the suspension lines, tests were made to determine effects of revised line attachments on the aerodynamic characteristics. Basic data for a model with eight keel lines and seven lines on each leading edge are presented in figure 17 and compared with results of the basic wing in figure 38. The comparison of data in figure 38 shows that the revised line attachments had very little effect on the maximum lift-drag ratio or the variation of lift-drag ratio with resultant-force coefficient.

Cambered keel.- Photographs of the basic wing presented in figure 4(a) show several large wrinkles in the fabric across the span of the canopy. Since these wrinkles are primarily normal to the free-stream direction, it was reasoned that removal of these

wrinkles could reduce the profile drag of the wing. The use of a cambered-keel model eliminated the most severe wrinkles near the keel, and gave a much smoother canopy shape than was obtained on the basic wing. The basic data of figure 19 and the summary results in figure 38 do not indicate however that removal of the wrinkles was favorable. Maximum lift-drag ratios obtained on the cambered-keel model were slightly lower than on the other configurations. Therefore, some of the wrinkles in the basic wing appeared to be beneficial, and in fact, attempts to remove the very deep crease evident (see fig. 4) at the second leading-edge line by lengthening the line caused the nose to collapse. An attempt was made to simulate this deep crease by the installation of a cloth dam (see fig. 18) on the cambered-keel model. The data presented in figure 19 for the model with and without the cloth dam indicate that the cloth dam increased the lift-drag ratios throughout the test angle-of-attack range. The deep wrinkle near the nose of the wing therefore appeared to provide a favorable pressure field that helped to inflate the nose.

Curved leading edges. - The curved-leading-edge modification was another attempt to improve the inflated-canopy shape. It was expected that the cloth added in the curved portion would allow the canopy to inflate without the severe discontinuities evident (see fig. 4) at each leading-edge-line attachment on the basic wing. Photographs of the model with curved leading edges (fig. 4(b)) show that the canopy leading edge was smoother than that of the basic wing; however, the data presented in figures 21 and 38 show that the maximum lift-drag ratios were lower than those of the basic wing. Observation of the wing during rigging adjustments in the tunnel indicated that the added cloth on the curved leading edge tended to make the leading edge collapse as the control lines were extended to decrease the angle of attack of the wing. Apparently the increased camber of the leading edge and early movement of the stagnation point to the upper surface of the leading edge caused the drag of the curved-leading-edge wing to be higher than that of the basic straight leading edge.

#### Performance Characteristics of Two Sizes of Wings

Results obtained for the 5-ft (1.524-m) wings are given in figures 9 and 11; those for the 8-ft (2.438-m) wings, in figures 13 and 15. Summary results for both sizes are given in figure 39. Data obtained on the smaller wings were for a wing-to-confluence distance of approximately  $1.25l_k$  (at the eighth keel line), and for the larger wings, a distance of approximately  $1.00l_k$ . The results presented in figure 39 show little difference in characteristics for the different models except the lower values of lift-drag ratio and resultant-force coefficients for the small glued wing. Although these data show little effects of model size or wing-to-confluence distance, results of many tests of 5-ft models of the basic planform (see ref. 5 and fig. 37) have indicated maximum lift-drag ratios of approximately 2.3, with a few models showing higher values (fig. 9, for example) and

some having lower values. Tests of 8-ft (2.438-m) wings (figs. 13 and 39) and 6.56-ft (2.0-m) wings (fig. 23 and unpublished data) have generally indicated maximum lift-drag ratios of approximately 2.5. It is therefore believed that a small increase in maximum lift-drag ratio can be expected in going from a 5-ft to 8-ft wing size.

#### Effect of Wing-to-Confluence Separation Distance

The basic data showing effects of wing-to-confluence separation distance are given in figure 23 and are summarized in figure 40. These tests were made to provide an aerodynamic assessment of effects of shortening the lines to accompany estimates of savings in line weight and packing volume that would accrue from line shortening. The variation in separation distance was achieved by shortening all lines from the basic lengths in increments of 50 cm, without adjusting any of the individual line lengths to maximize performance as was done in the work of reference 5. The data of figures 23 and 40 show fairly consistent reductions in resultant-force coefficient as the lengths of all the suspension lines were reduced.

Maximum lift-drag ratios decreased as the separation distance varied from  $1.25l_k$  to  $0.50l_k$ . The data of figure 23 indicate that the loss in lift that accompanied shortening of the lines was primarily responsible for the decrease in maximum lift-drag ratio.

#### Aerodynamic Characteristics of Slotted Wings

Slotted canopies have been used in many parachute designs for the purpose of alleviating the opening shock and to provide better stability during descent. Deployments of all-flexible parawings have been characterized by positive, rapid inflation and high opening shock loads, and means for reducing the opening loads have been investigated. The use of a slotted canopy to reduce opening loads of all-flexible parawings is one of the methods that has been investigated in flight tests. The present investigation recognized this potential value of a slotted canopy; however, the use of slots for other purposes such as flow control over the wing may also have value in the glide and landing portions of flight.

Basic data for the slotted wings investigated are presented in figures 25, 26, 28, and 30, and a summary of the performance characteristics is presented in figure 41. Longitudinal characteristics obtained for the wing with multiple slots in figure 25 show a somewhat larger test angle-of-attack range than for the 5-ft (1.524-m) unslotted wings of figures 7 to 11. The loss in lift-drag ratio with increased angle of attack was more gradual and was smaller for the wing with multiple slots than for the unslotted wings; however, the maximum lift-drag ratio was slightly less (a value of 2.2) for the slotted wing. Observation of the slotted wing during testing indicated that many of the slots were practically closed, particularly in areas of the canopy having large spanwise curvature.

In order to provide additional open-slot area, the trailing edges of the rear two rows of slots were scalloped as shown in figure 24. A comparison of the data for the straight slot edges (fig. 25) and the scalloped edges (fig. 26) indicates that the scalloped slot edges provided a higher lift-drag ratio (a value of 2.4) over the wing with straight slot edges. (See fig. 41.)

Flow surveys were made over the upper surface of a basic unslotted wing by means of a tuft probe. These surveys indicated that a fairly extensive region of separated flow occurred over the rear inboard part of the wing. This region was approximately triangular in shape, extended from the keel outward and rearward to the trailing edge, and was confined inboard of the maximum lobe height. The fairly large extent of this flow separation suggested that substantial reductions in drag could possibly be realized by improving the flow characteristics. The wing having two rows of slots (fig. 27) was investigated as an attempt to improve the flow in a manner similar to a slotted high-lift flap. The test results presented for this wing in figure 28 show a maximum lift-drag ratio of about 2.3 and somewhat lower resultant-force coefficients than the configurations with multiple slots.

Observations of the canopy during tests of the wing with the two rows of single slots revealed that the slots were closed over the inboard half and open only over the outboard half. The slots appeared to be closed over the portion of the wing where they were needed most. The behavior of this slotted configuration illustrates a point of interest for all of the slotted wings investigated. The slot details for the various models were selected on the basis of the best guess as to an appropriate slot arrangement. For multiple-slotted, high-lift flaps on conventional aircraft wings, the basic slot parameters such as slot gap, airfoil shape, and slot location have to be carefully determined in order to obtain an efficient slot configuration. It is therefore believed that the test results for the slotted wings investigated do not represent the performance potential for the use of slots on all-flexible parawings.

Another approach to a slotted parawing is illustrated in the wing with multiple slots and radial tapes. The wing configuration shown in figure 29 can be considered similar to one-quarter of a Ring Sail parachute. Basic test results for this wing are presented in figure 30, and the performance characteristics for zero control deflection are summarized in figure 41. The results of figure 41 show that the slotted wing with radial tapes had a lower value of maximum lift-drag ratio than the other slotted wings; however, the lift-drag ratio was practically invariant with resultant-force coefficient. During tests of the wing, it appeared that the minimum angle of attack that could be obtained was limited by collapse of the leading-edge points at the nose. These points appeared to give more difficulty than the points formed by the straight nose cut used for the other wings. A small improvement in performance might be expected, therefore, if the shape of the planform nose were modified.

### **Effect of Control-Line Shortening**

The tests of the present investigation were made with the sting angle of attack as the primary variable. The spread rigging mount used for the control lines provided an effective control input when the sting angle was varied, so that the effect of an increase in sting angle was similar to that of shortening the three rear control lines. In addition to this control effect, the spread rigging mount also provided untrimmed negative pitching moments throughout this investigation since the moment reference was left at the confluence point. No attention has been given to the pitching-moment data because they are not generally applicable and can be used only for the same mount-attachment geometry used in these tests. The discussion of control effects therefore will be concerned primarily with the effects of control-line shortening on lift-drag ratio and resultant-force coefficients. In regard to an assessment of these parameters to indicate the aerodynamic potential for each wing, it is believed that the data are generally applicable.

Basic wing.- Test results which show effects of shortening only the tip lines or the rear keel line are given in figures 11 and 42(a). The results of figure 42(a) show that shortening only the tip lines reduced the lift-drag ratio at a given value of resultant-force coefficient and caused a slight reduction in the maximum resultant-force coefficient. Shortening of only the rear keel line caused a general increase in resultant-force coefficient and had very little effect on the maximum lift-drag ratio. It should be noted also that the range available for modulating either lift-drag ratio or resultant-force coefficient was very restricted. For an assumed wing loading of 1.0 and sea-level altitude, the available resultant-force range would allow the flight velocity to be varied from approximately 25 ft/sec (7.62 m/sec) to 31 ft/sec (9.45 m/sec).

Wing with multiple slots and scalloped slot edges.- Test results which show effects of shortening both the rear keel and tip lines together for the multiple-slotted wing having scalloped slot edges are presented in figures 26 and 42(b). The summary characteristics given in figure 42(b) show very little overall effect of combined line shortening on the variation of lift-drag ratio with resultant-force coefficient. The basic data of figure 26 show large effects of line shortening at a given sting angle of attack. When the data of figure 26 for the various control deflections are compared at the same wing angle of attack ( $\alpha_w$ ), however, the results are in fairly close agreement. It appears therefore that shortening the three rear lines together had essentially the same effect as increasing the angle of attack of the rigging mount since it rotated the wing to a higher angle of attack.

Wing with multiple slots and radial tapes.- Data which show effects of three different modes of line shortening are presented in figures 30(b) and 42(c). Shortening only

the tip lines provided an increase in resultant-force coefficient and an attendant decrease in lift-drag ratio (fig. 42(c)) through the stall. Shortening of only the rear keel line gave a much larger increment in resultant-force coefficient than the same shortening of only the tip lines and provided a higher maximum value of resultant-force coefficient. The combination of a smaller tip and keel deflection gave about the same resultant-force coefficients, but the lift-drag ratios were generally lower with the combined deflection than with the keel line alone.

The results obtained for the wing with multiple slots and radial tapes (see fig. 42(c)) did not show the overlap of the  $L/D$  and  $C_R$  variation shown for the wing with multiple slots and scalloped slot edges for the combined keel and tip deflection (fig. 42(b)). The reason for this difference in results is that the same wing angle-of-attack range was not covered with shortenings of 0 and 0.042 for the slotted wing with radial tapes. The line spread was smaller in relation to the wing size (see table I) for the wing with radial tapes, and therefore, the ability of the sting and rigging mount to vary the wing angle of attack was less than for the wing with scalloped slots. If, for example, the sting-angle range could have been extended an additional  $10^\circ$  for the wing with radial tapes, the  $L/D$  variation with  $C_R$  should overlap for line shortenings of 0 and 0.042.

An overall assessment of the effects of shortening the control lines indicates that shortening of only the rear keel line provided the largest increase in resultant-force coefficient of the three modes investigated. Shortening of the rear keel line and tip lines together might be expected to have little effect on the variation of  $L/D$  with  $C_R$  and would cause primarily a change in angle of the rigging mount for a suspended payload. Shortening of only the wing tip lines would be expected to give lower maximum resultant-force coefficients than with either of the other modes of shortening.

#### Four-Lobe Parawings

Exploratory research on parawing planforms and configurations has been continued in an effort to identify wing designs that may have improved aerodynamic characteristics in comparison with the basic single-keel design. Test results from the exploratory studies on four-lobe parawings are presented in figures 32, 34, and 36. In addition to the wind-tunnel tests, the  $35^\circ$  swept and rectangular unswept wings were flight tested by gliding the models from an altitude of about 90 ft (27.4 m).

The test results presented in figure 34 for the  $35^\circ$  swept four-lobe wing show a maximum lift-drag ratio of 2.6, which was an improvement of 0.1 to 0.3 over the single-keel wing.

The  $35^\circ$  swept wing was difficult to rig for the tunnel tests, and during subsequent free-gliding tests, an undesirable fore and aft oscillation of the tips occurred. Maximum

lift-drag ratios of the other four-lobe wings (figs. 32 and 36) were even lower than those of the basic two-lobe (single-keel) wing and no further wind-tunnel tests were made, although flight tests were made with the rectangular wing.

The most significant aspect of the tests of the four-lobe wings is that pieces of completely flexible fabric of widely differing shapes could be rigged for gliding flight. The task of rigging the 35° swept wing and the rectangular wing was the most difficult rigging determination encountered on all-flexible parawings. Successful accomplishment of this task has provided a valuable background of experience that has been applied to other improved multilobed wing configurations.

#### SUMMARY OF RESULTS

The results of a low-speed wind-tunnel investigation of the effects of canopy construction methods, wing design details, and canopy slots on the longitudinal aerodynamic characteristics of all-flexible parawings may be summarized as follows:

1. Construction details such as type of nonporous canopy fabric, glued or sewed seams, tape reinforcement, or cloth-weave orientation had little effect on maximum lift-drag ratios and resultant-force coefficients.
2. Canopy modifications which incorporated a curved-leading-edge planform or a cambered keel gave a smoother inflated-canopy shape than the unmodified wing, but did not provide an improvement in measured aerodynamic characteristics.
3. Maximum lift-drag ratios obtained on the various single-keel, unslotted parawings ranged from approximately 2.2 to 2.5.
4. Incremental reductions in the length of all the suspension lines caused a corresponding reduction in the resultant-force coefficients and maximum lift-drag ratios.
5. Maximum lift-drag ratios obtained on the slotted parawings ranged from approximately 2.2 to 2.4. Visual observation of the individual slot openings during the tests indicated that some of the slots were not open, and therefore, some detailed development would be required to obtain an efficient slot design.
6. The available range for modulation of resultant-force coefficient or lift-drag ratio by control-line shortening was limited. Changing the length of only the rear keel line was the most effective means for varying the resultant-force coefficient.

Langley Research Center,  
National Aeronautics and Space Administration,  
Hampton, Va., June 5, 1970.

## REFERENCES

1. Polhamus, Edward C.; and Naeseth, Rodger L.: Experimental and Theoretical Studies of the Effects of Camber and Twist on the Aerodynamic Characteristics of Parawings Having Nominal Aspect Ratios of 3 and 6. NASA TN D-972, 1963.
2. Naeseth, Rodger L.; and Gainer, Thomas G.: Low-Speed Investigation of the Effects of Wing Sweep on the Aerodynamic Characteristics of Parawings Having Equal-Length Leading Edges and Keel. NASA TN D-1957, 1963.
3. Croom, Delwin R.; Naeseth, Rodger L.; and Sleeman, William C., Jr.: Effect of Canopy Shape on Low-Speed Aerodynamic Characteristics of a  $55^{\circ}$  Swept Parawing With Large-Diameter Leading Edges. NASA TN D-2551, 1964.
4. Bugg, Frank M.: Effects of Aspect Ratio and Canopy Shape on Low-Speed Aerodynamic Characteristics of  $50.0^{\circ}$  Swept Parawings. NASA TN D-2922, 1965.
5. Naeseth, Rodger L.; and Fournier, Paul G.: Low-Speed Wind-Tunnel Investigation of Tension-Structure Parawings. NASA TN D-3940, 1967.
6. Gillis, Clarence L.; Polhamus, Edward C., Jr.; and Gray, Joseph L., Jr.: Charts for Determining Jet-Boundary Corrections for Complete Models in 7- by 10-Foot Closed Rectangular Wind Tunnels. NACA WR L-123, 1945. (Formerly NACA ARR L5G31.)
7. Herriot, John G.: Blockage Corrections for Three-Dimensional-Flow Closed-Throat Wind Tunnels, With Consideration of the Effect of Compressibility. NACA Rep. 995, 1950. (Supersedes NACA RM A7B28.)

TABLE I.- PARAWING LINE ATTACHMENT DIMENSIONS

[Symbols are indicated in figure 2]

Figure	$h_1/l_k$	$h_2/l_k$	$d_1/l_k$	$d_2/l_k$	$y/l_k$	$y_1/l_k$
7-11	0.0271	0.0323	0.1333	0.1500	0.0833	
13, 15	.0169	.0202	.0833	.0938	.0521	
17, 19, 21-26, 28	.0271	.0323	.1333	.1500	.0833	
30	.0169	.0202	.0833	.0938	.0521	
32	.0271	.0323	.1333	.1500	.0833	
34	.0338	.0404	.1667	.1875	.1042	0.0625
36	.0637	.0760	.3137	.3529	.1961	.1569

TABLE II.- CANOPY AND LINE MATERIALS FOR EACH PARAWING INVESTIGATED

Parawing configuration	Model drawing figure	Data figure	Canopy material (a)	Line			Canopy construction	Keel length, $l_k$		
				Material	Rated strength			ft	m	
					lb	N				
Basic	5(a), 6	7, 11	A	Nylon	100	445	Glued	5.0	1.524	
Basic	5(a), 6	8	B	Dacron	130	578	Glued	5.0	1.524	
Basic	5(b), 6	9	A	Dacron	130	578	Sewed	5.0	1.524	
Bias trailing edge	6	10	A	Dacron	130	578	Sewed	5.0	1.524	
Basic	12	13	A	Braided nylon	85	378	Sewed	8.0	2.438	
Tape reinforcement	14	15	A	Braided nylon	85	378	Sewed	8.0	2.438	
Revised line attachments	16	17	A	Dacron	130	578	Sewed	5.0	1.524	
Cambered keel	18	19	A	Dacron	130	578	Sewed	5.0	1.524	
Curved leading edge	20	21	A	Nylon	100	445	Glued	5.0	1.524	
Basic	22	23	C	Dacron	130	578	Sewed	6.56	2.0	
Multiple slots	24	25	A	Dacron	130	578	Sewed	5.0	1.524	
Multiple slots with scalloped slot edge	24	26	A	Dacron	130	578	Sewed	5.0	1.524	
Two rows of single slots	27	28	A	Dacron	130	578	Sewed	5.0	1.524	
Multiple slots with radial tapes	29	30	A	Braided nylon	85	378	Sewed	8.0	2.438	
Composite four lobe	31	32	B	Dacron	130	578	Glued	5.0	1.524	
$\Lambda_0 = 35^\circ$ four lobe	33	34	A	Dacron	130	578	Sewed	4.0	1.219	
Rectangular four lobe	35	36	D	Dacron	130	578	Sewed	2.125	.648	

<sup>a</sup>Material designations are as follows:

- A: 1.1 oz/yd<sup>2</sup> (37.3 g/m<sup>2</sup>) acrylic-coated nylon
- B: 2.2 oz/yd<sup>2</sup> (74.6 g/m<sup>2</sup>) calendered nylon
- C: 0.75 oz/yd<sup>2</sup> (25.3 g/m<sup>2</sup>) resin-impregnated nylon
- D: 0.75 oz/yd<sup>2</sup> silicone-impregnated nylon

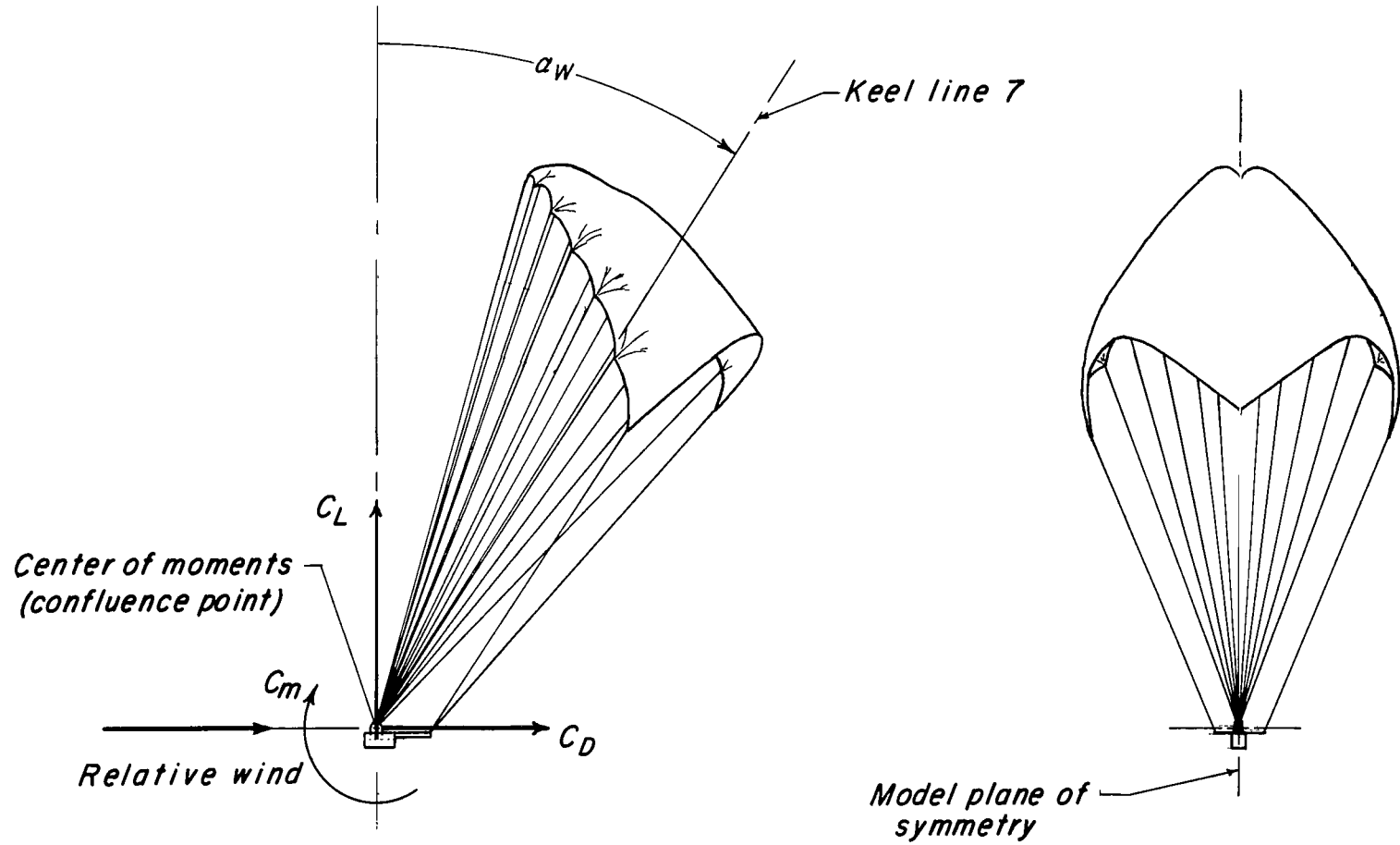


Figure 1.- Sketch showing positive directions of forces, moment, and angle used in presentation of data.

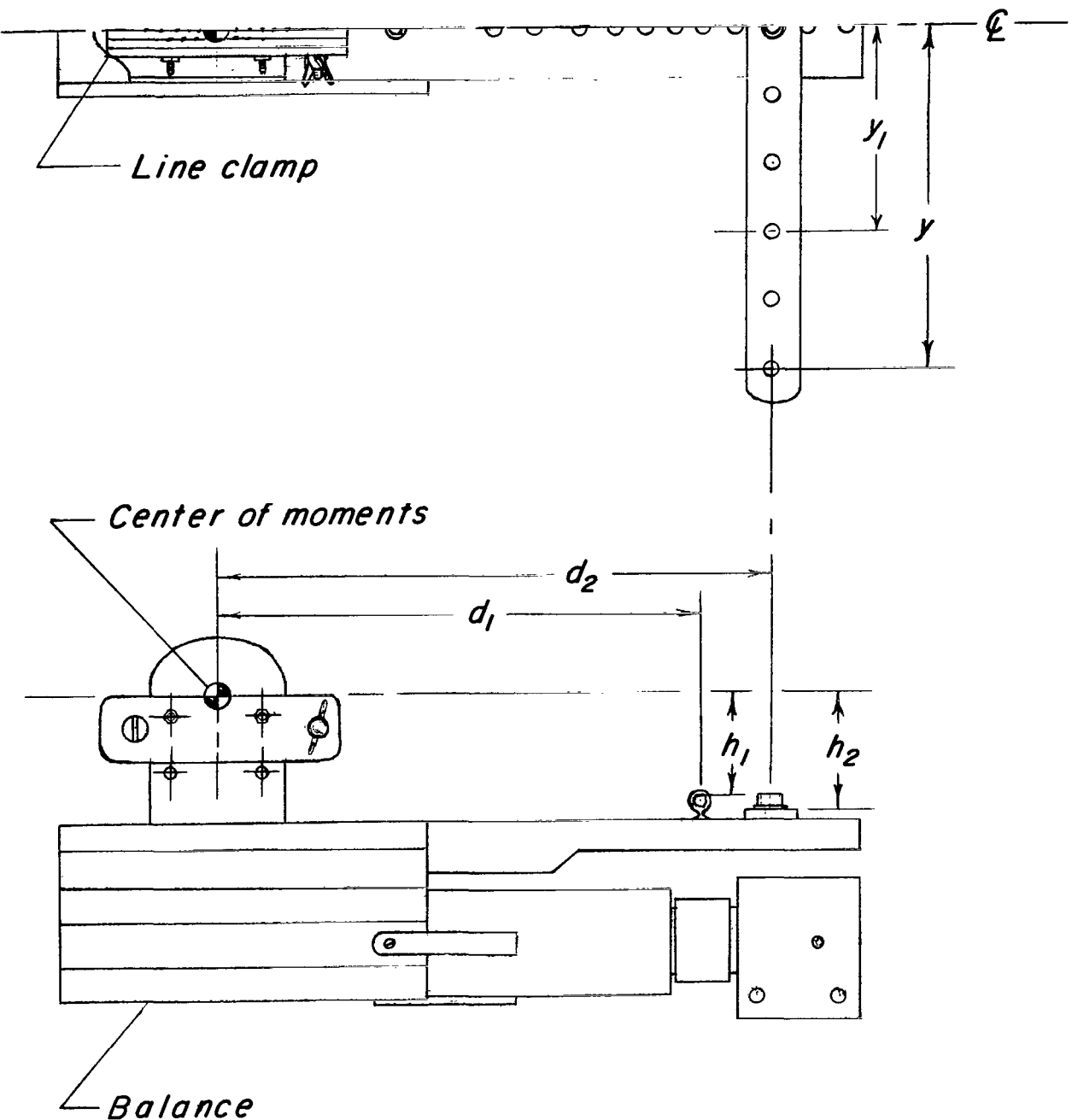
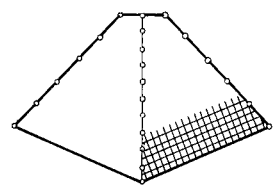
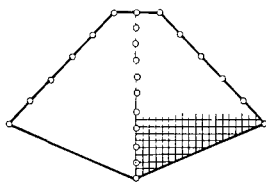


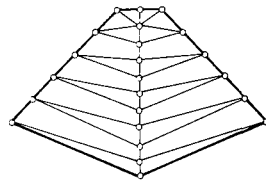
Figure 2.- Parawing line attachments to balance used for tethered tests. Dimensions are given in table I.



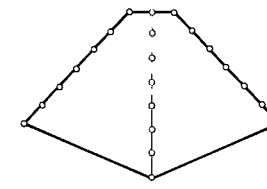
BASIC CONFIGURATION



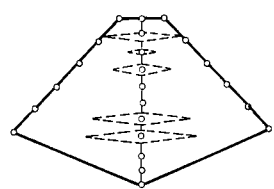
BIAS TRAILING EDGE



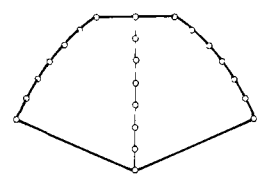
TAPE REINFORCEMENT



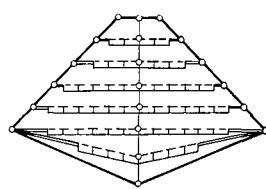
REVISED LINE ATTACHMENTS



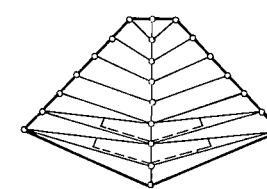
CAMBERED KEEL



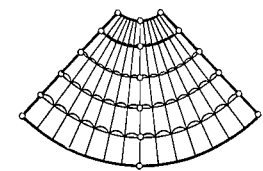
CURVED LEADING EDGE



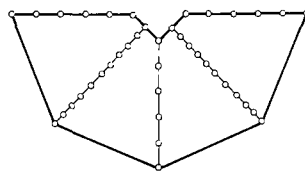
MULTIPLE SLOTS



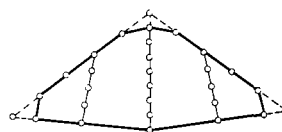
TWO ROWS OF SLOTS



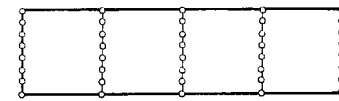
MULTIPLE SLOTS AND RADIAL TAPES



COMPOSITE WING

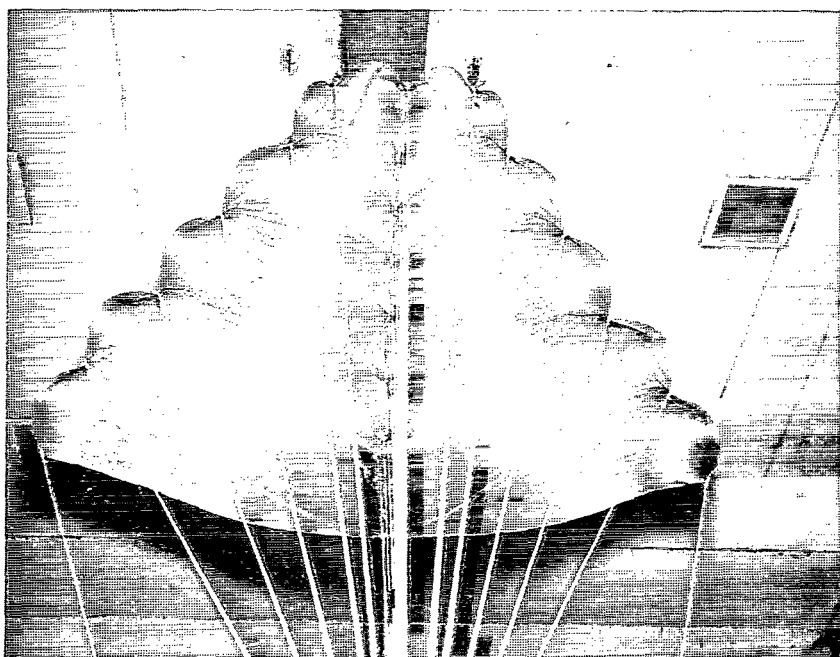


35° SWEPT WING

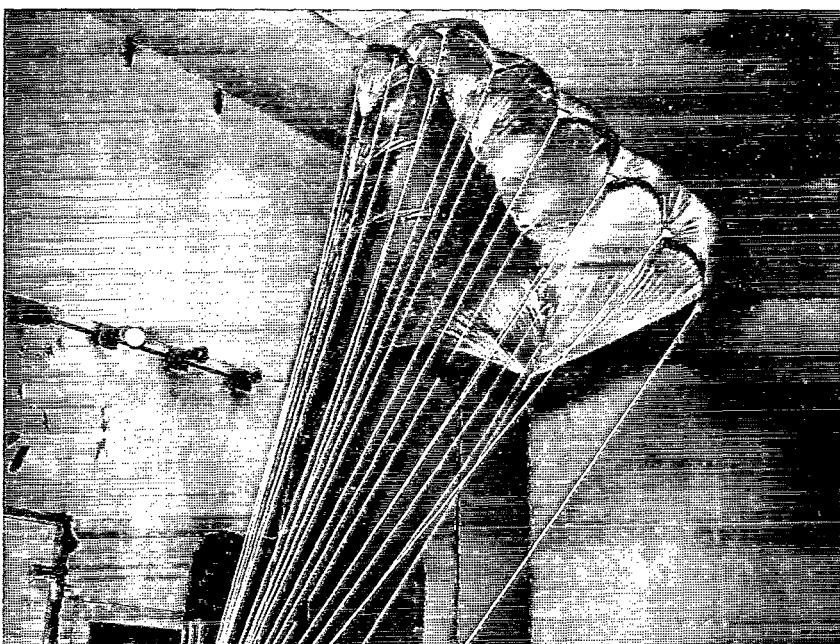


RECTANGULAR WING

Figure 3.- Planform sketches of wing configurations investigated.



*Plan view*

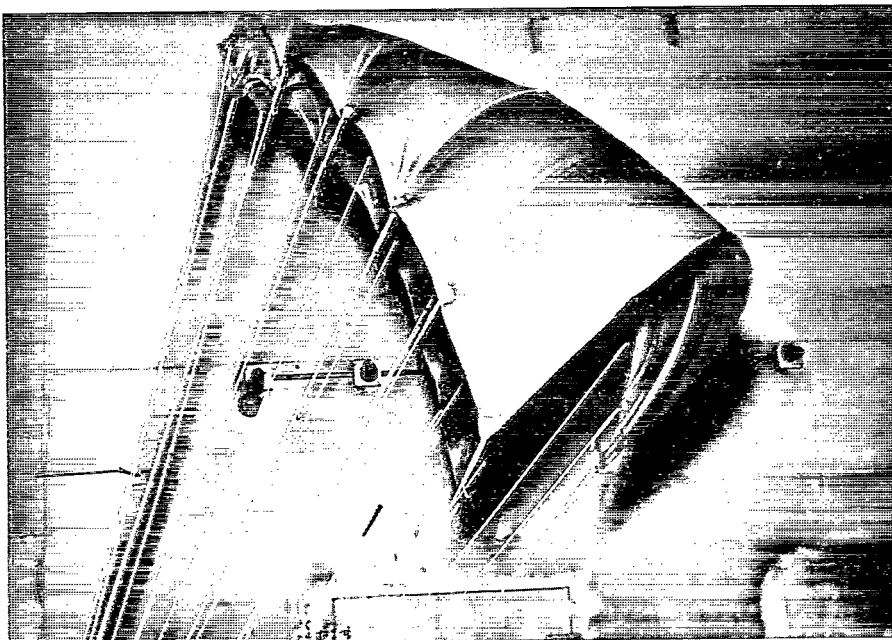


*Three-quarter front view*

(a) Basic planform.

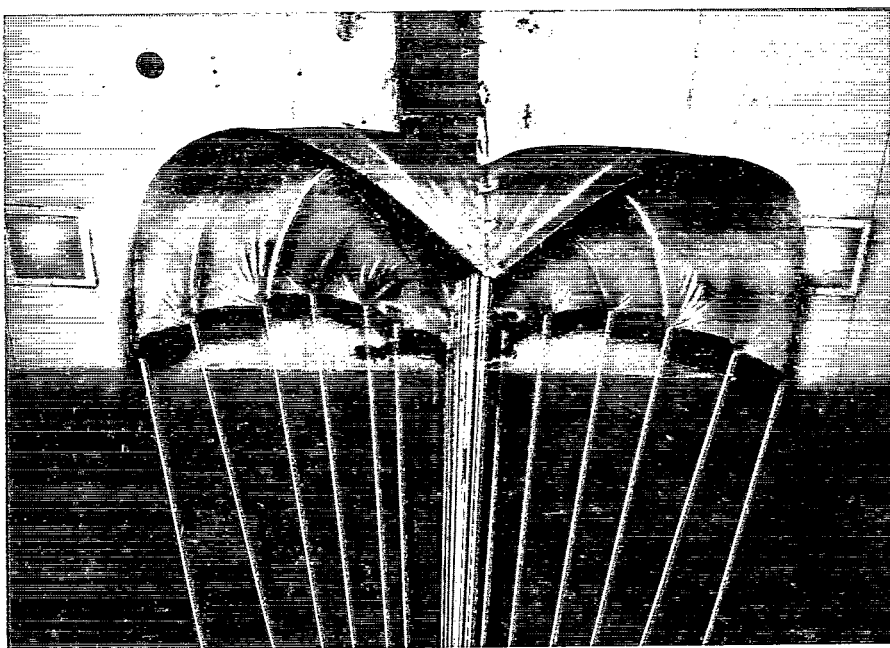
L-65-2356

Figure 4.- Parawing models during testing.



*Side view*

L-65-2354

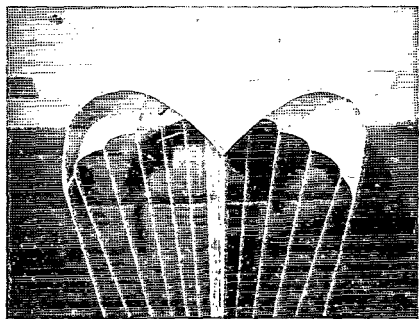


*Rear view*

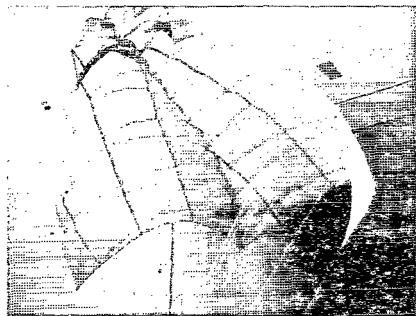
(a) Concluded.

L-65-2360

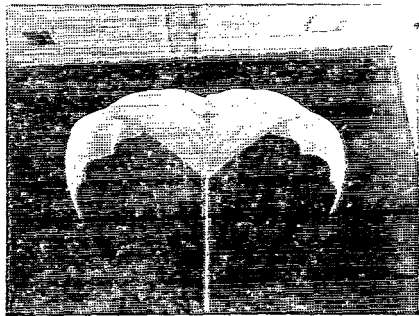
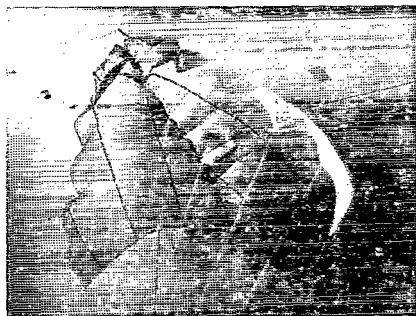
Figure 4.- Continued.



$\Delta_0 = 45^\circ$  Cambered-keel wing



$\Delta_0 = 45^\circ$  Basic wing, tape construction

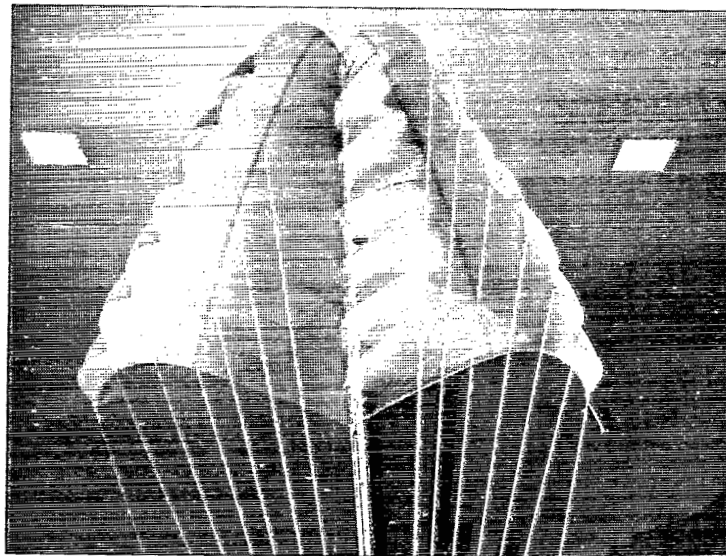
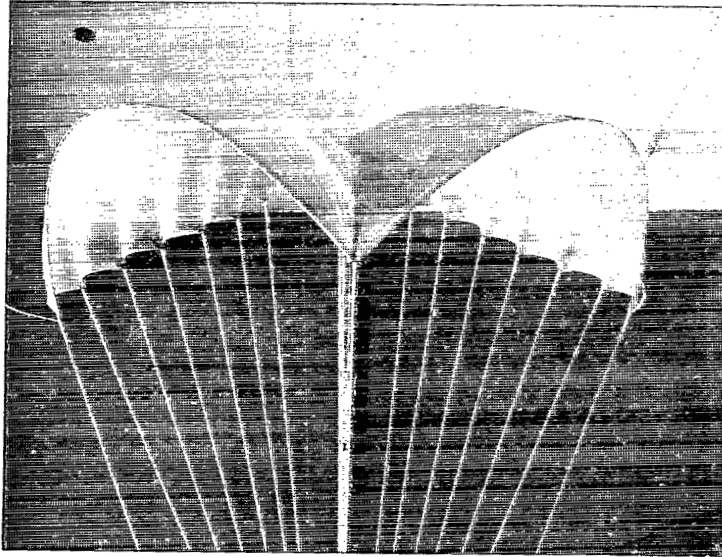


$\Delta_0 = 45^\circ$  Basic wing, sewed construction

(b) Modifications to basic planform.

L-70-1671

Figure 4.- Continued.

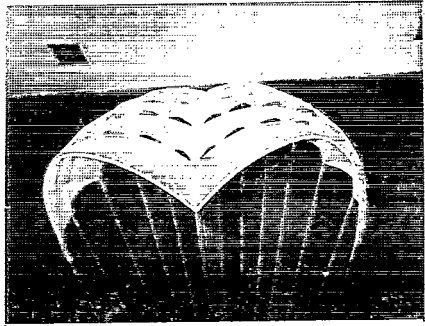
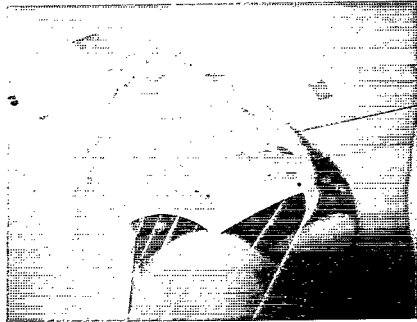


*Curved leading edge*

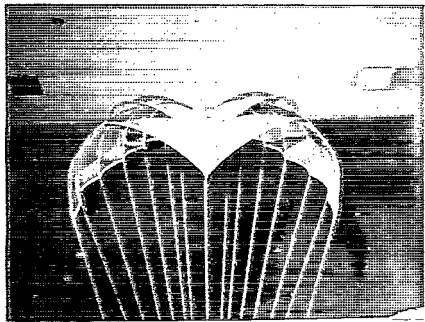
(b) Concluded.

L-70-1672

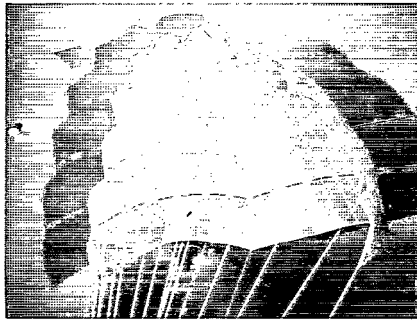
Figure 4.- Continued.



$\Delta_o = 45^\circ$  Multiple slotted wing



$\Delta_o = 45^\circ$  Wing with two rows of slots



$\Delta_o = 45^\circ$  Radial tape wing

(c) Slotted planforms.

L-70-1673

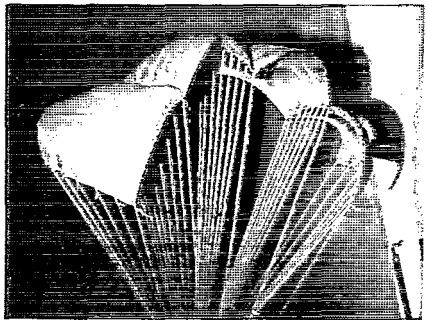
Figure 4.- Continued.



$\Delta_0 = 0^\circ$  Four-lobe wing (Two basic wings joined)



$\Delta_0 = 35^\circ$  Four-lobe wing

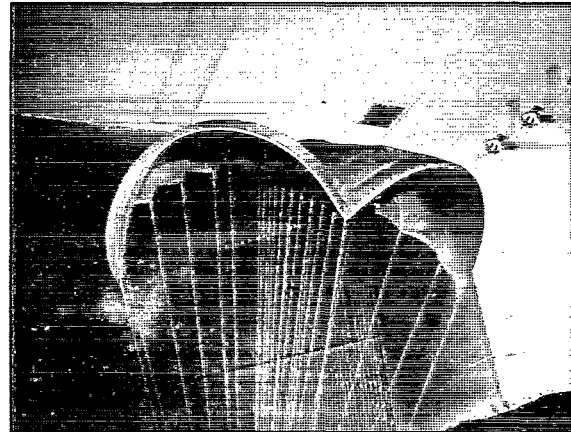


$\Delta_0 = 0^\circ$  Rectangular four-lobe wing

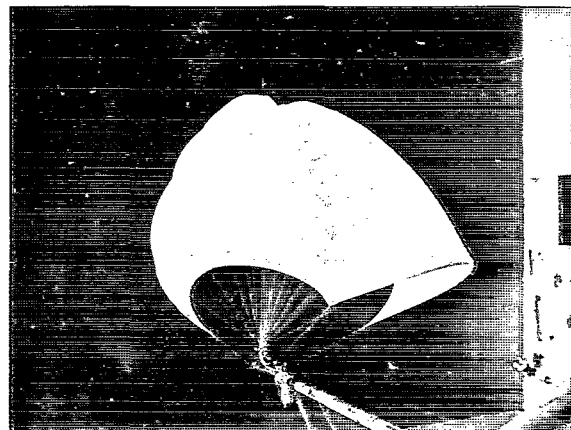
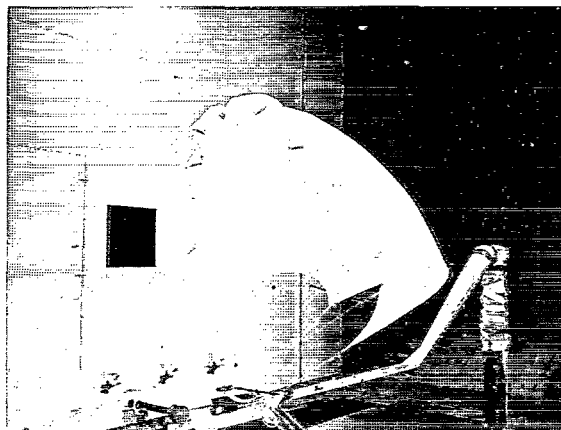
(d) Four-lobe planforms.

L-70-1674

Figure 4.- Continued.



Basic rigging.

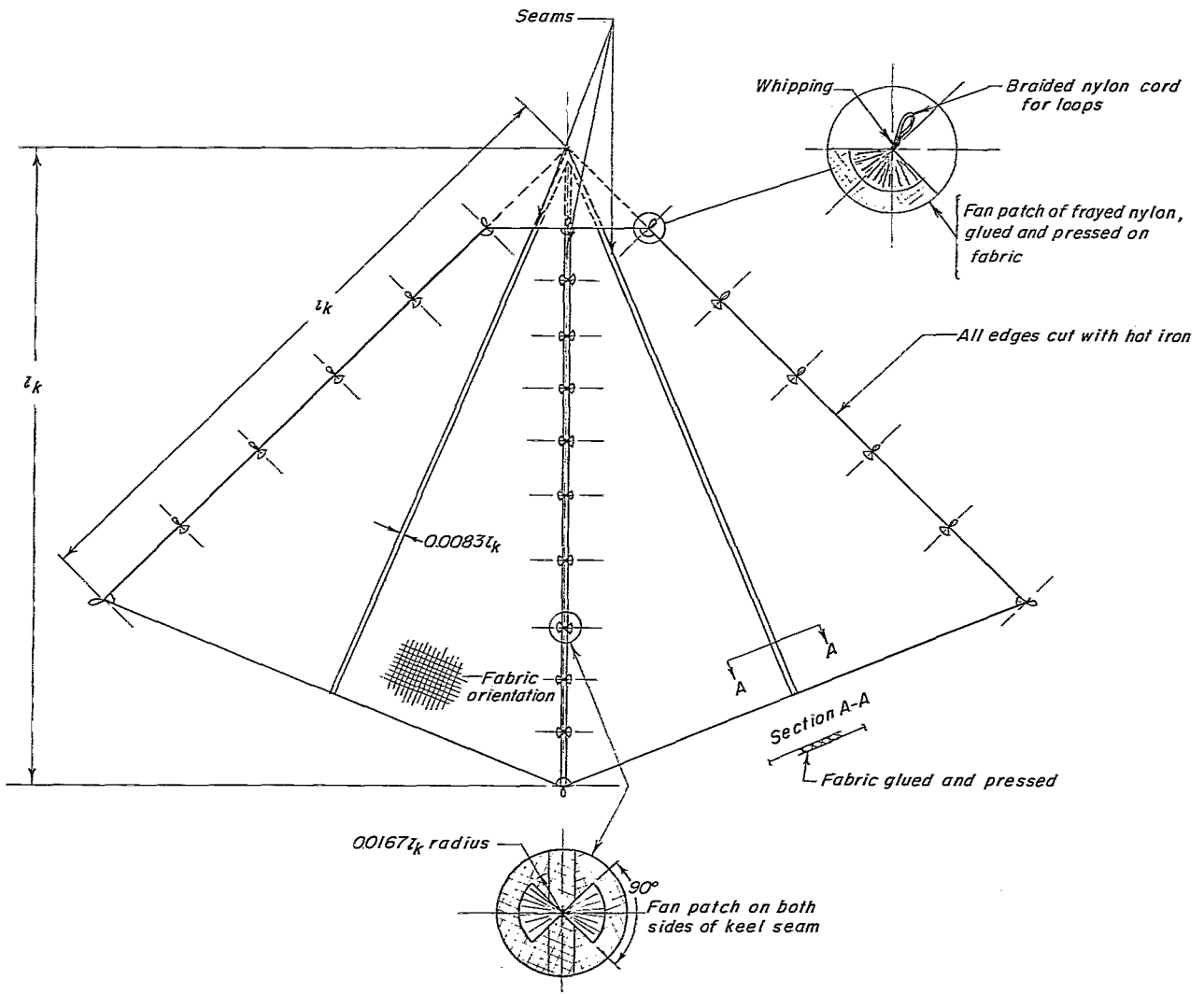


Shortening of all canopy lines,  $\Delta l/l_k = .75$ .

(e) Basic wing with two wing-to-confluence distances.

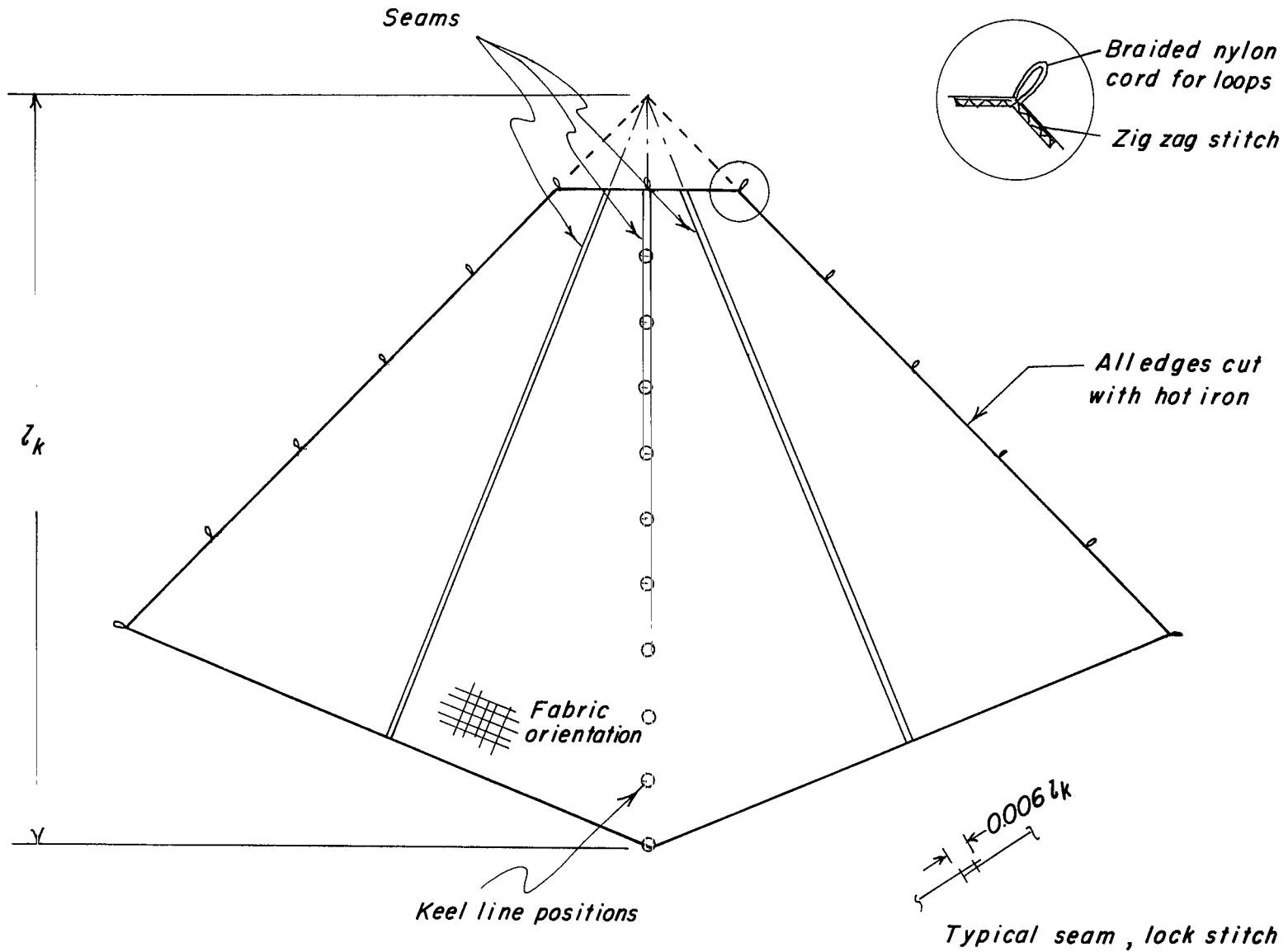
L-70-1675

Figure 4.- Concluded.



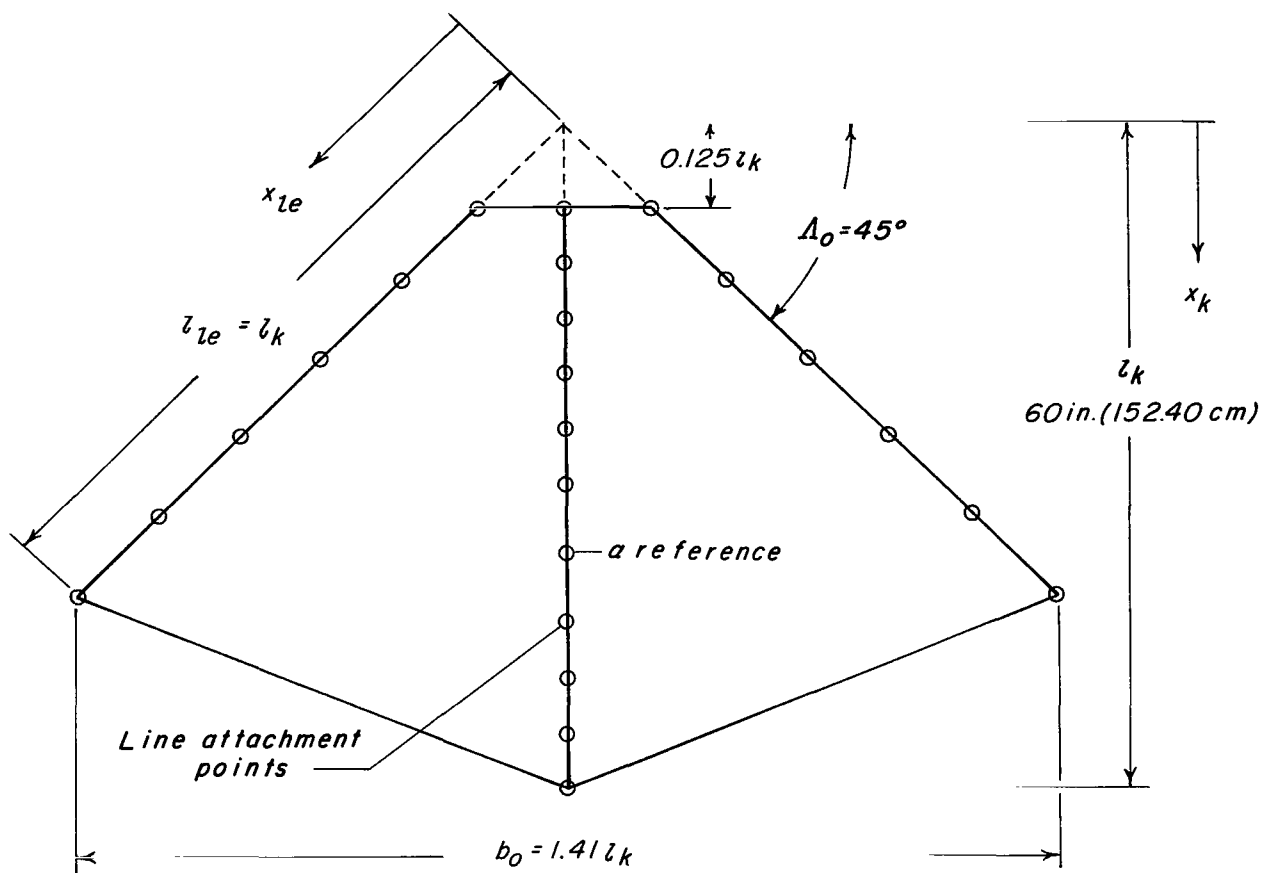
(a) Glued construction.

Figure 5.- Typical construction details for the basic parawing.  $\Lambda_0 = 45^\circ$ ; nose cutoff of  $0.125t_k$ .



(b) Sewed construction.

Figure 5.- Concluded.



$x/l_k$

KeeI	Leading edge
.125	.177
.208	.333
.292	.500
.375	.667
.459	.833
.542	1.000
.645	
.750	
.833	
.917	
1.000	

Line attachment location

Figure 6.- Planform of basic 5-ft (1.524-m) parawing.

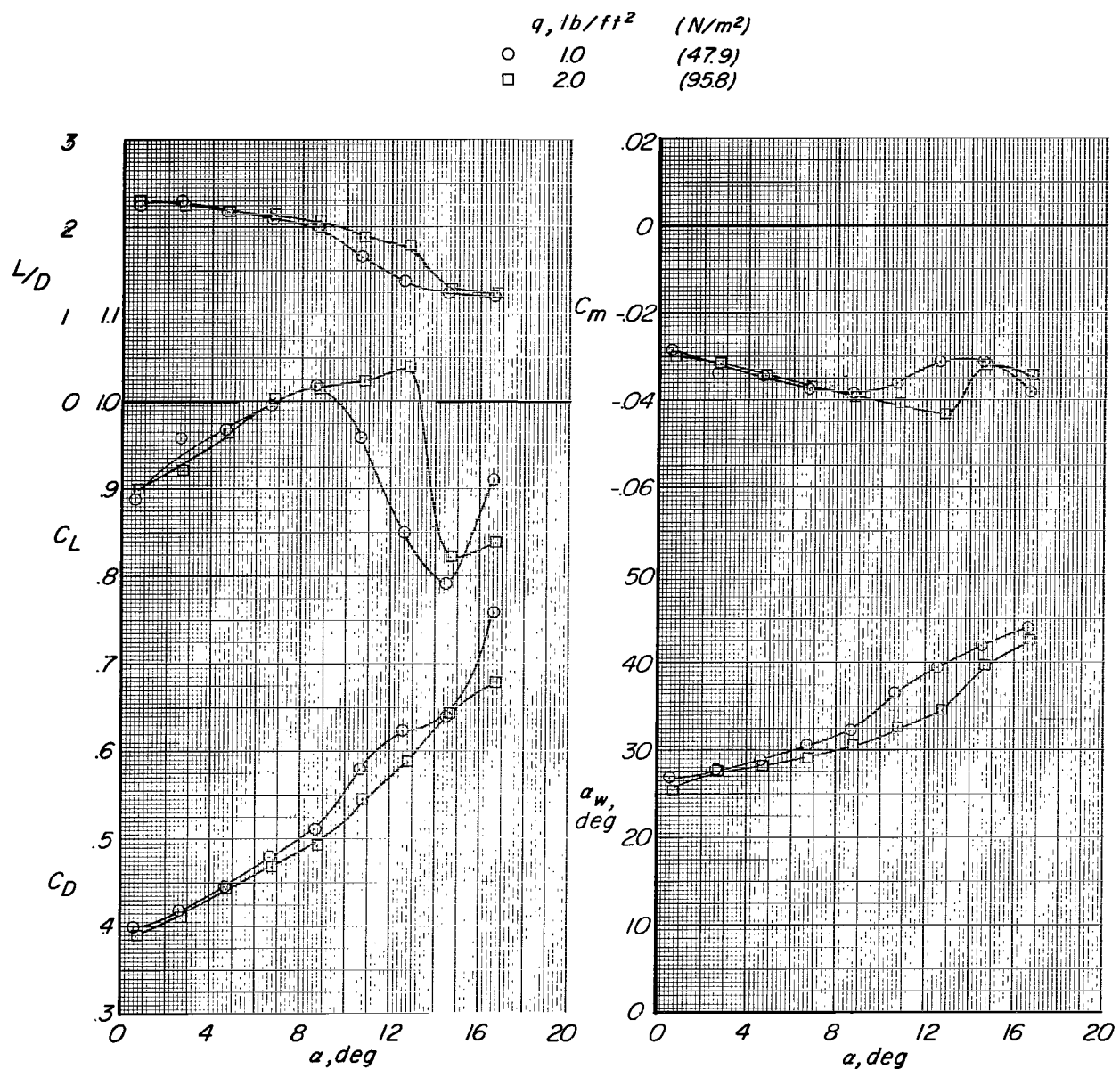


Figure 7.- Longitudinal aerodynamic characteristics of basic parawing with  $1.1 \text{ oz/yd}^2$  ( $37.3 \text{ g/m}^2$ ) acrylic-coated nylon canopy. Glued construction; nylon lines;  $l_k = 5 \text{ ft}$  ( $1.524 \text{ m}$ ).

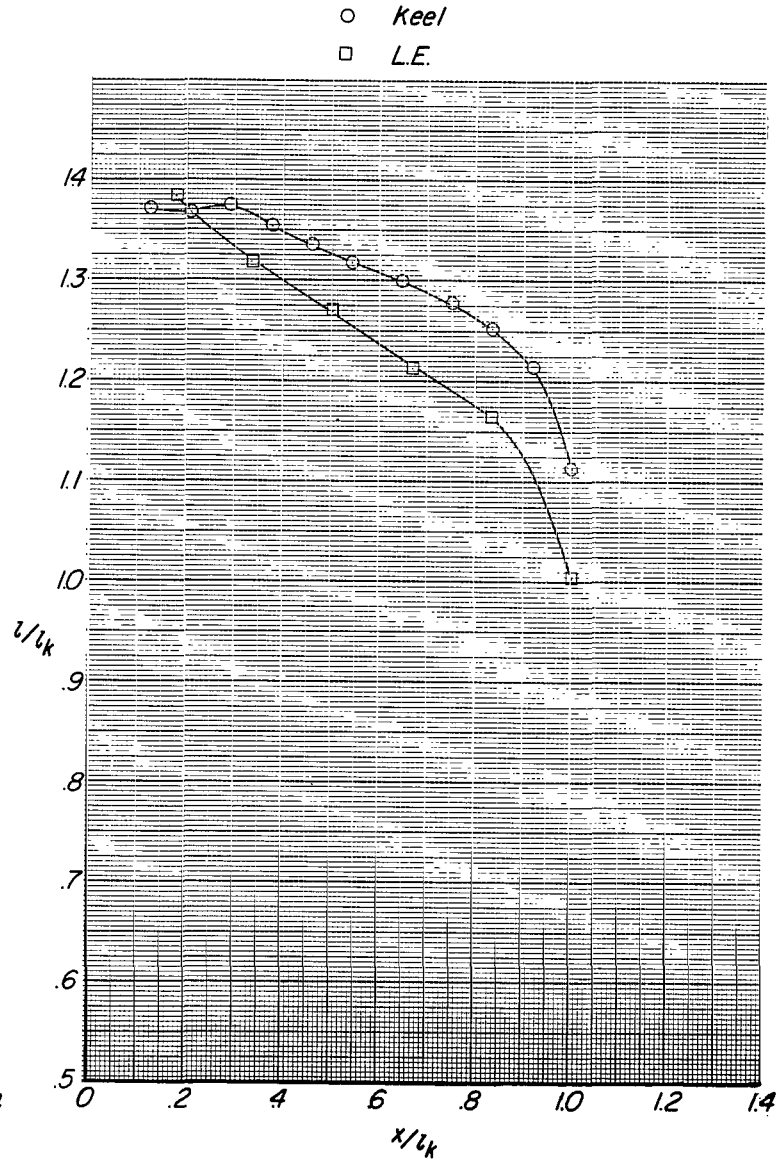
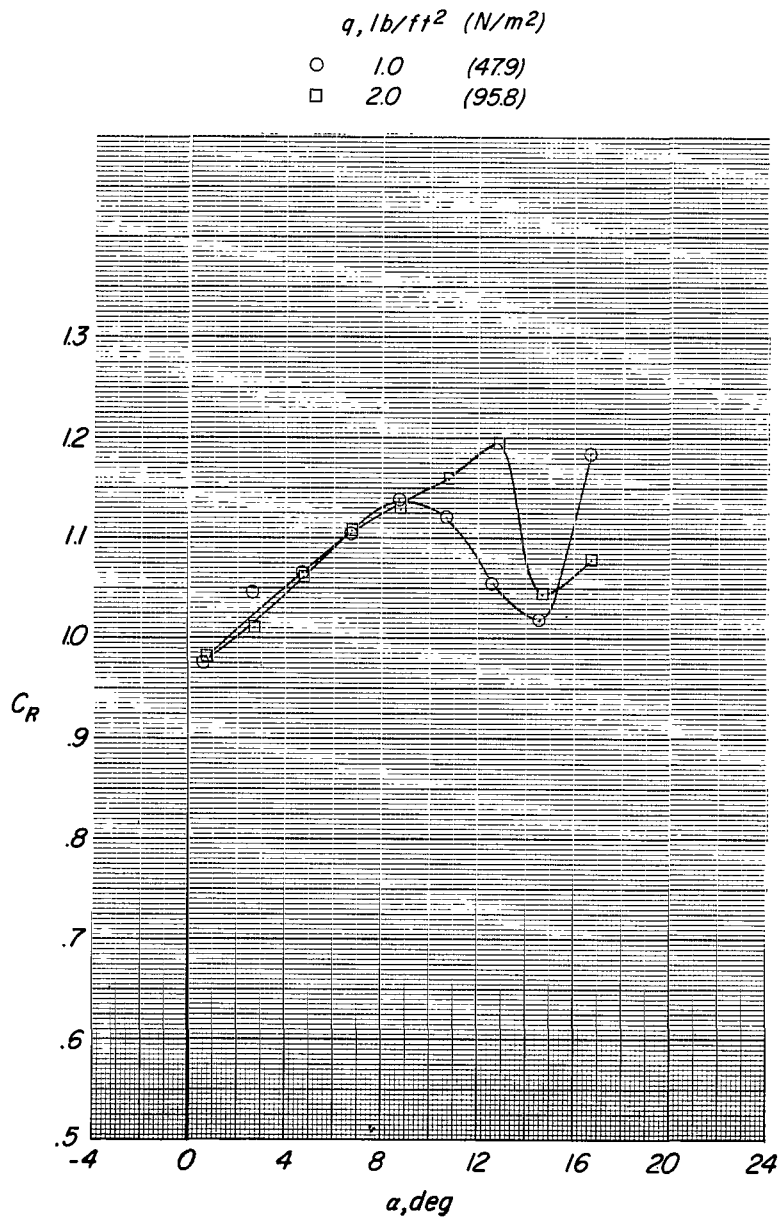


Figure 7.- Concluded.

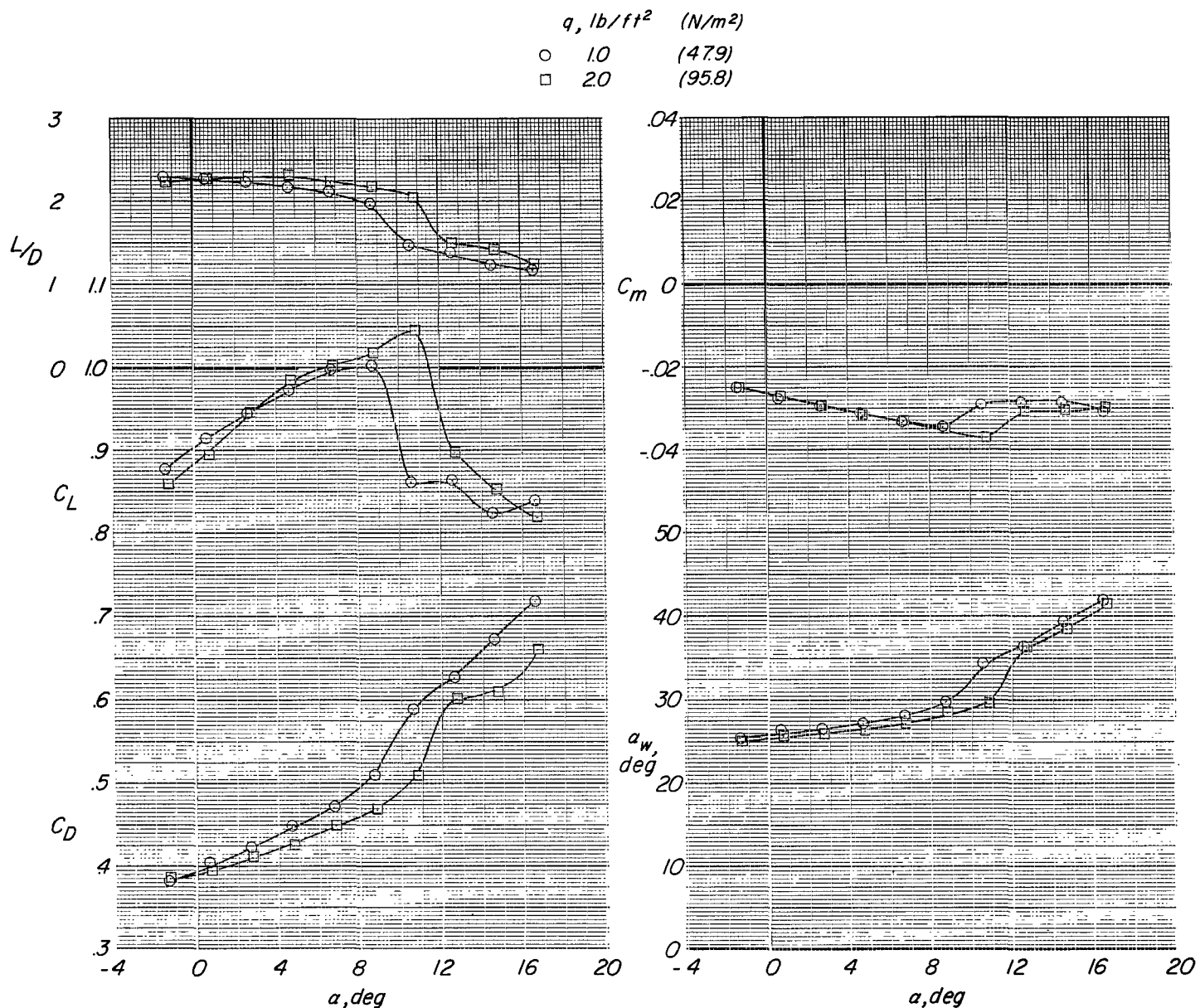


Figure 8.- Longitudinal aerodynamic characteristics of basic parawing with  $2.2 \text{ oz/yd}^2$  ( $74.6 \text{ g/m}^2$ ) calendered nylon canopy. Glued construction; dacron lines;  $l_k = 5 \text{ ft}$  ( $1.524 \text{ m}$ ).

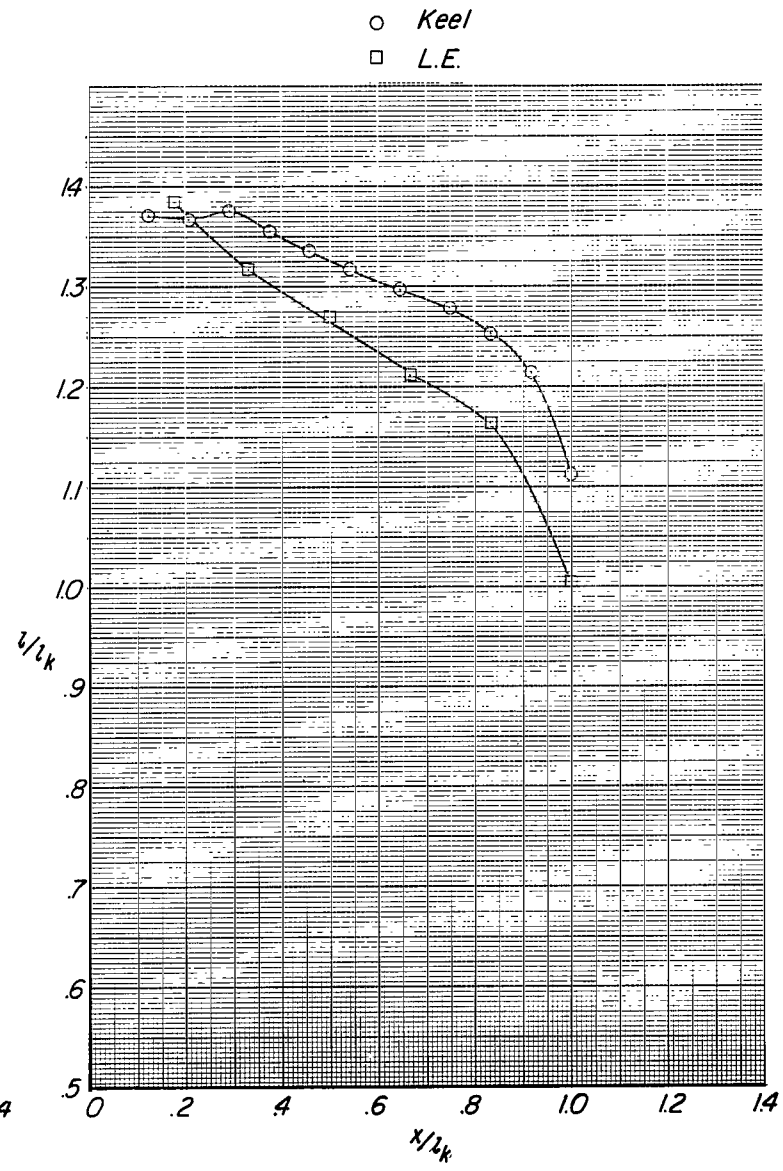
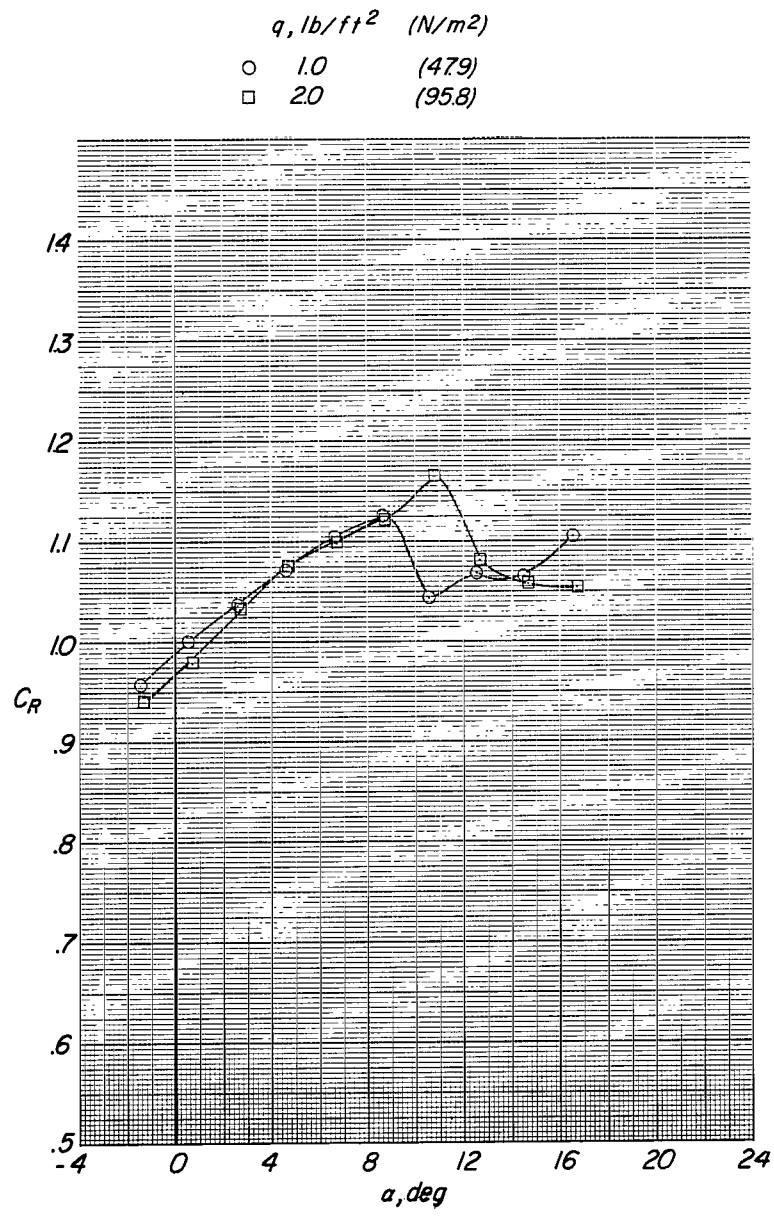


Figure 8.- Concluded.

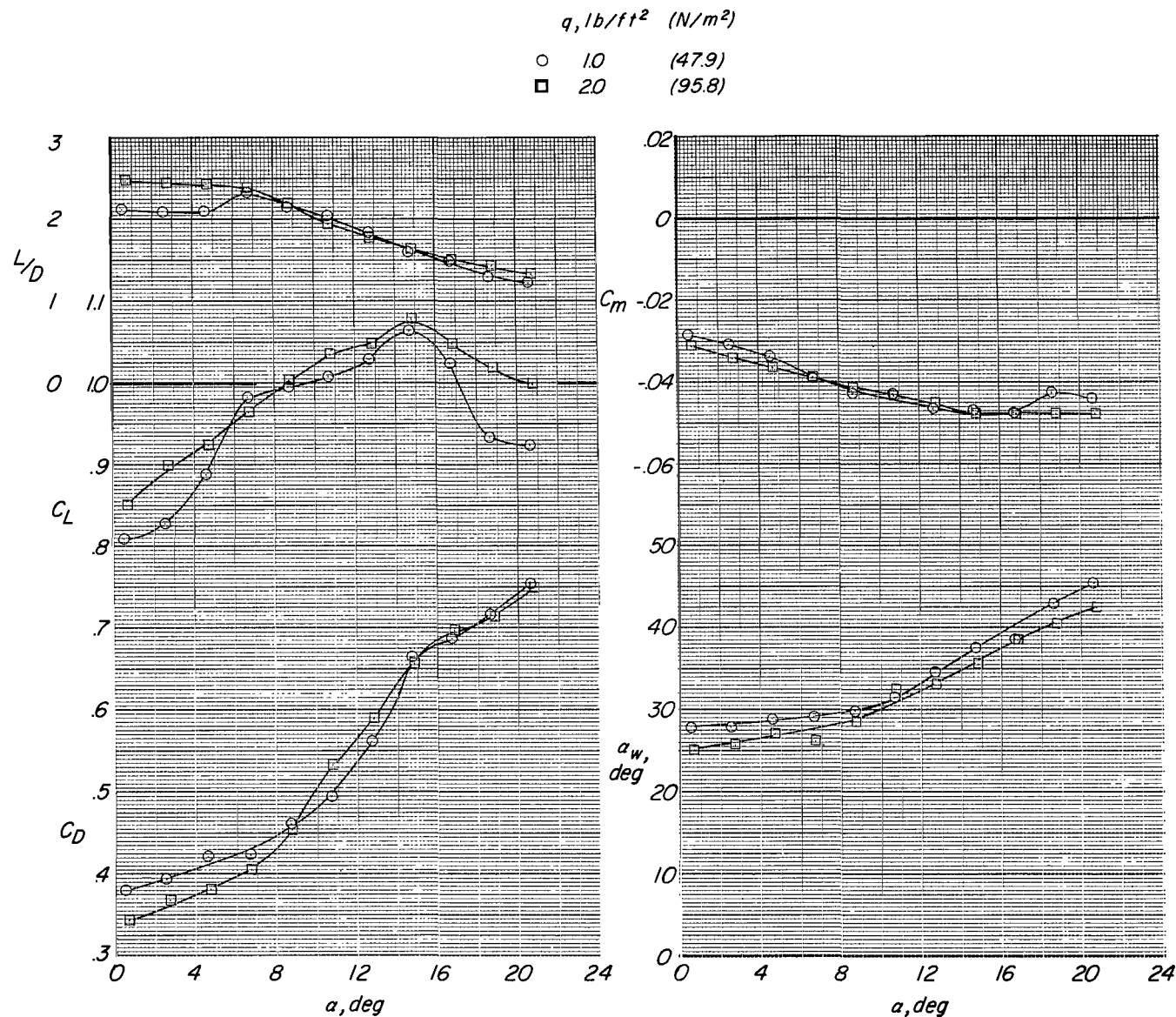


Figure 9.- Longitudinal aerodynamic characteristics of the basic parawing with  $1.1 \text{ oz/yd}^2$  ( $37.3 \text{ g/m}^2$ ) acrylic-coated nylon canopy. Sewed construction; dacron lines;  $l_k = 5 \text{ ft}$  ( $1.524 \text{ m}$ ).

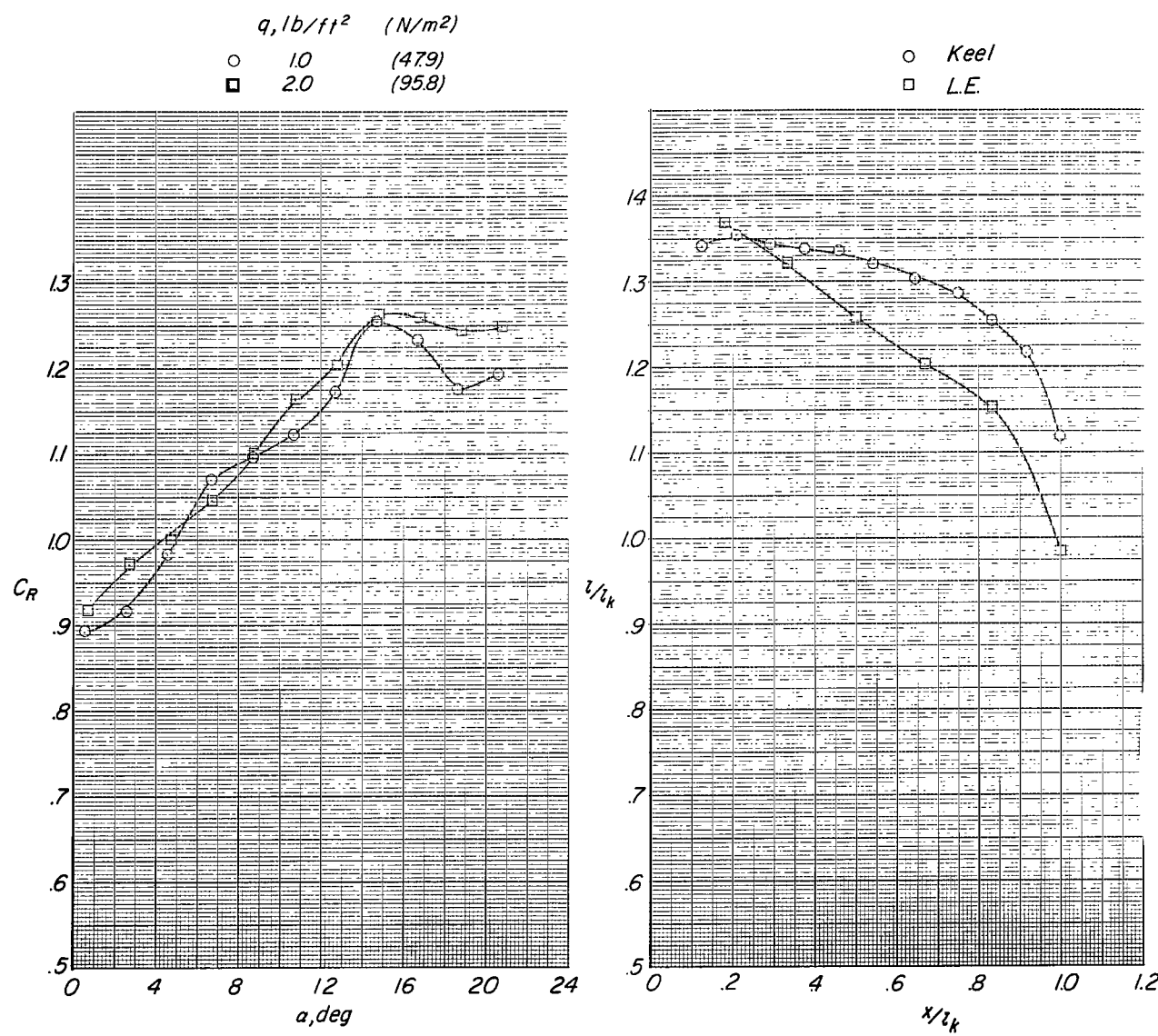


Figure 9.- Concluded.

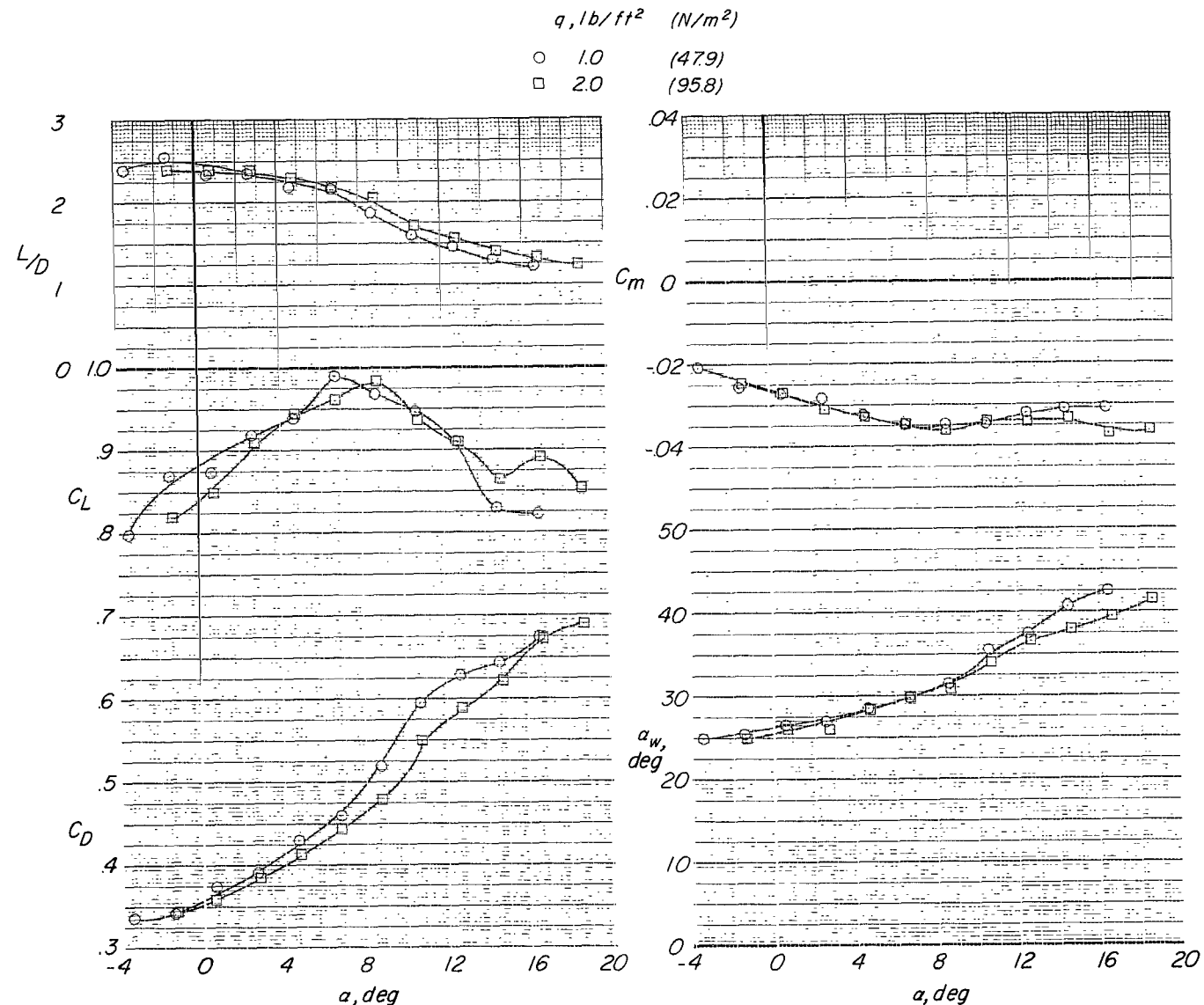


Figure 10.- Longitudinal aerodynamic characteristics of basic parawing with bias-cut trailing edge.  $1.1 \text{ oz}/\text{yd}^2$  ( $37.3 \text{ g}/\text{m}^2$ ) acrylic-coated nylon canopy; sewed construction; dacron lines;  $l_k = 5 \text{ ft}$  ( $1.524 \text{ m}$ ).

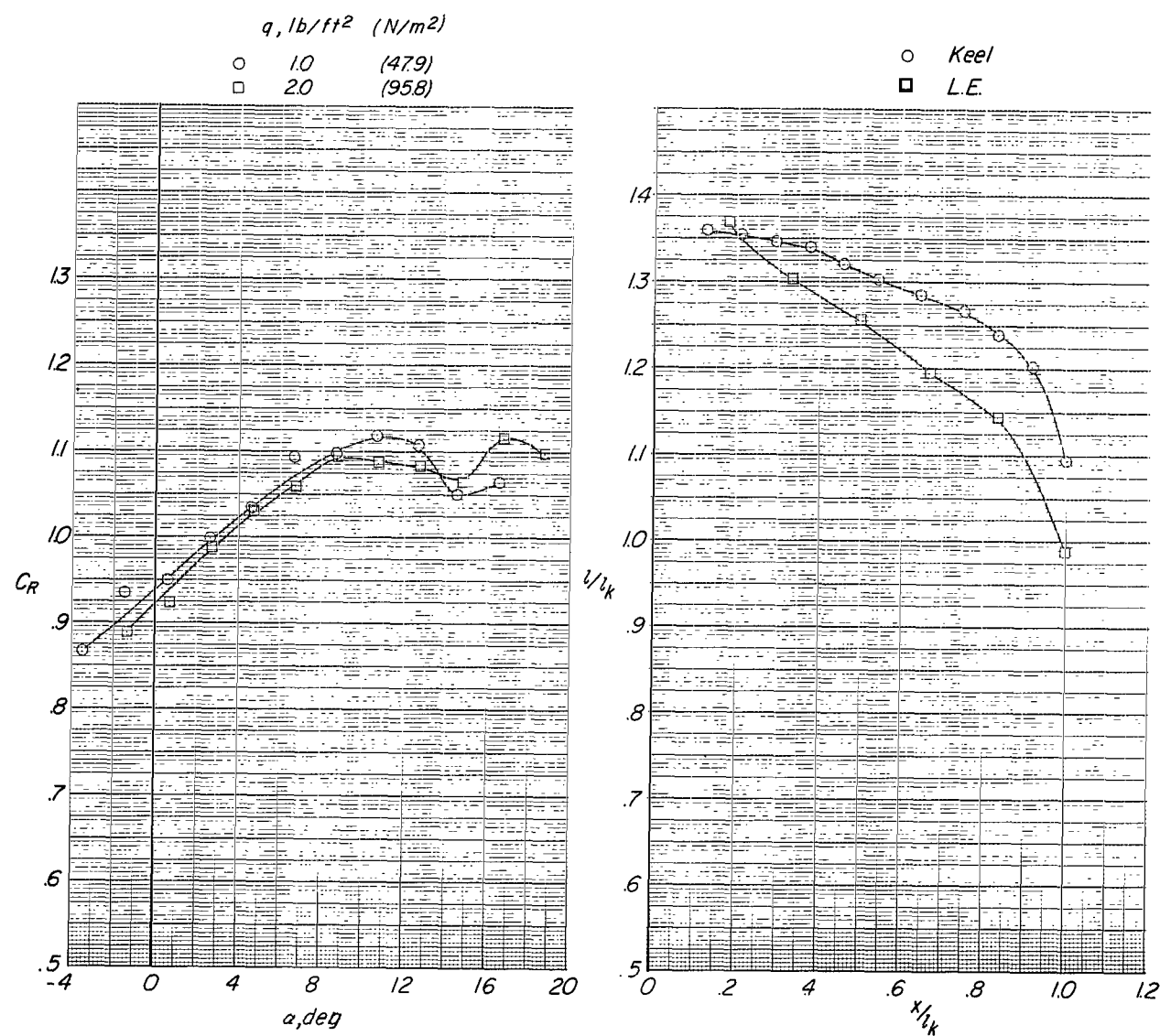


Figure 10.- Concluded.

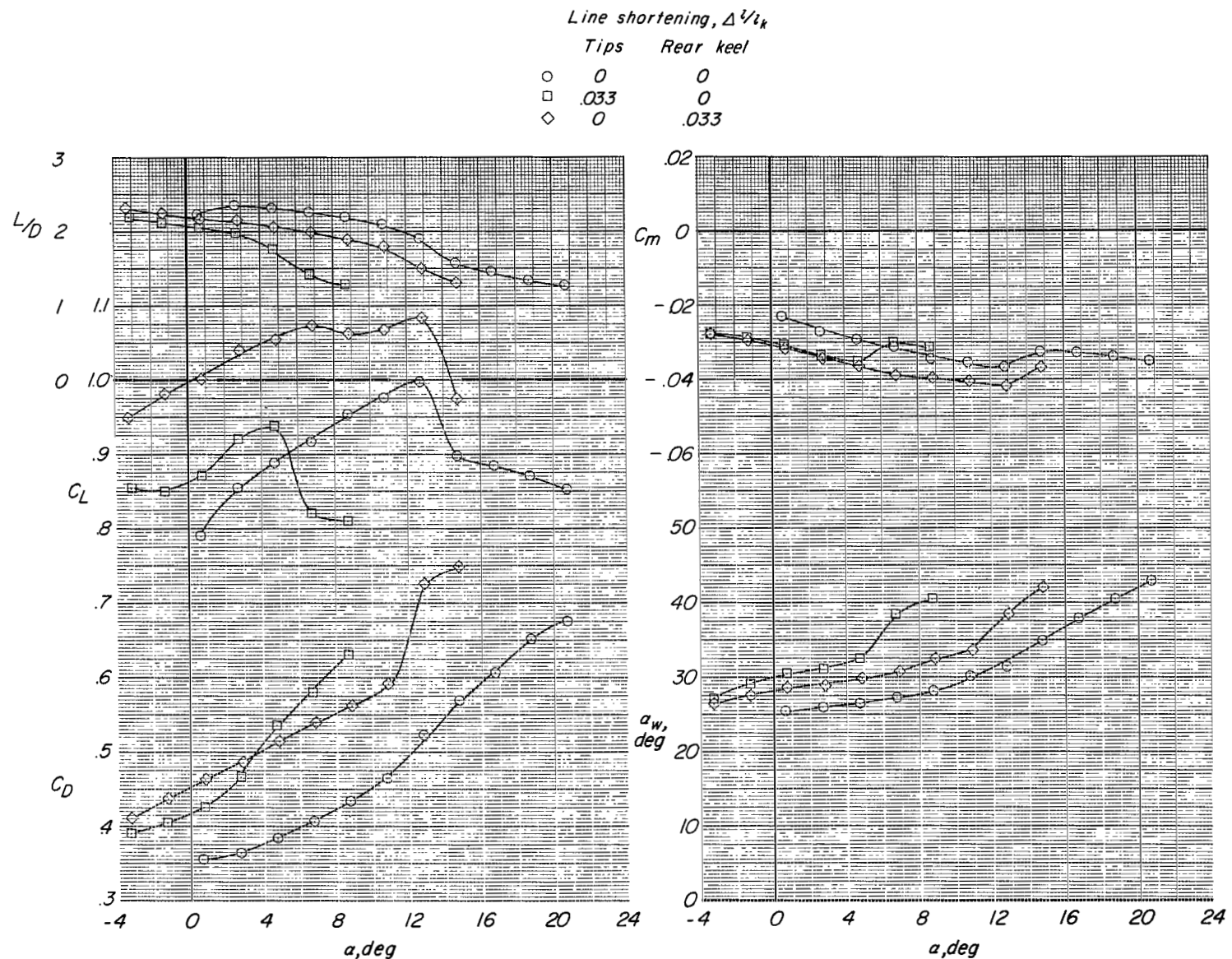


Figure 11.- Longitudinal aerodynamic characteristics of basic parawing with different modes of longitudinal control. 1.1 oz/yd<sup>2</sup> (37.3 g/m<sup>2</sup>) acrylic-coated nylon canopy; glued construction; nylon lines;  $q = 2.0 \text{ lb/ft}^2$  (95.8 N/m<sup>2</sup>).

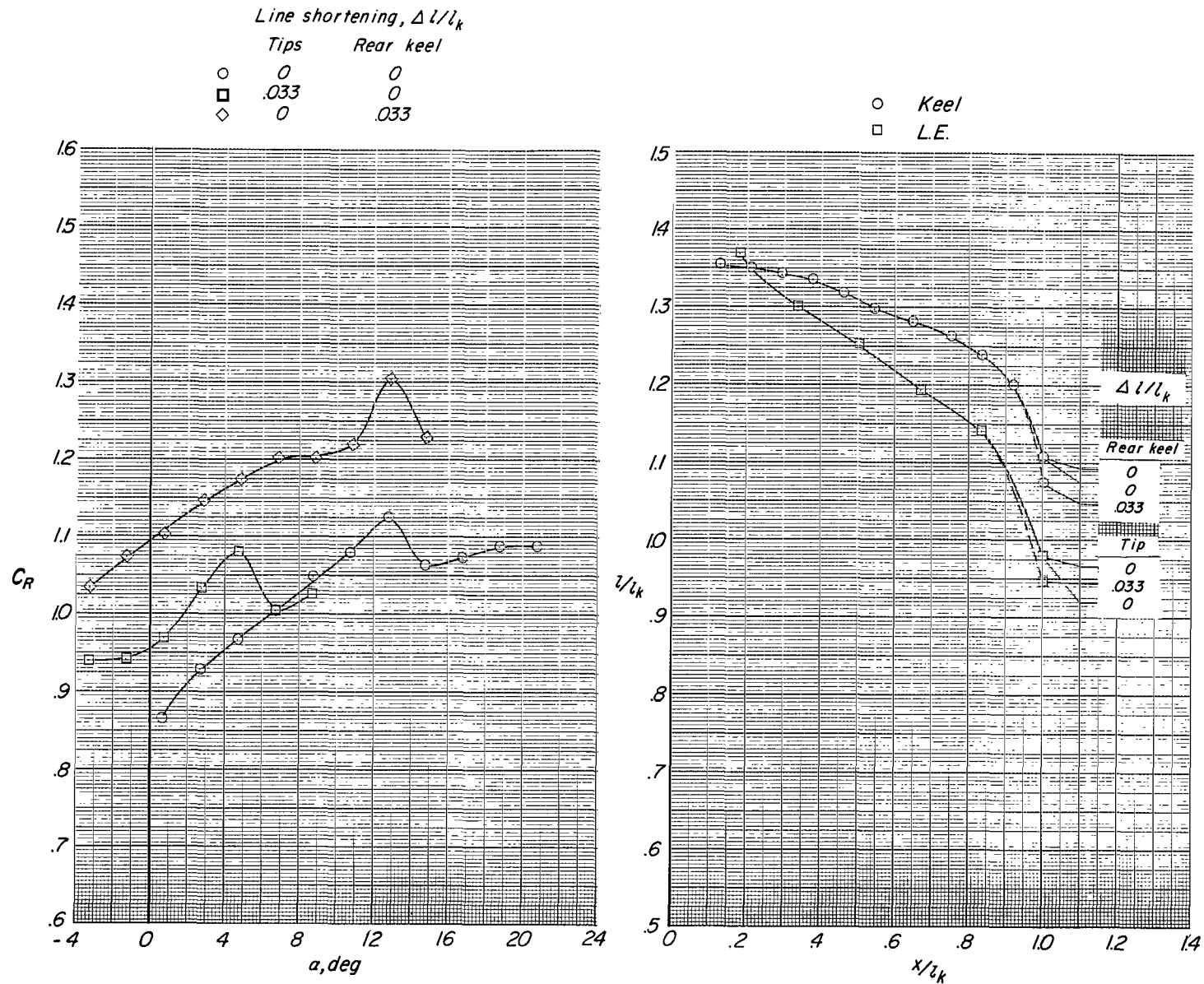


Figure 11.- Concluded.

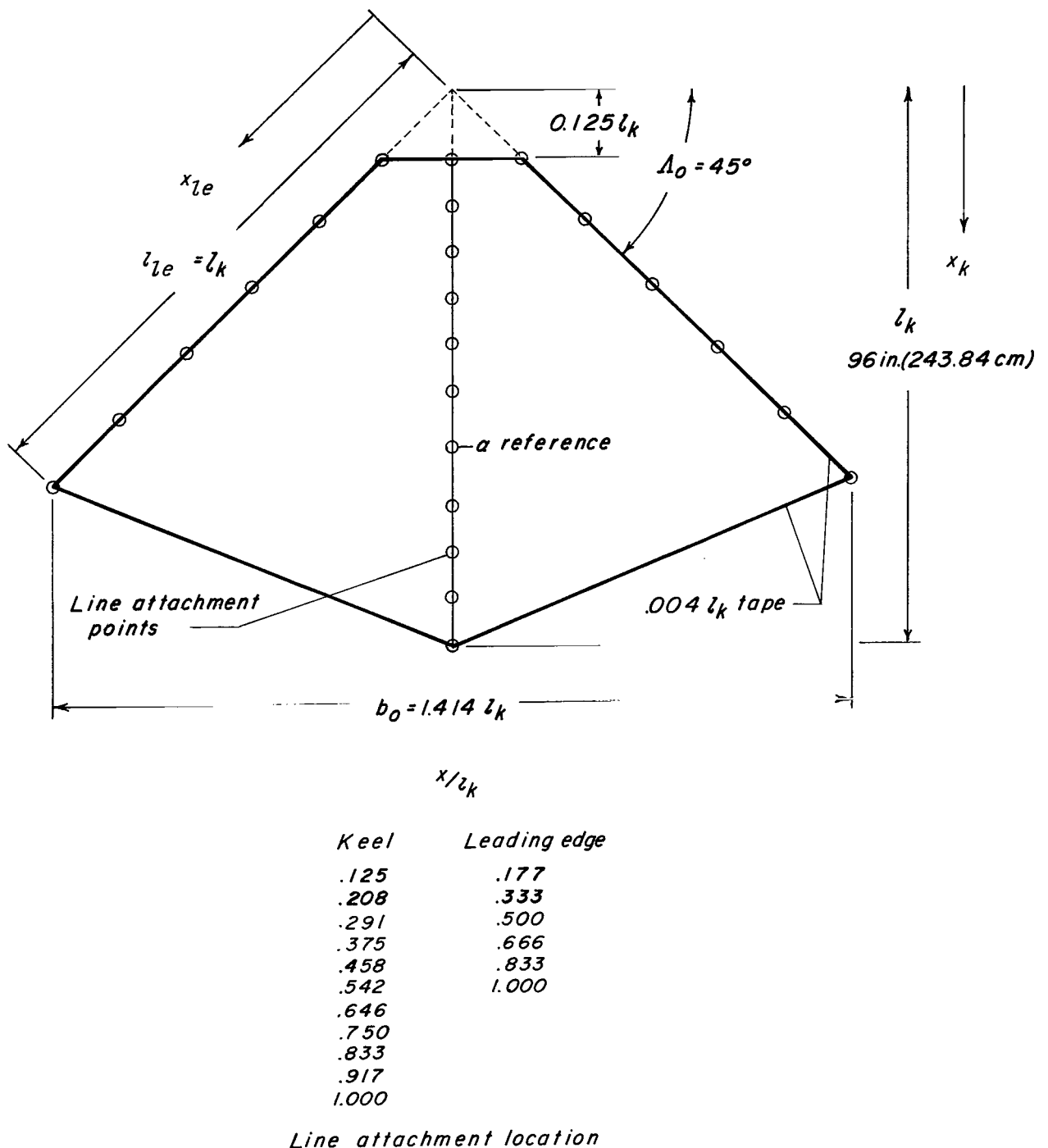


Figure 12.- Planform of basic 8-ft (2.438-m) parawing.

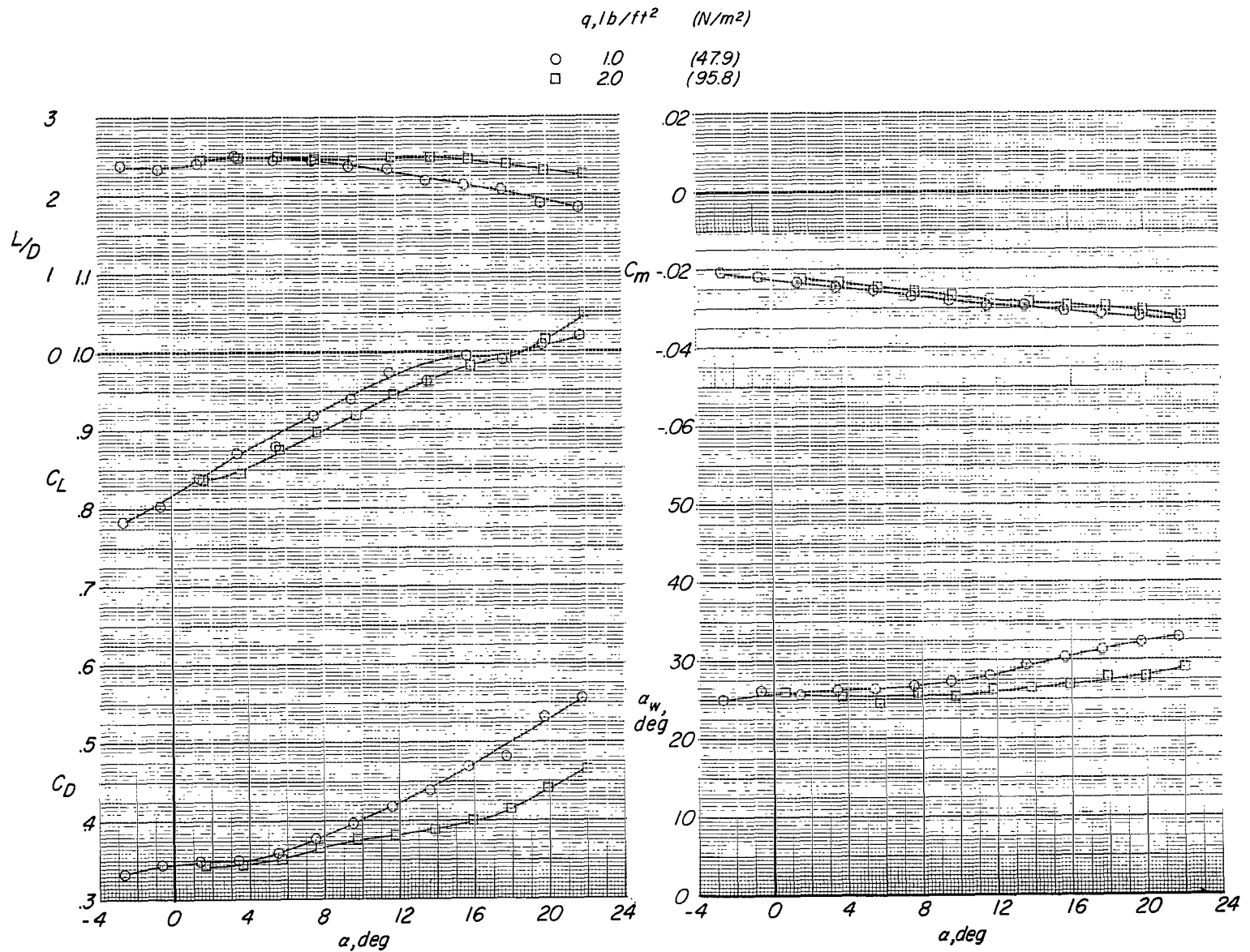


Figure 13.- Longitudinal aerodynamic characteristics of basic 8-ft (2.438-m) parawing with 1.1 oz/yd<sup>2</sup> (37.3 g/m<sup>2</sup>) acrylic-coated nylon canopy.  
Sewn construction; braided nylon lines.

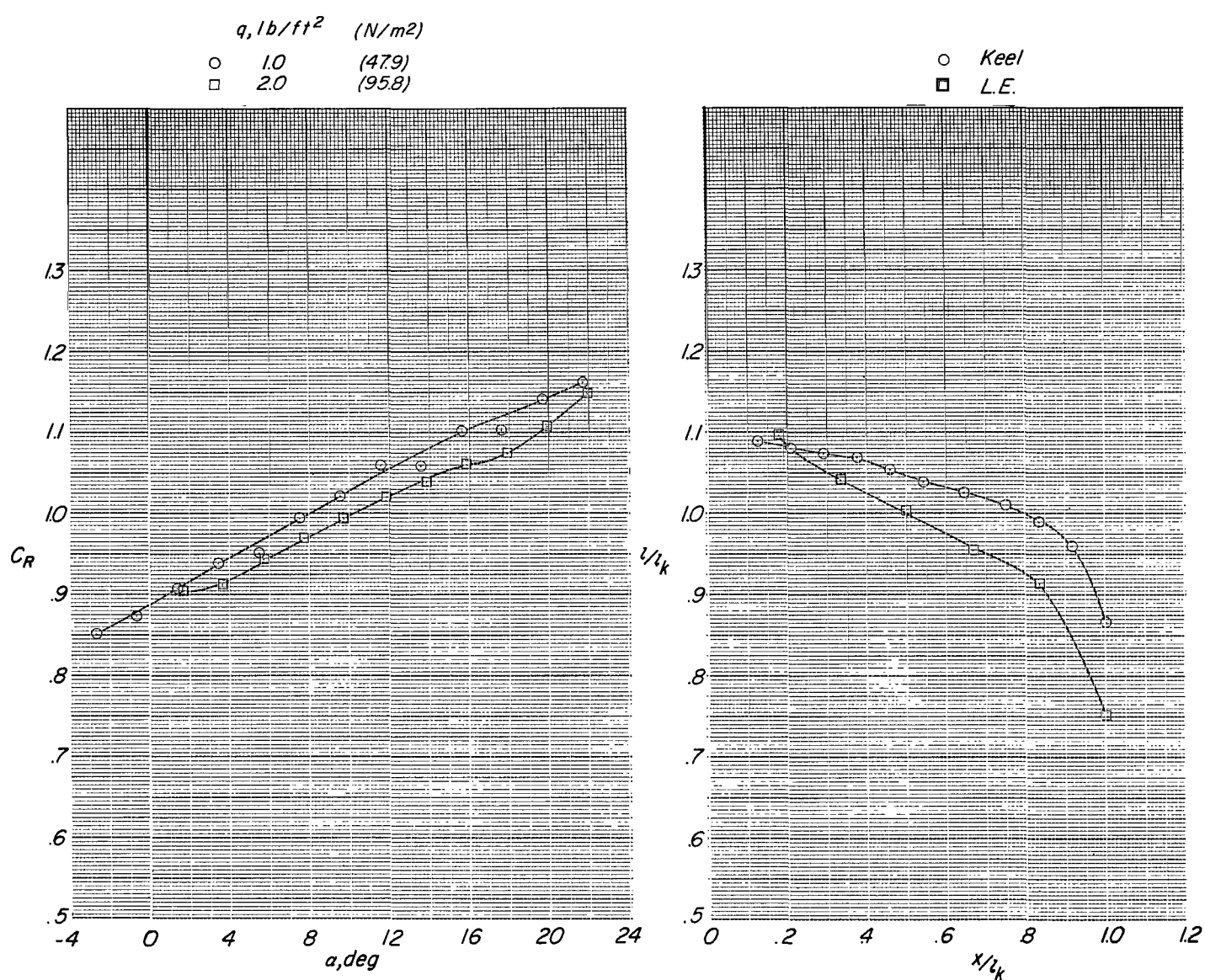
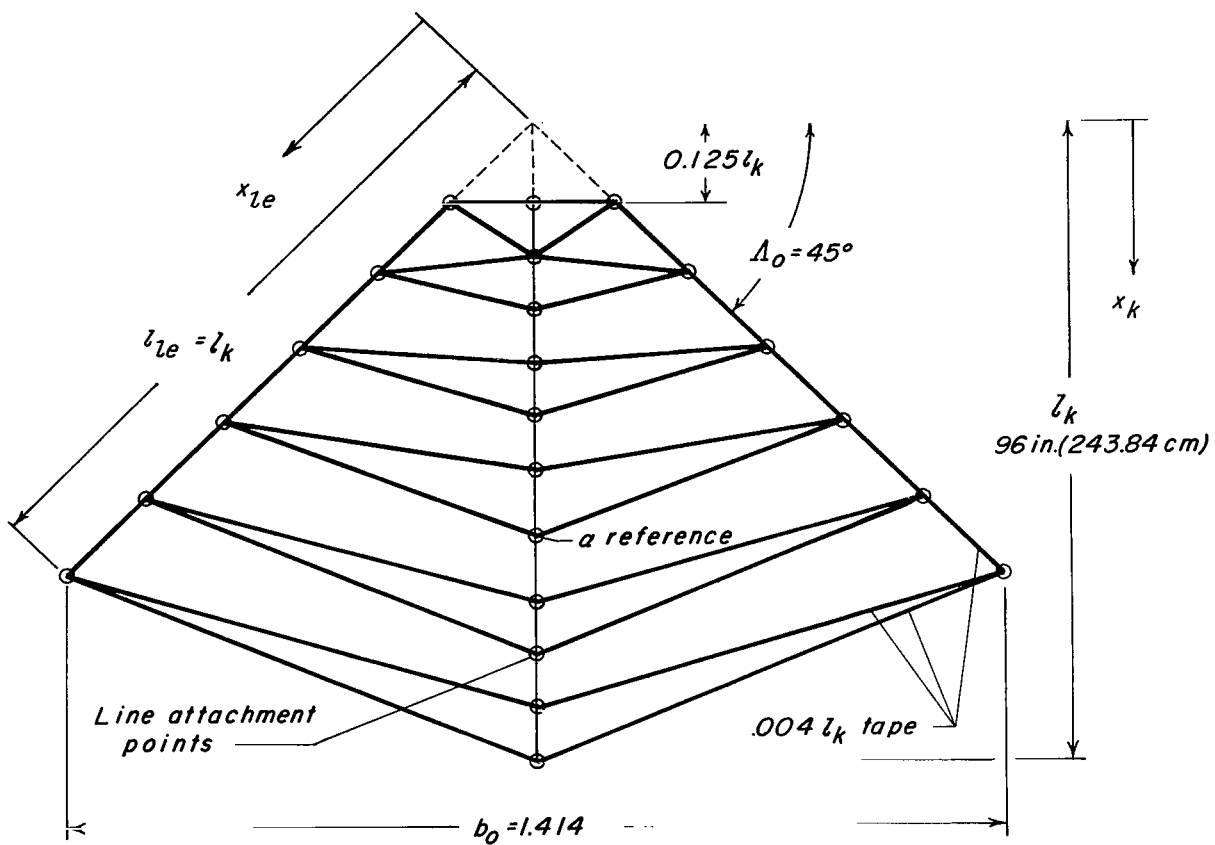


Figure 13.- Concluded,



$x/l_k$

*Keel              Leading edge*

.125	.177
.208	.333
.291	.500
.375	.666
.458	.833
.542	1.000
.646	
.750	
.833	
.917	
1.000	

*Line attachment location*

Figure 14.- Planform of parawing with tape reinforcement.

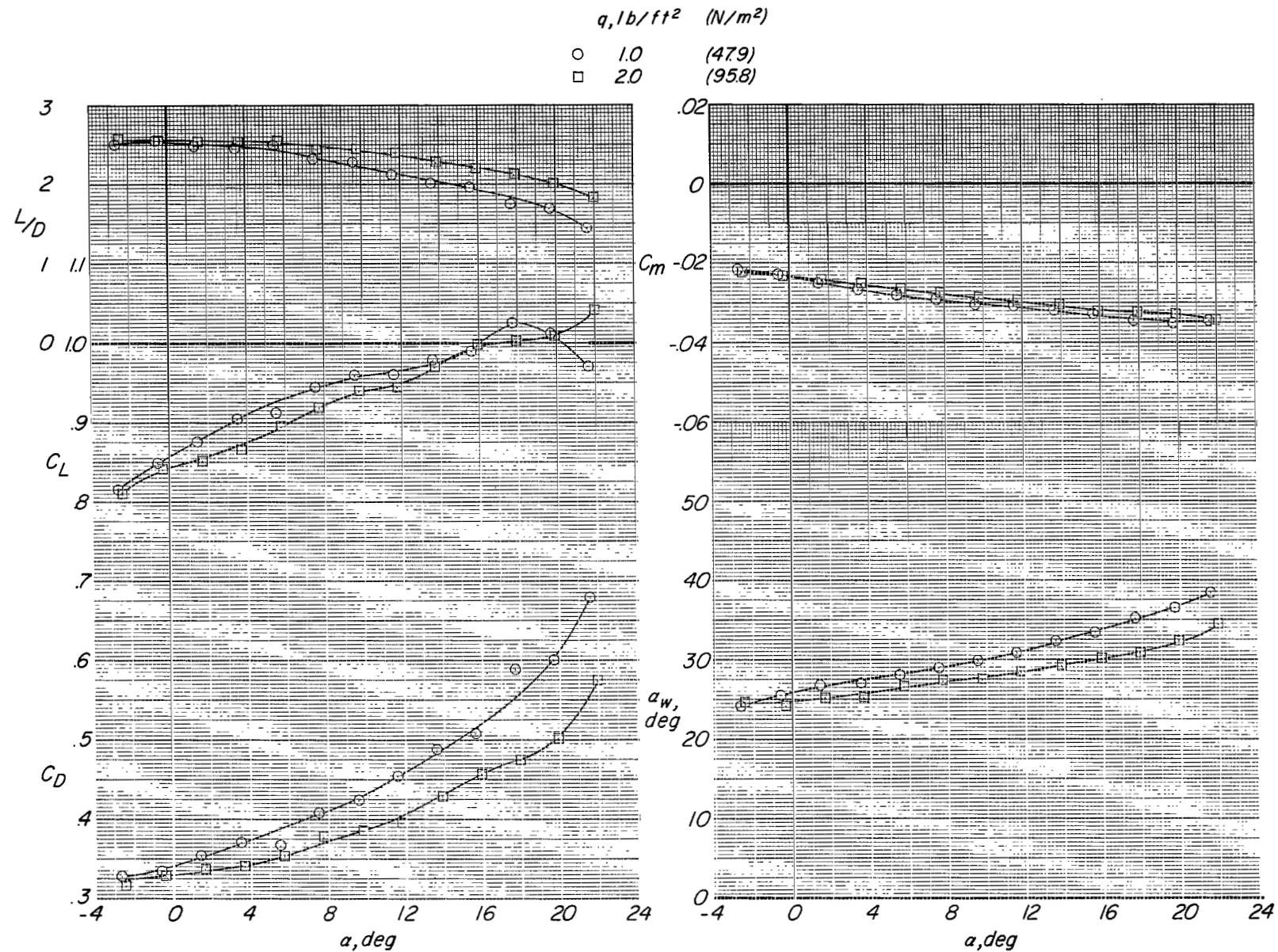


Figure 15.- Longitudinal aerodynamic characteristics of parawing with tape reinforcement  $l_k = 8 \text{ ft}$  (2.438 m).

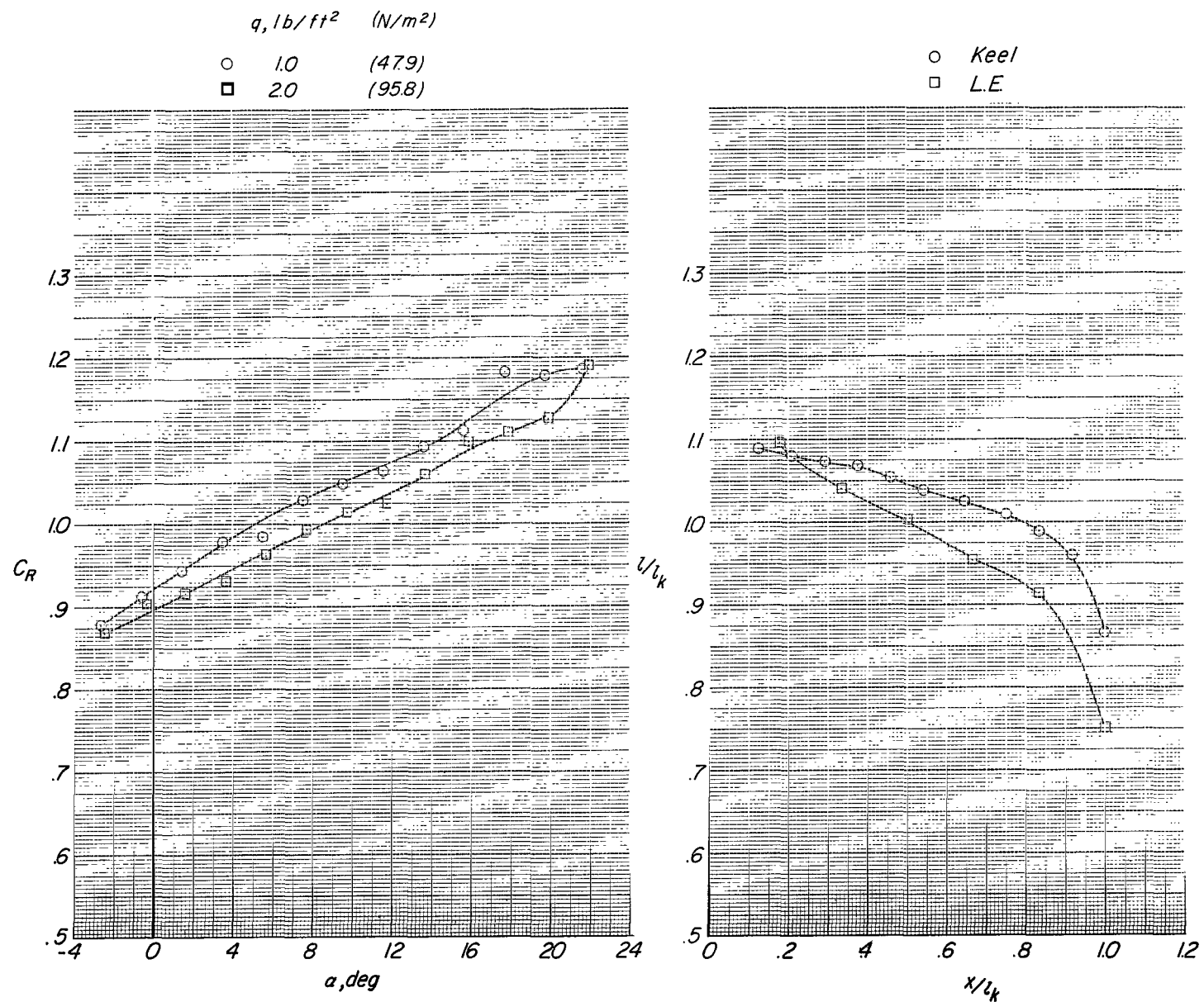


Figure 15.- Concluded.

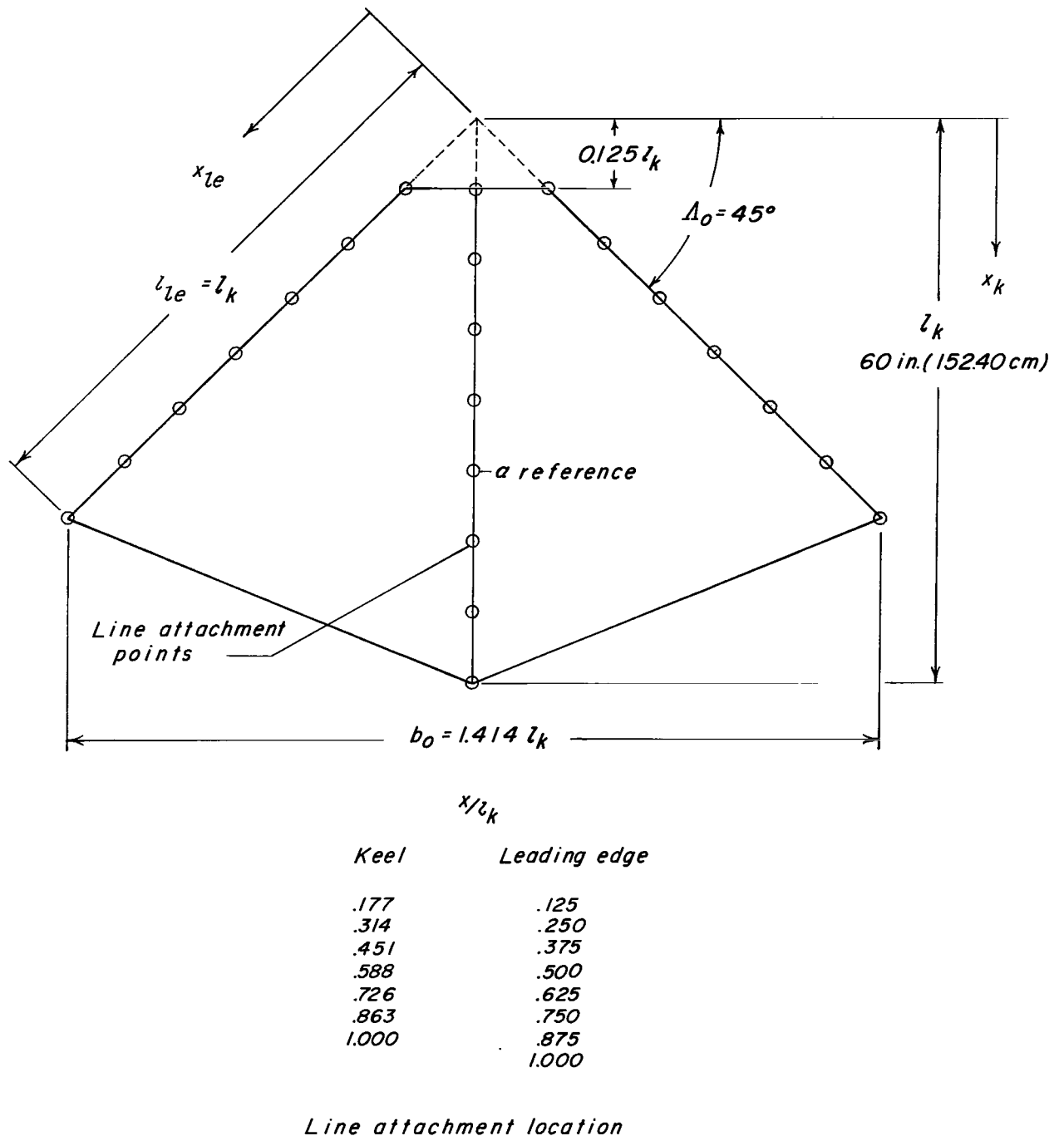


Figure 16.- Planform of parawing with revised line attachment locations (eight keel and seven leading-edge lines).

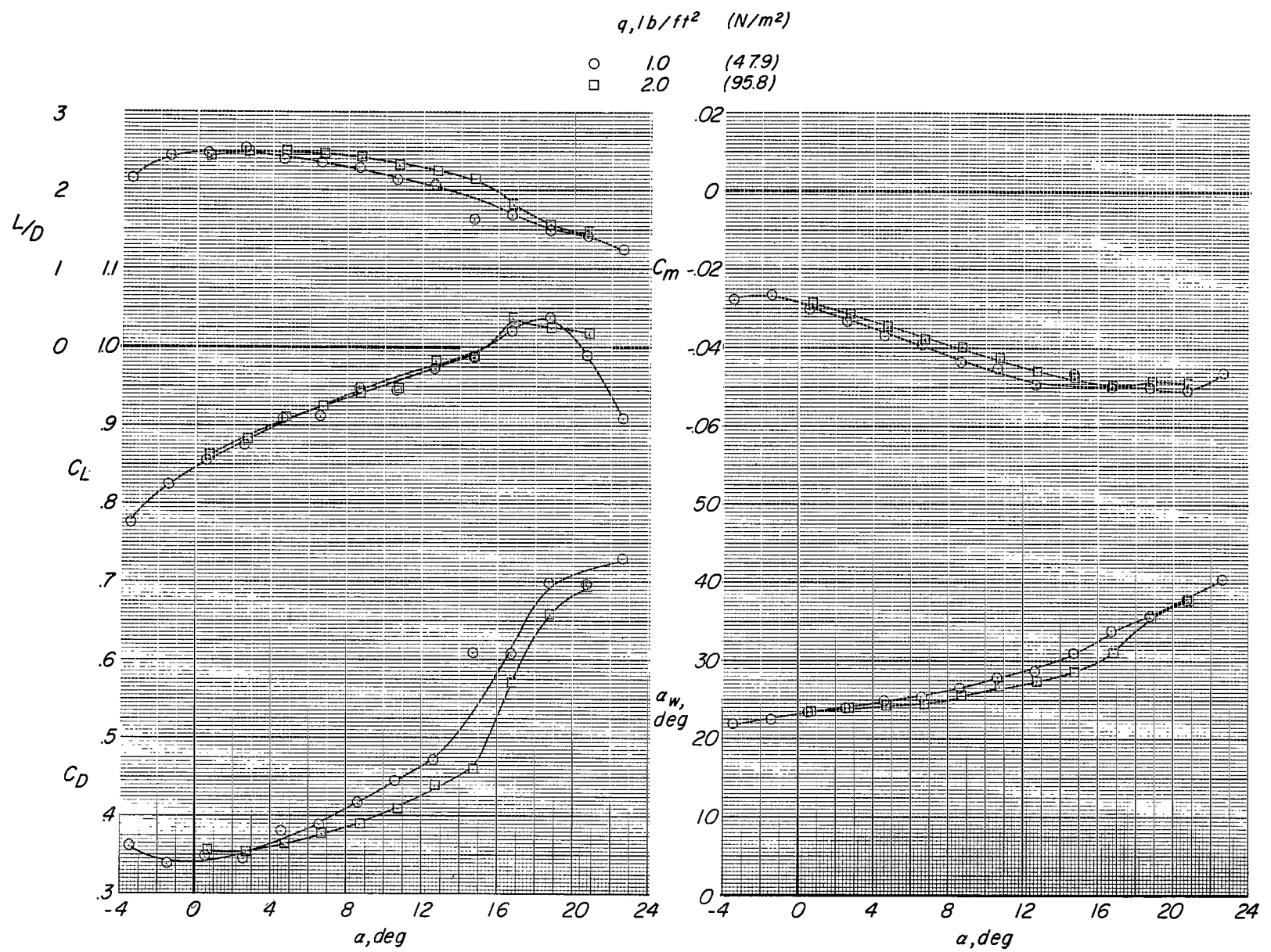


Figure 17.- Longitudinal aerodynamic characteristics of parawing with revised line attachment locations.

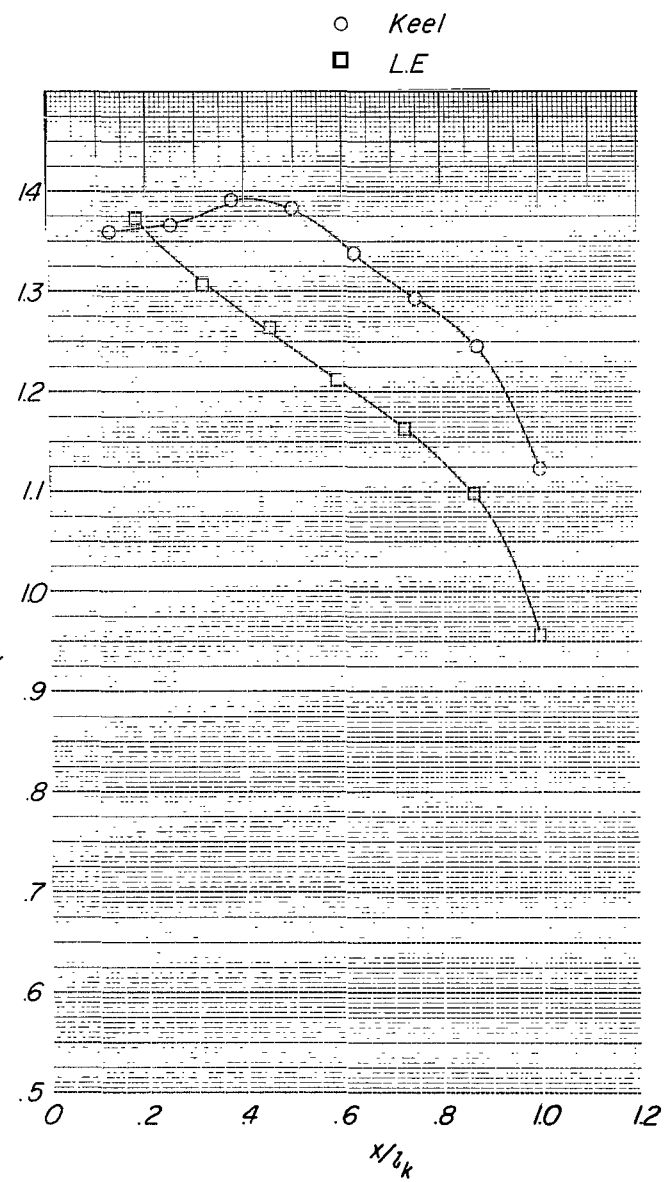
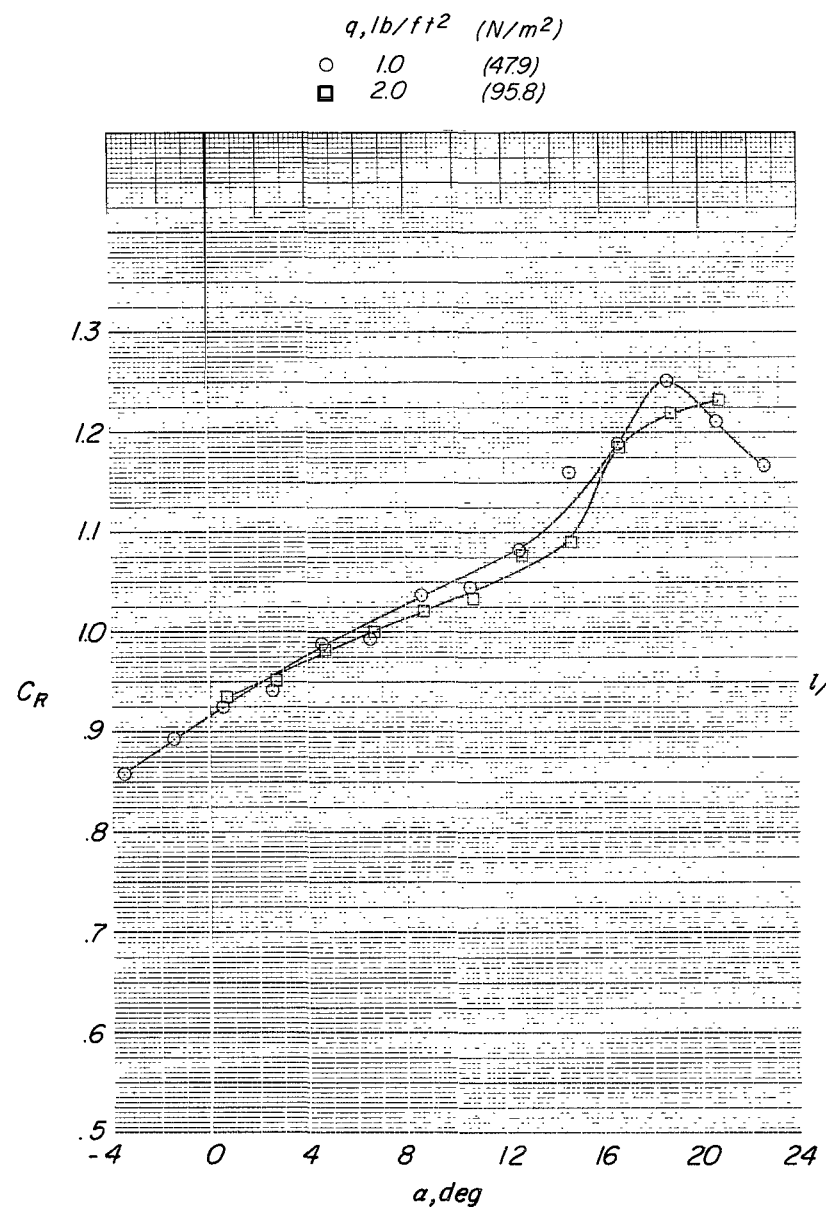
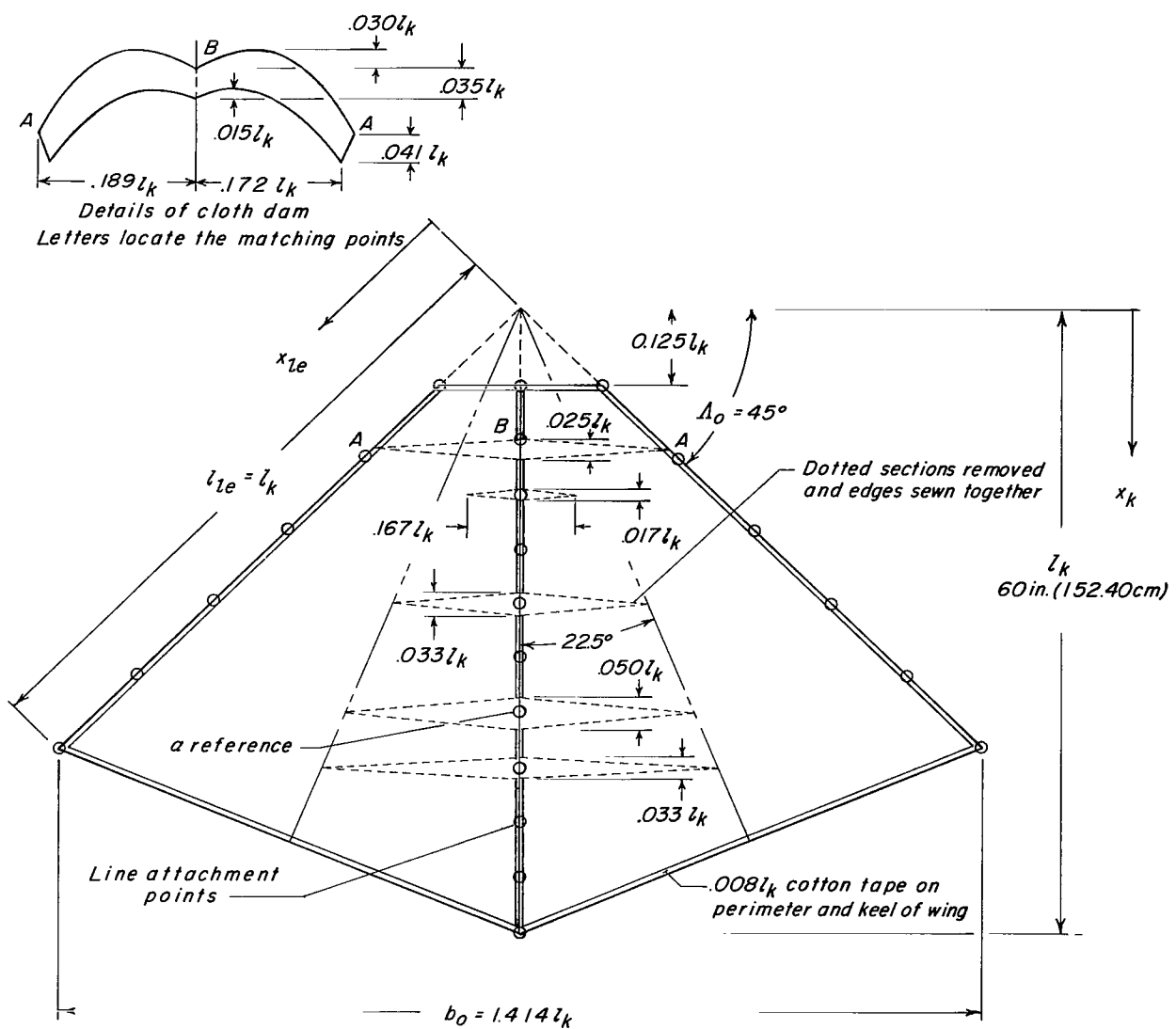


Figure 17.- Concluded.



$x/l_k$

Keel	Leading edge
.125	.177
.208	.333
.292	.500
.375	.667
.459	.833
.542	1.000
.645	
.750	
.833	
.917	
1.000	

Line attachment location

Figure 18.- Planform of parawing with cambered keel.

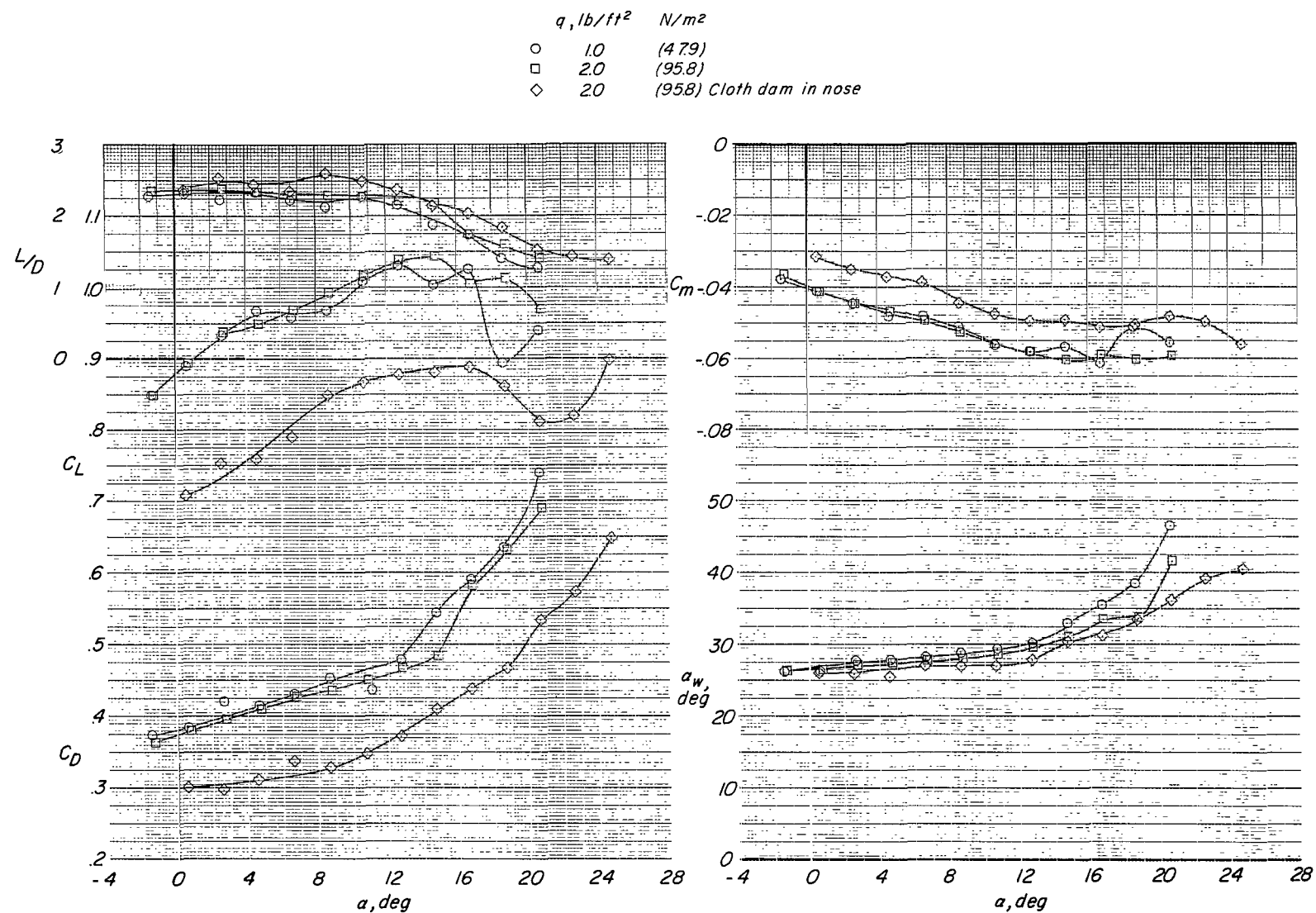


Figure 19.- Longitudinal aerodynamic characteristics of parawing with cambered keel.

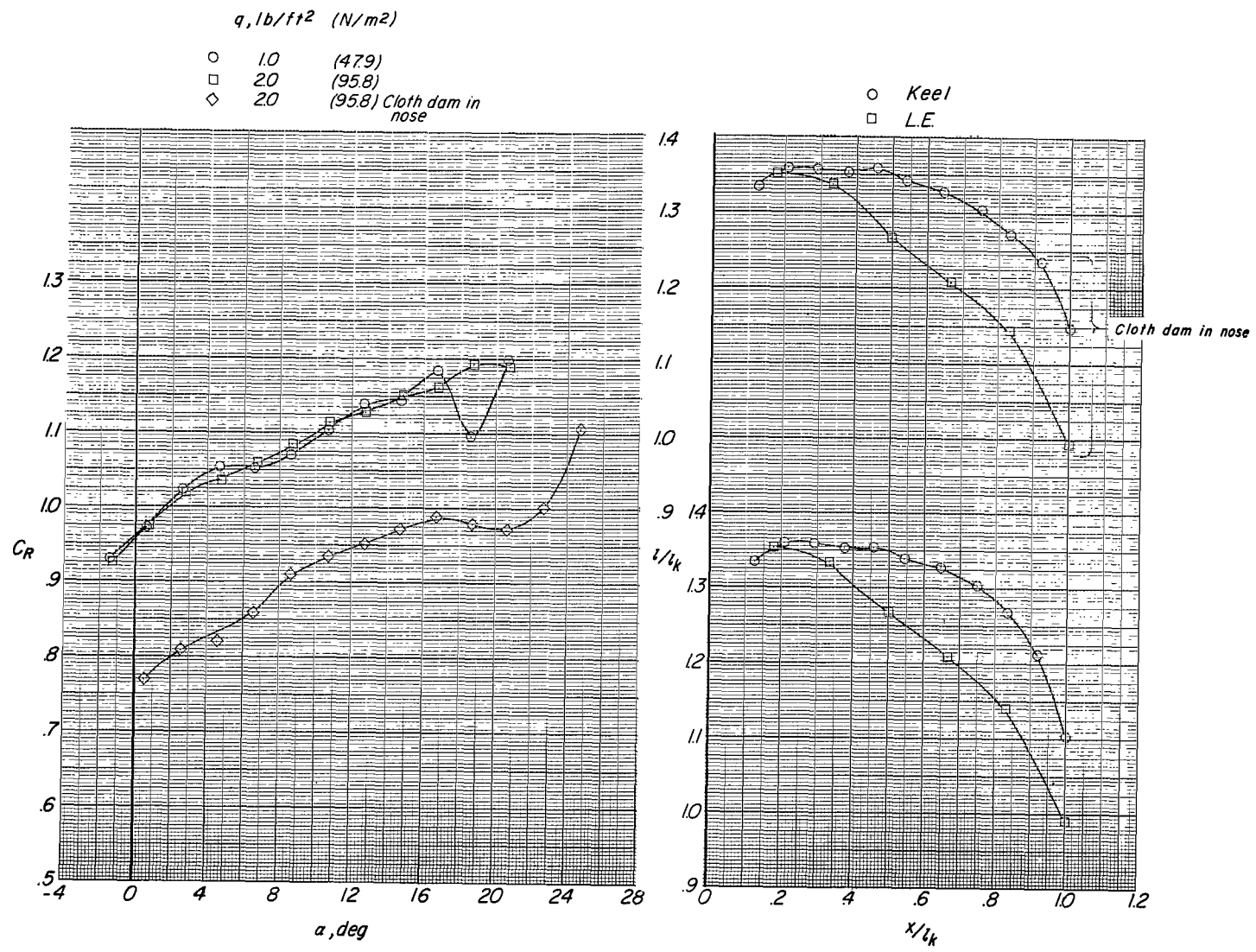
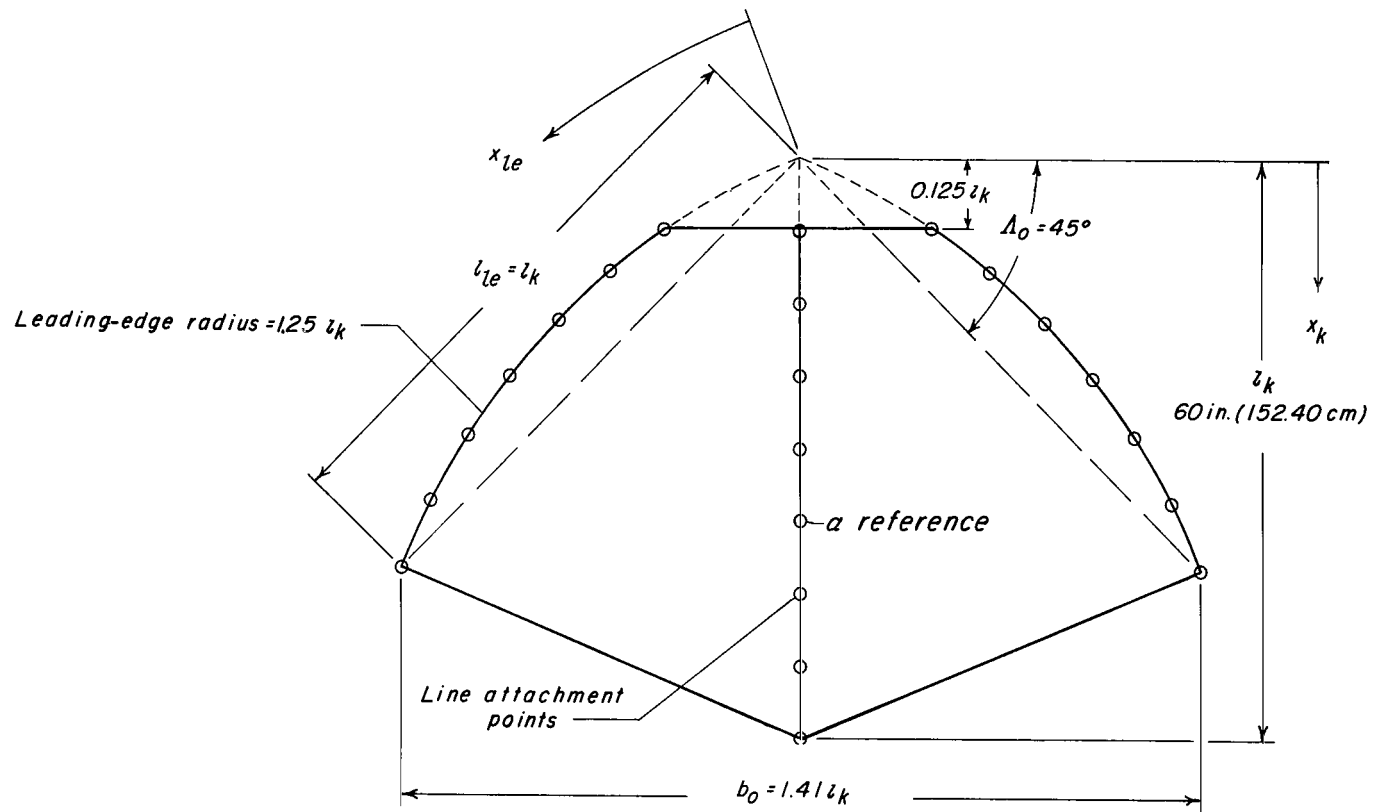


Figure 19.- Concluded.



Kee $\ell$	Leadi $ng$ edge $\ell$
.125	.259
.250	.389
.375	.518
.500	.647
.625	.776
.750	.905
.875	1.034
1.000	

Line attachment location

Figure 20.- Planform of parawing with curved leading edges.

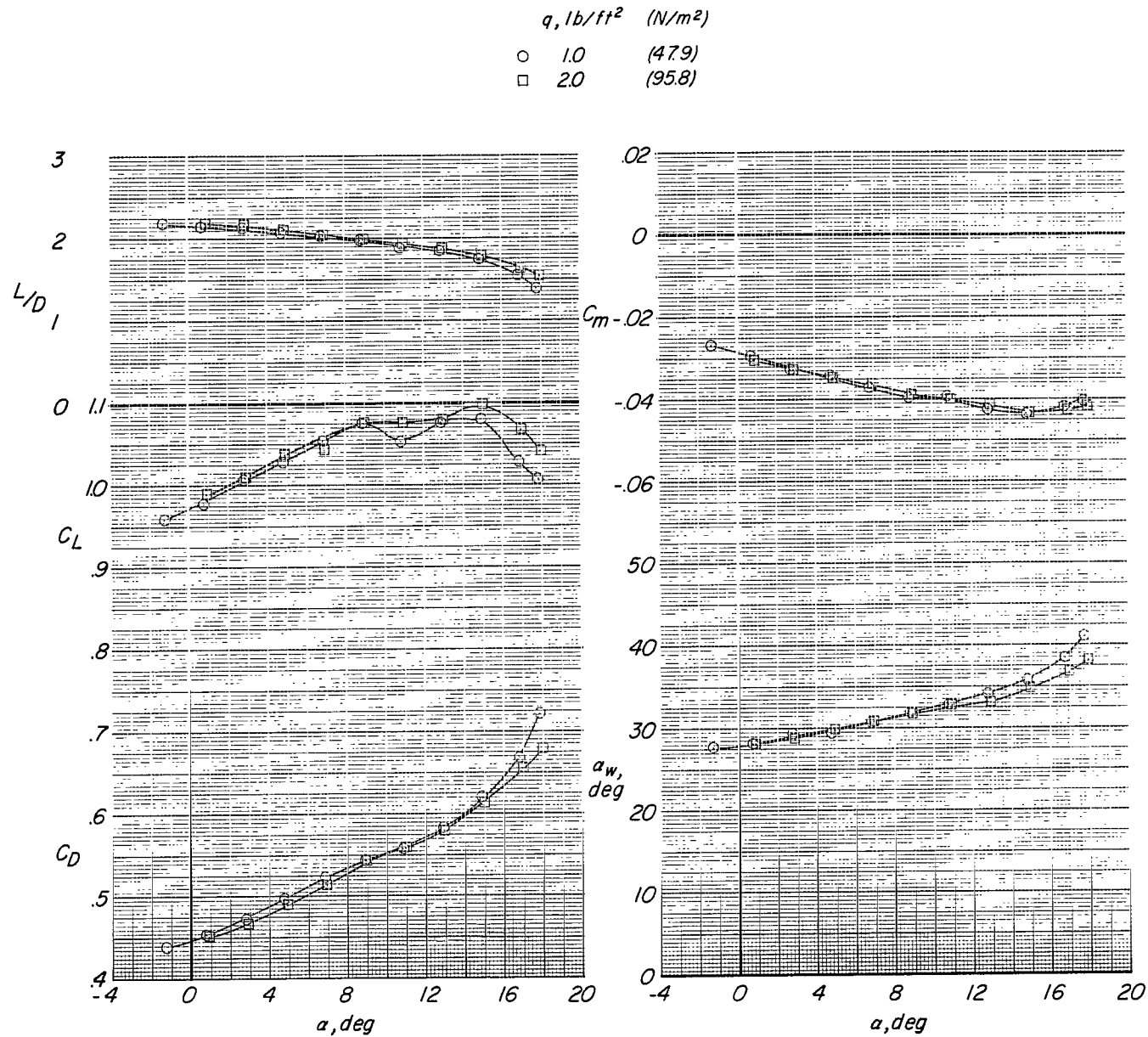


Figure 21.- Longitudinal aerodynamic characteristics of parawing with a curved-leading-edge planform.

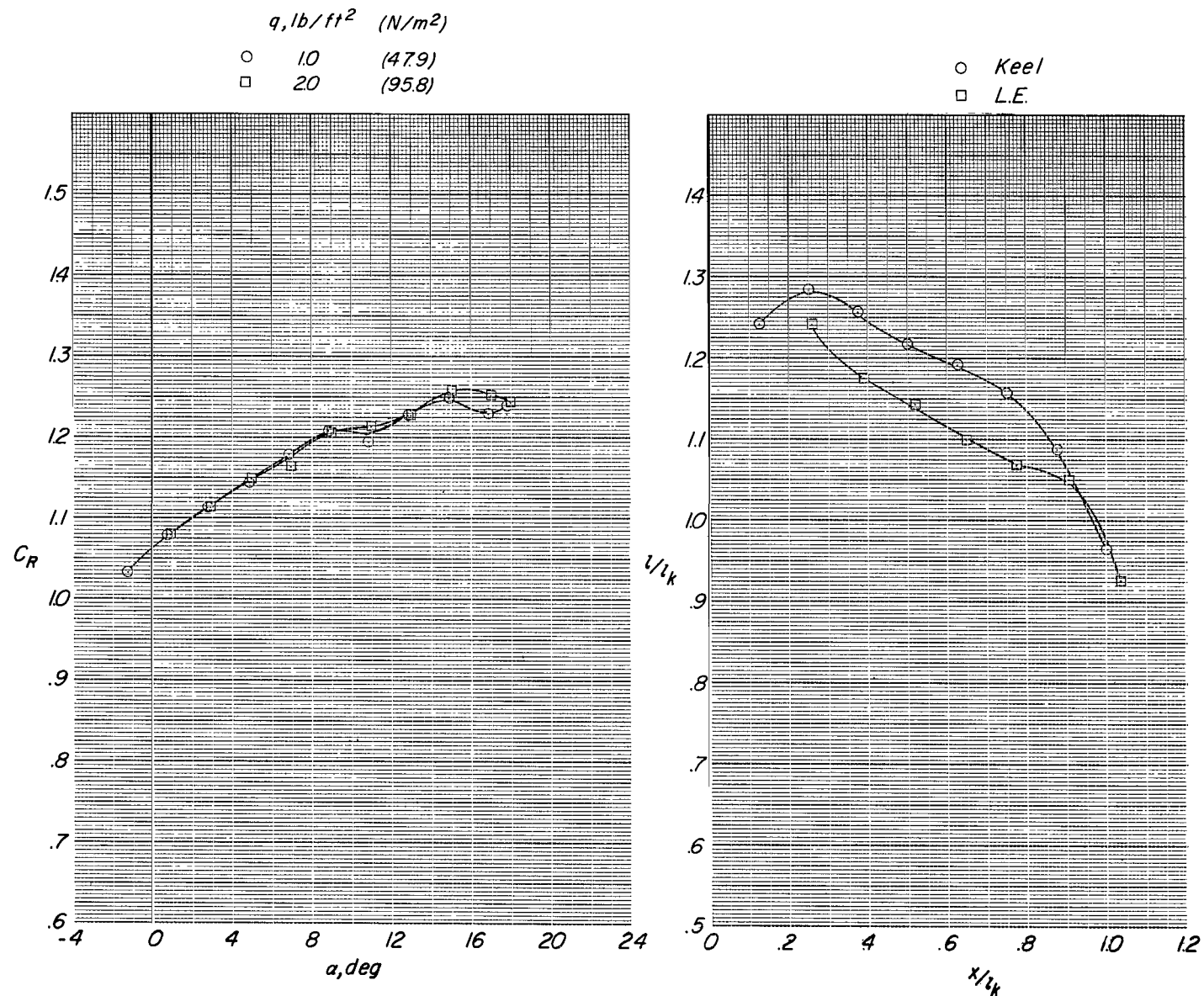
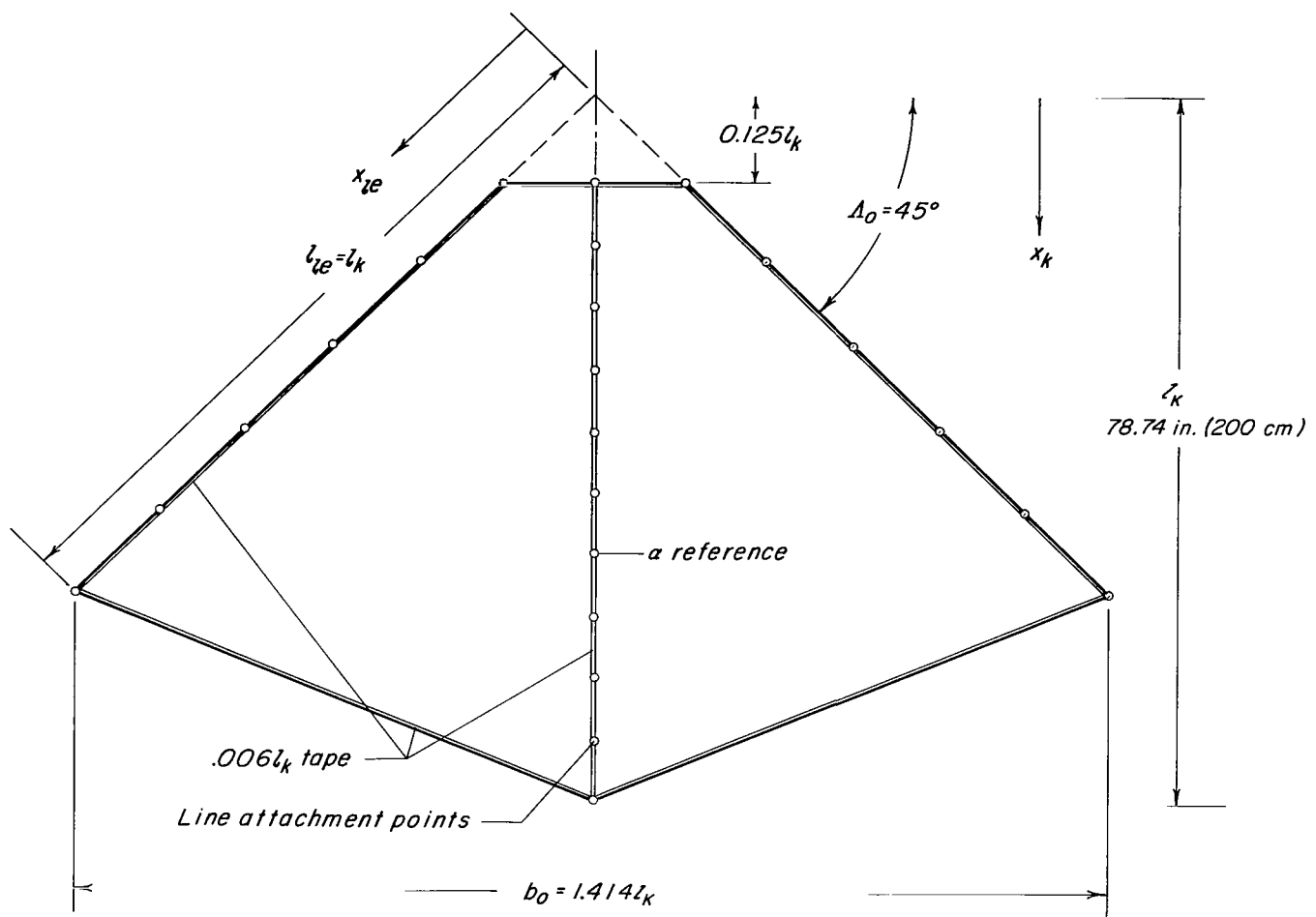


Figure 21.- Concluded.



$x/l_k$

Keel	Leading edge
.125	.177
.213	.342
.300	.507
.388	.672
.475	.837
.563	1.000
.650	
.738	
.825	
.913	
1.000	

Line attachment locations

Figure 22.- Planform of basic 2-meter parawing.

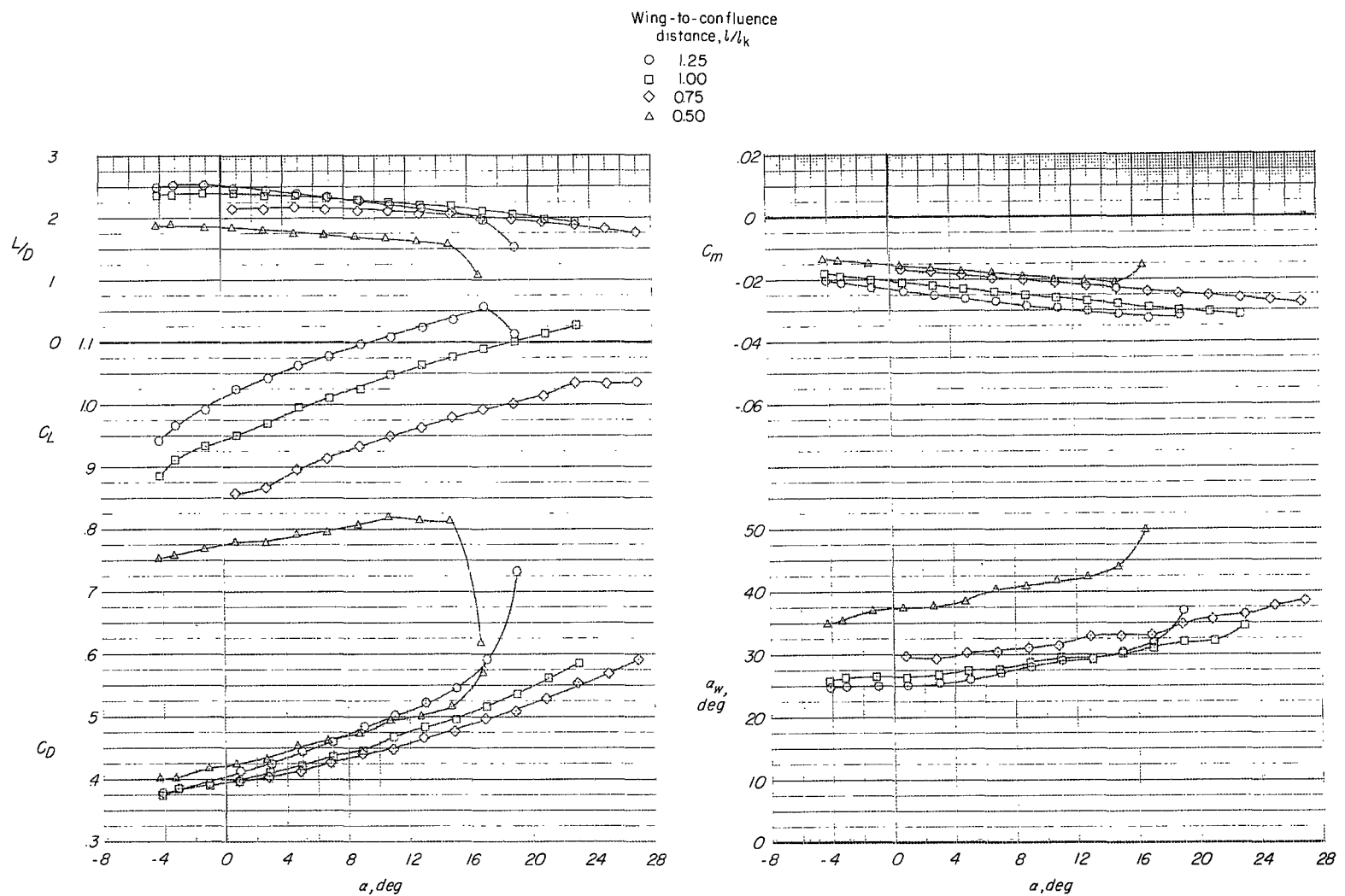


Figure 23.- Effects of decreasing wing-to-confluence distance on longitudinal aerodynamic characteristics of a basic parawing.

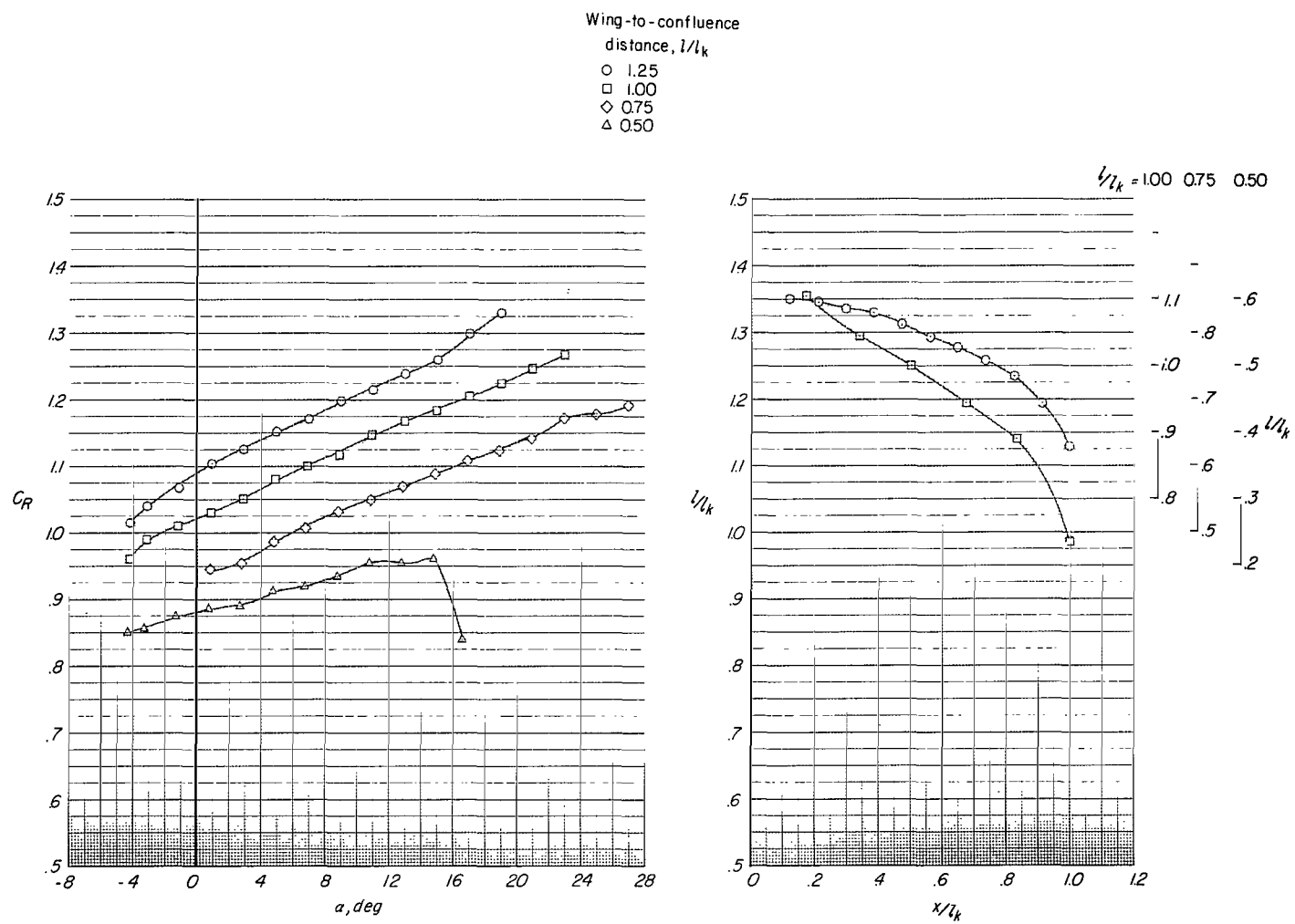


Figure 23.- Concluded.

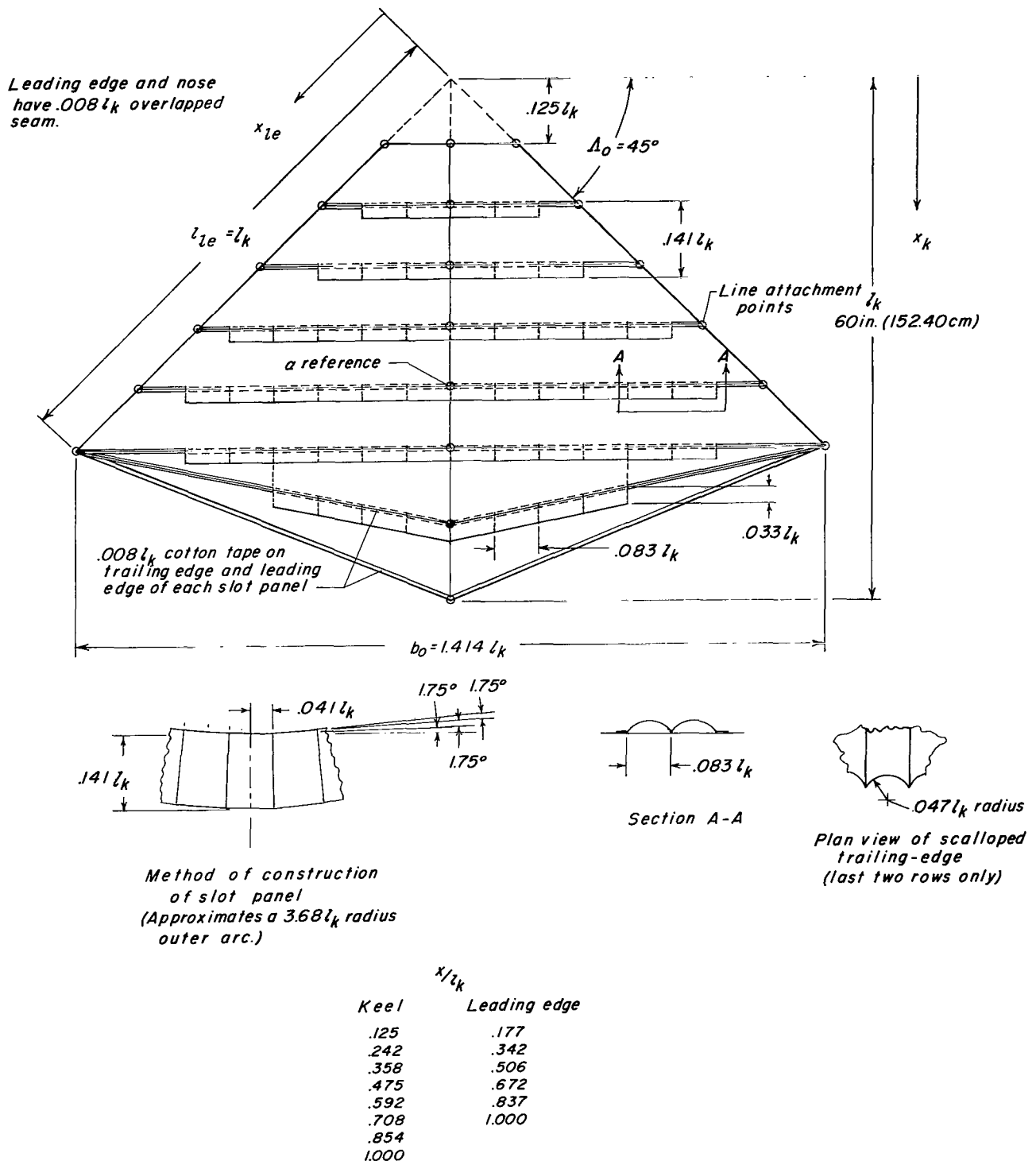


Figure 24.- Planform of parawing with multiple slots.

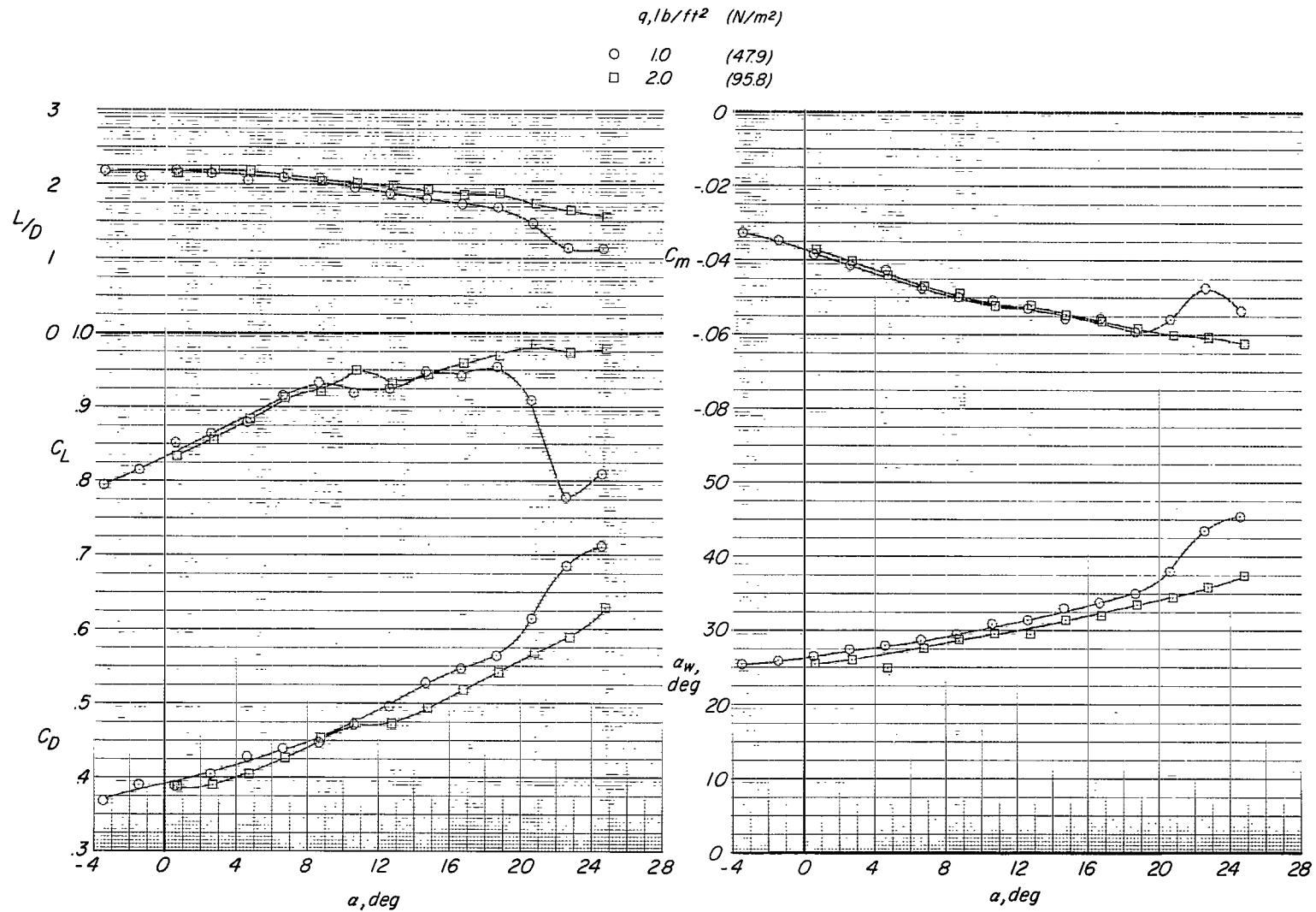


Figure 25.- Longitudinal aerodynamic characteristics of parawing with multiple slots and straight trailing edges on the slots.

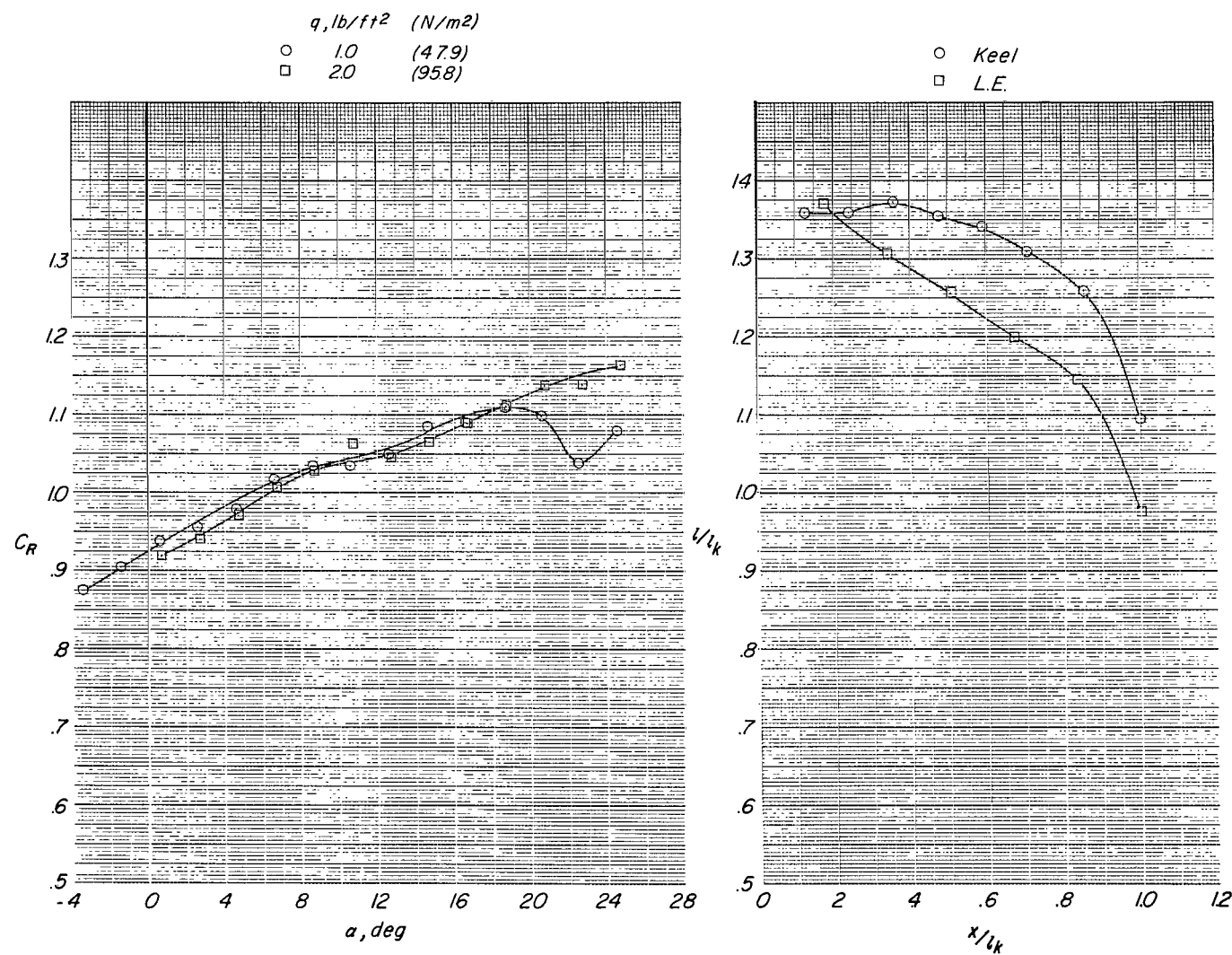


Figure 25.- Concluded.

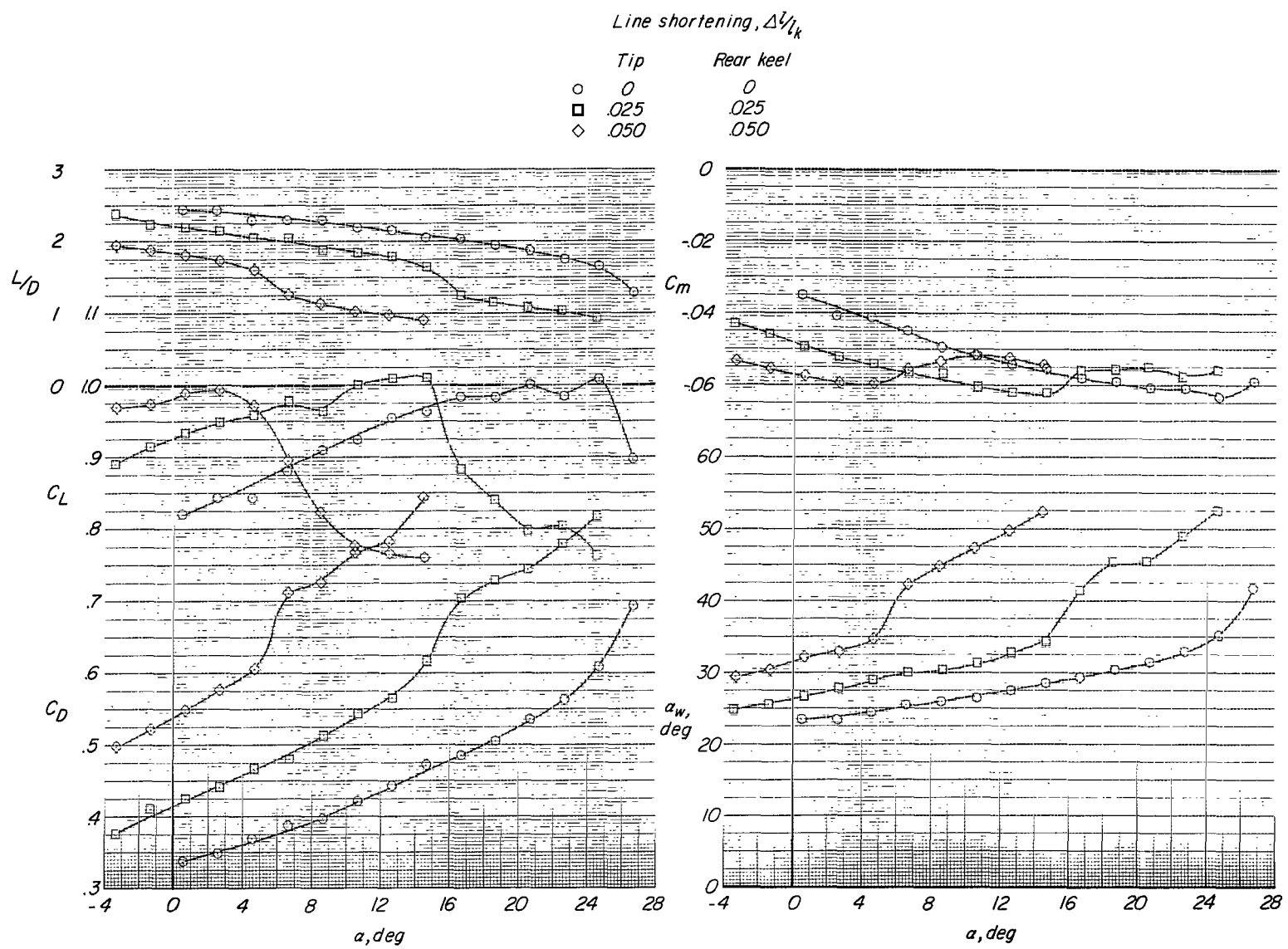


Figure 26.- Longitudinal aerodynamic characteristics of parawing with multiple slots and scalloped trailing edges on the rear slots.  $q = 1.5 \text{ lb/ft}^2$  ( $71.8 \text{ N/m}^2$ ).

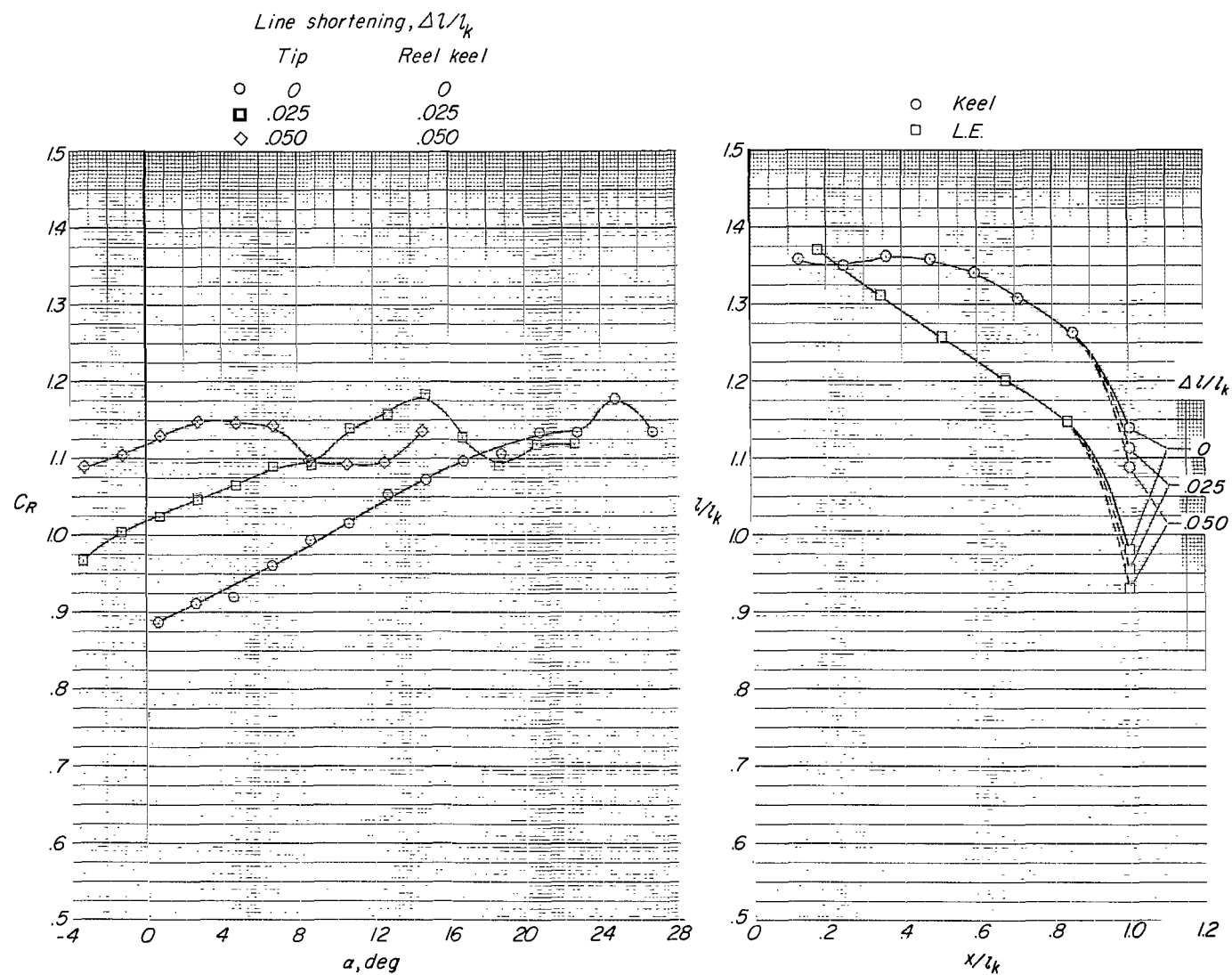
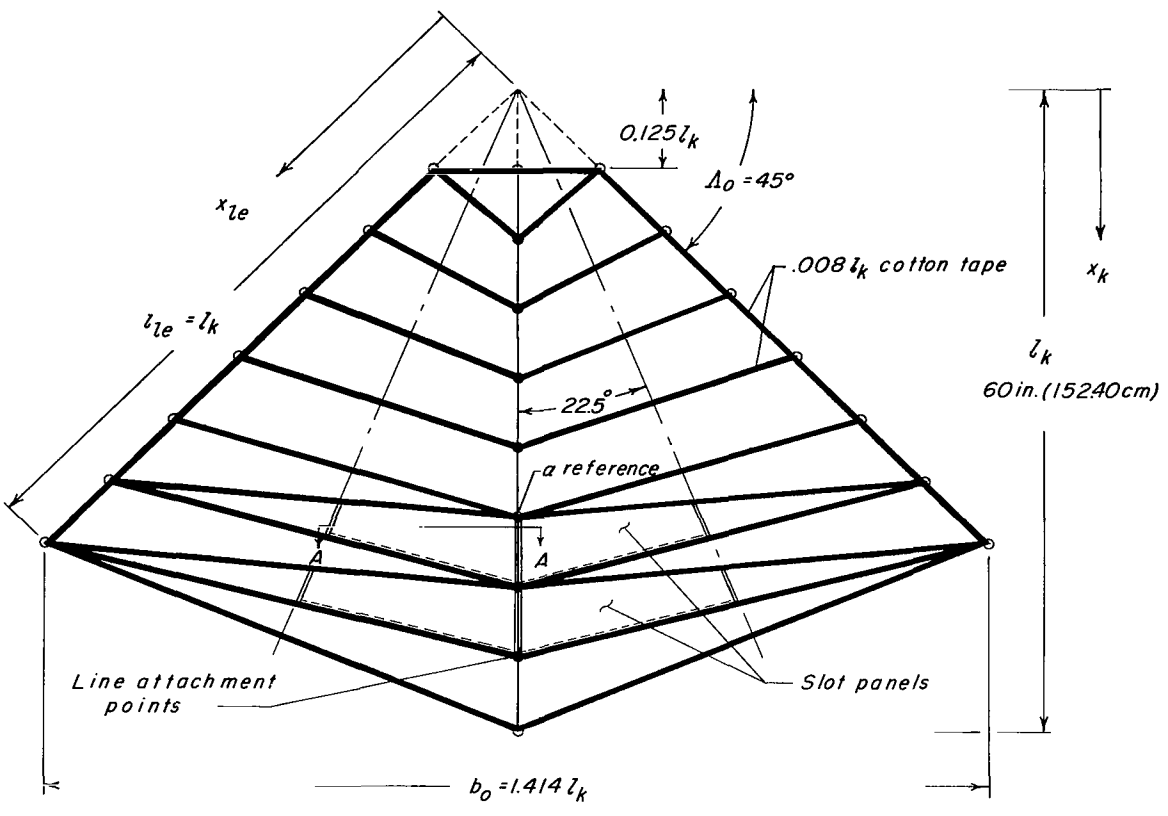


Figure 26.- Concluded.



Typical slot panel, note excess of 5° at each end to give fullness.

$x/l_k$	Keel	Leading edge
.125		.177
.233		.314
.342		.452
.450		.588
.558		.726
.667		.863
.775		1.000
.883		
1.000		

#### Line attachment location

Figure 27.- Planform of parawing with two rows of single slots.

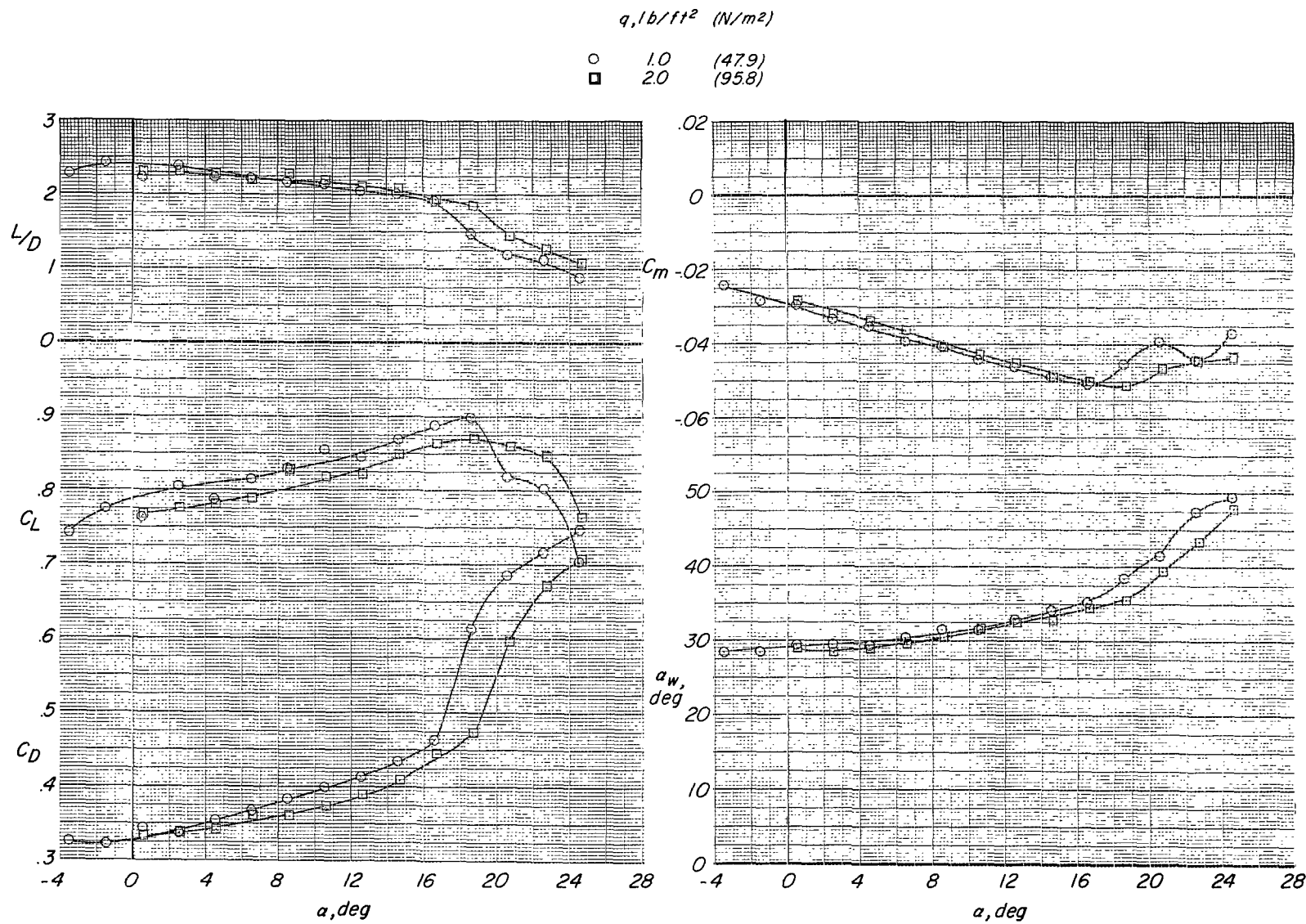


Figure 28.- Longitudinal aerodynamic characteristics of the parawing with two rows of single slots.

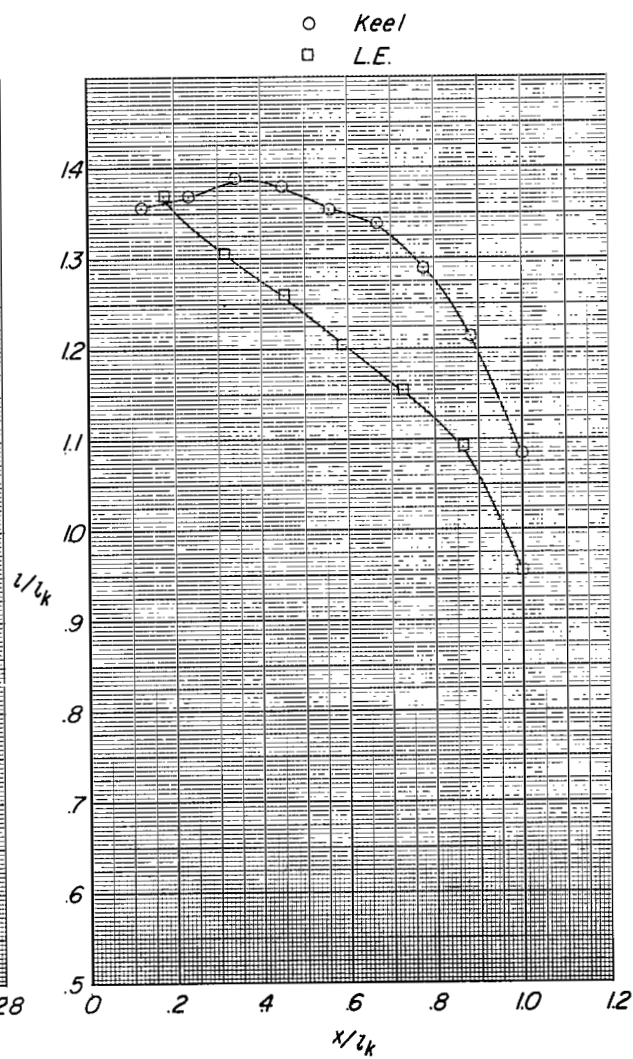
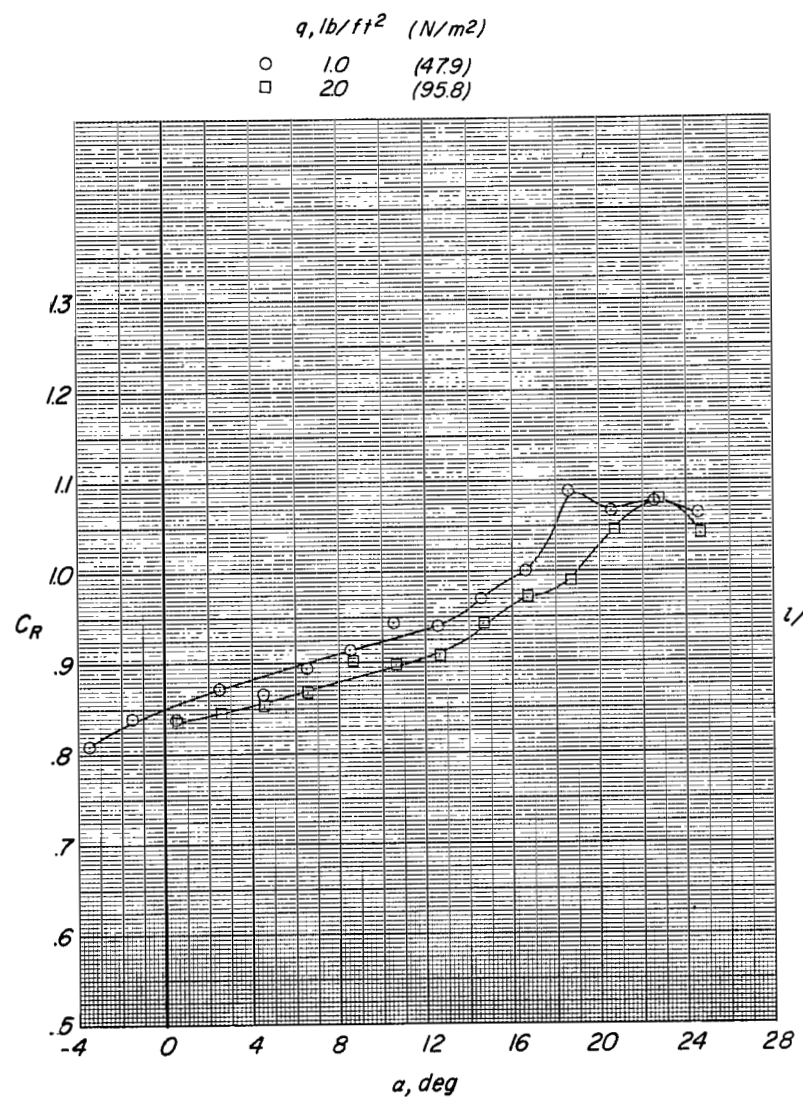
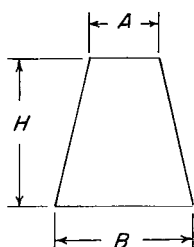
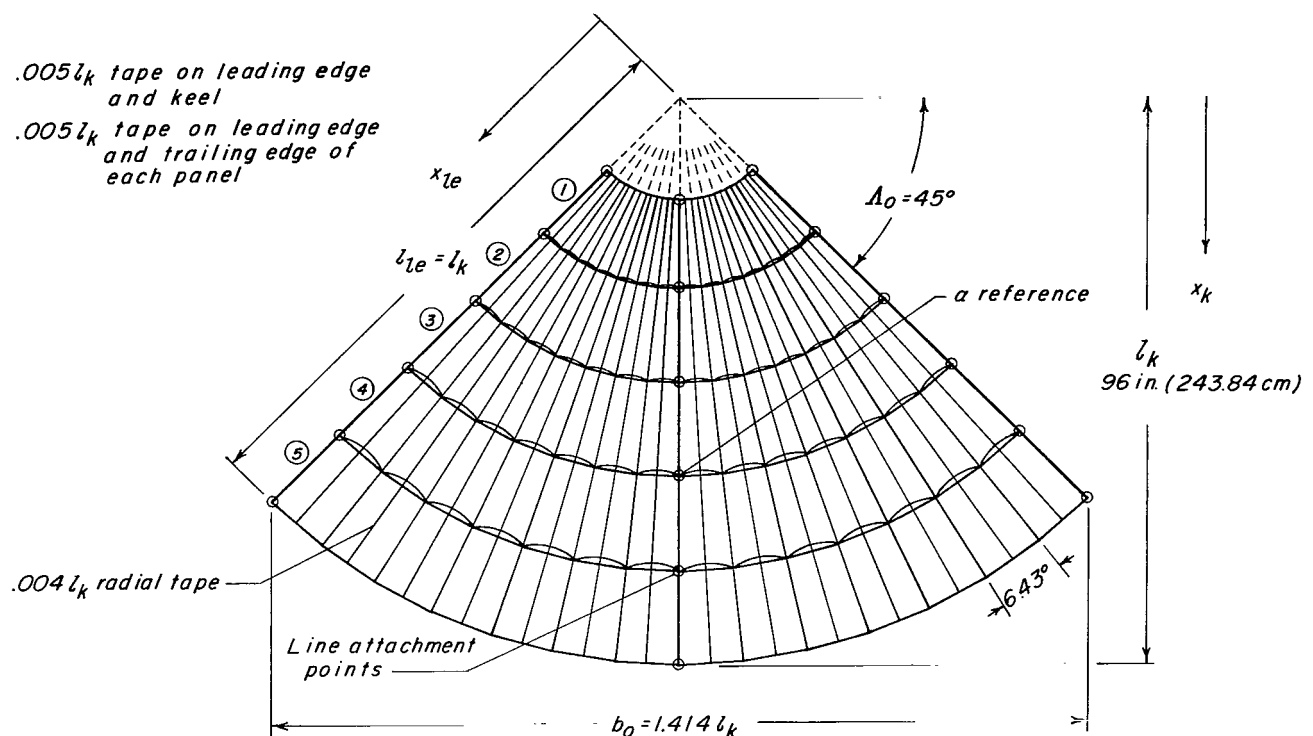


Figure 28.- Concluded.



Panel	Dimension, fraction of $l_k$		
	A	B	H
1	.0198	.0378	.157
2	.0374	.0572	.167
3	.0561	.0770	.167
4	.0748	.0972	.167
5	.0935	.1120	.165

Typical panel

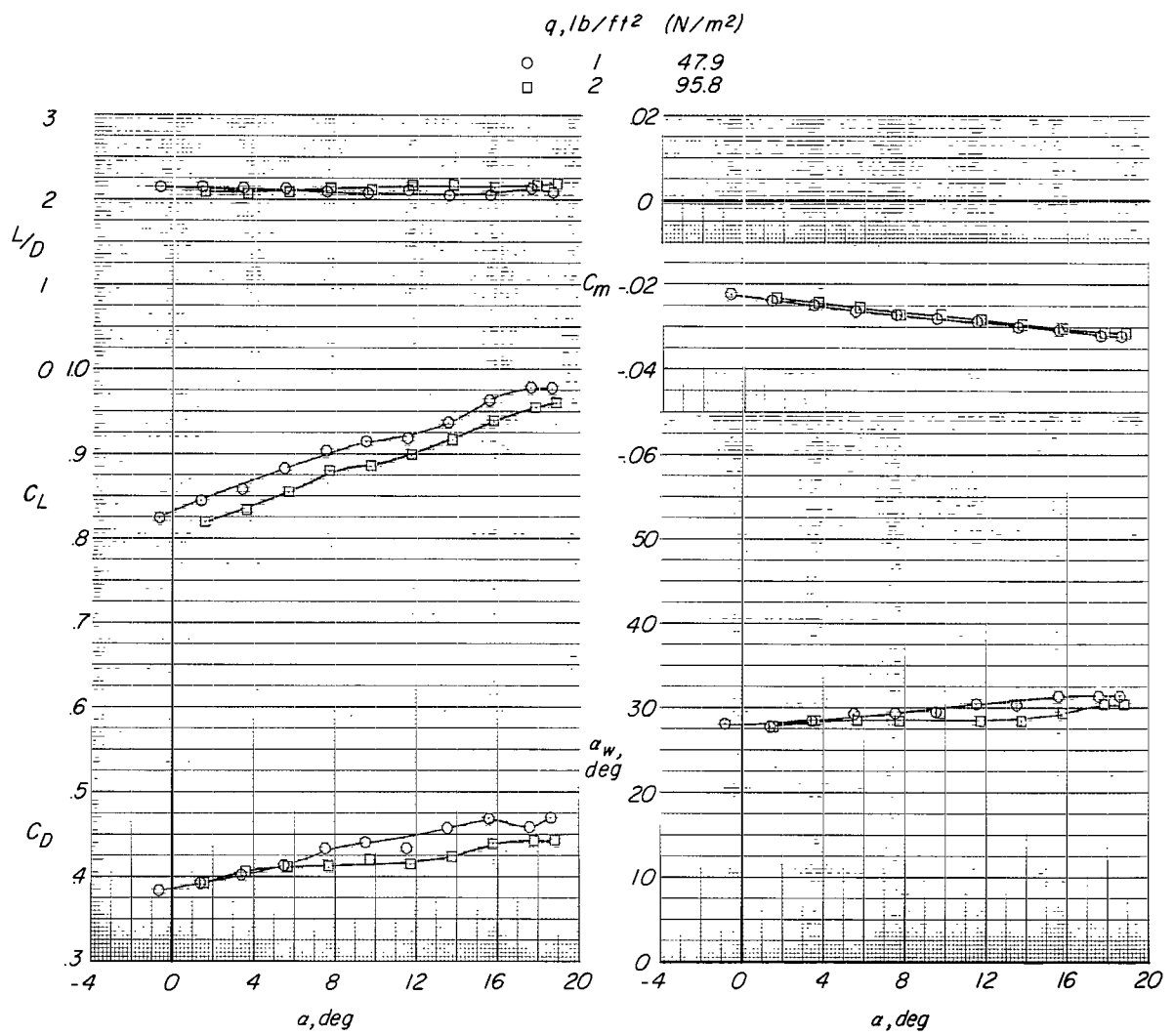
$x/l_k$

Keel and leading edge

.177  
 .334  
 .501  
 .668  
 .835  
 1.000

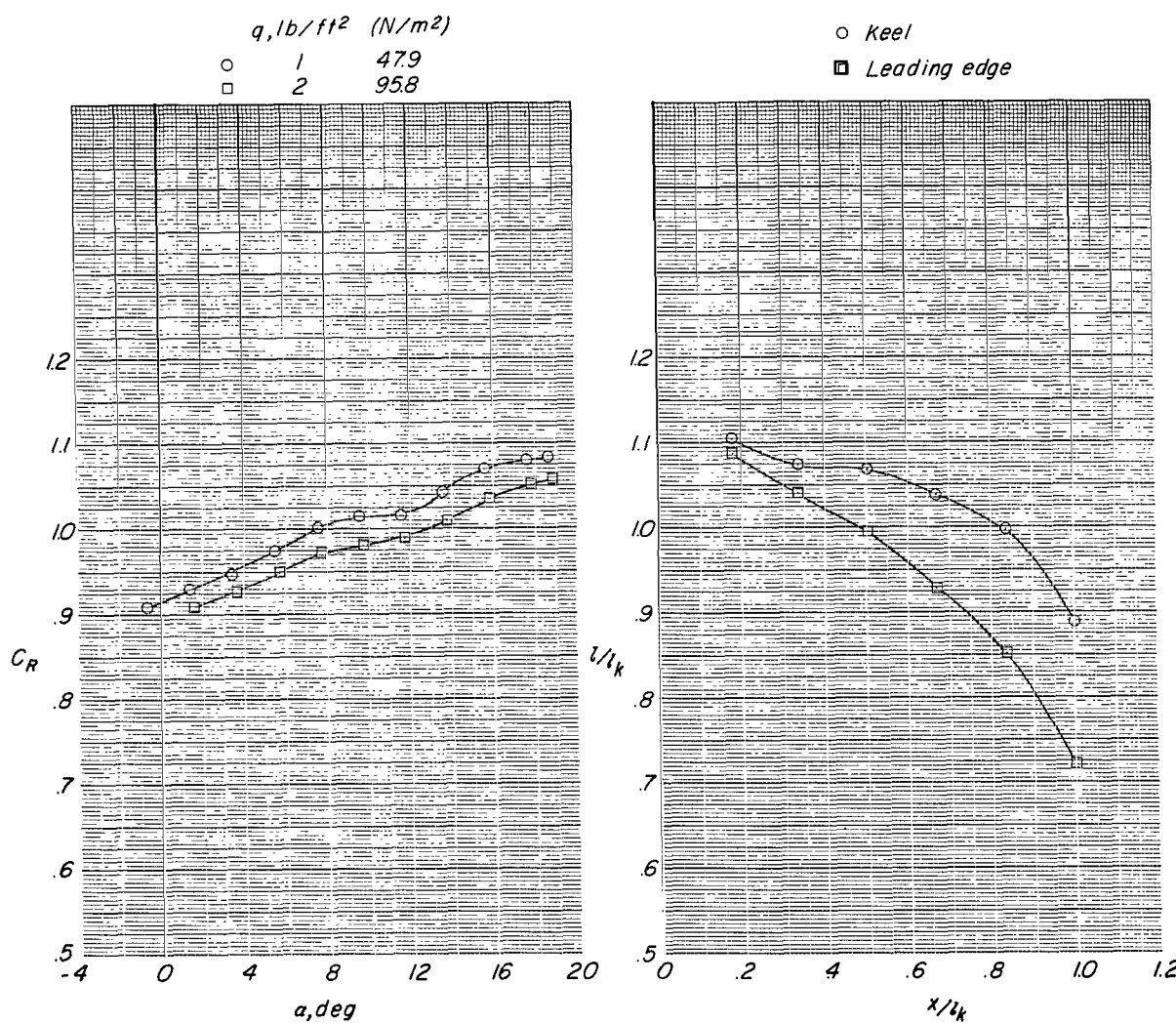
Line attachment location

Figure 29.- Planform of parawing with multiple slots and radial tapes.



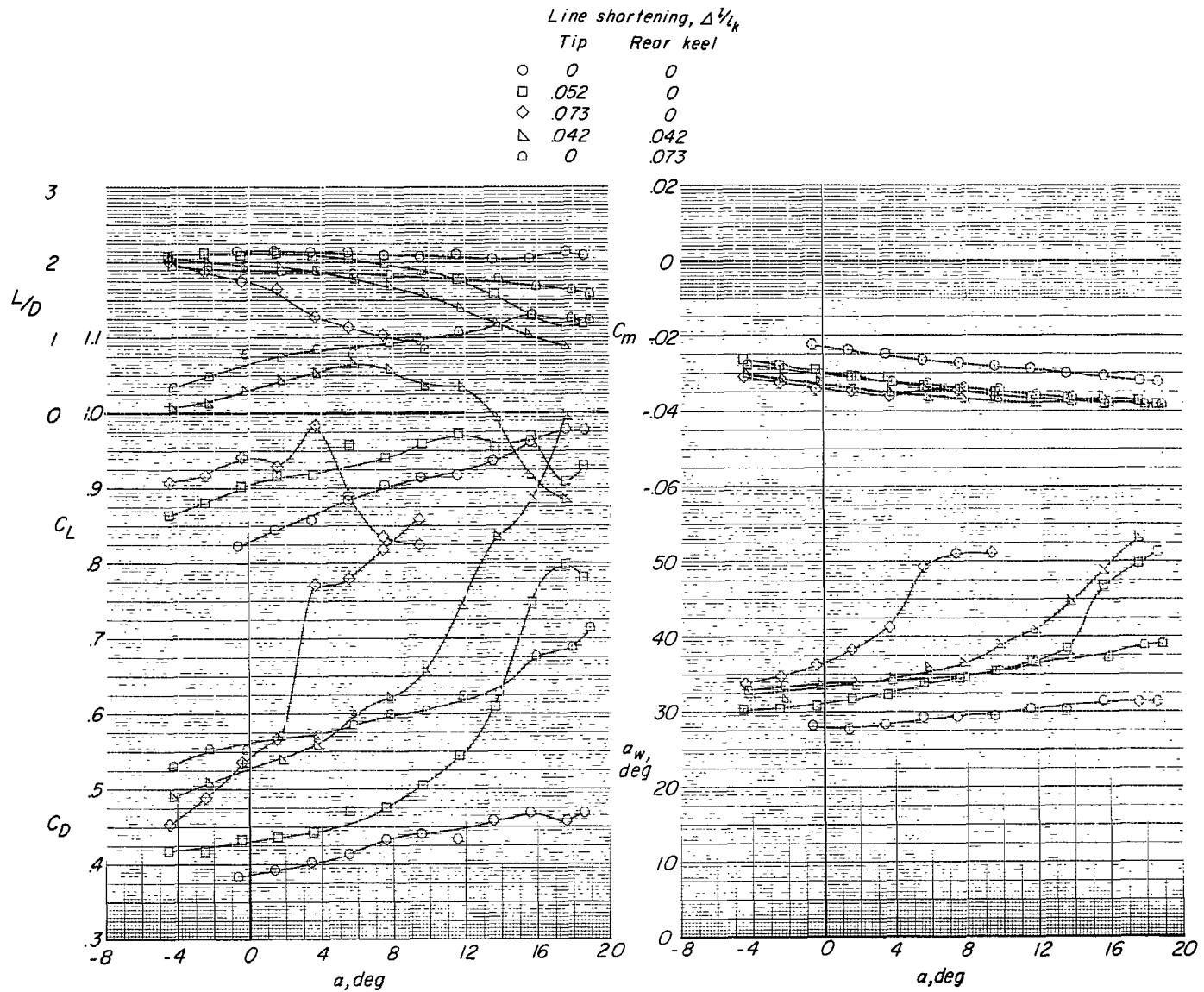
(a) Effect of dynamic pressure, no line shortening.

Figure 30.- Longitudinal aerodynamic characteristics of parawing with multiple slots and radial tapes.



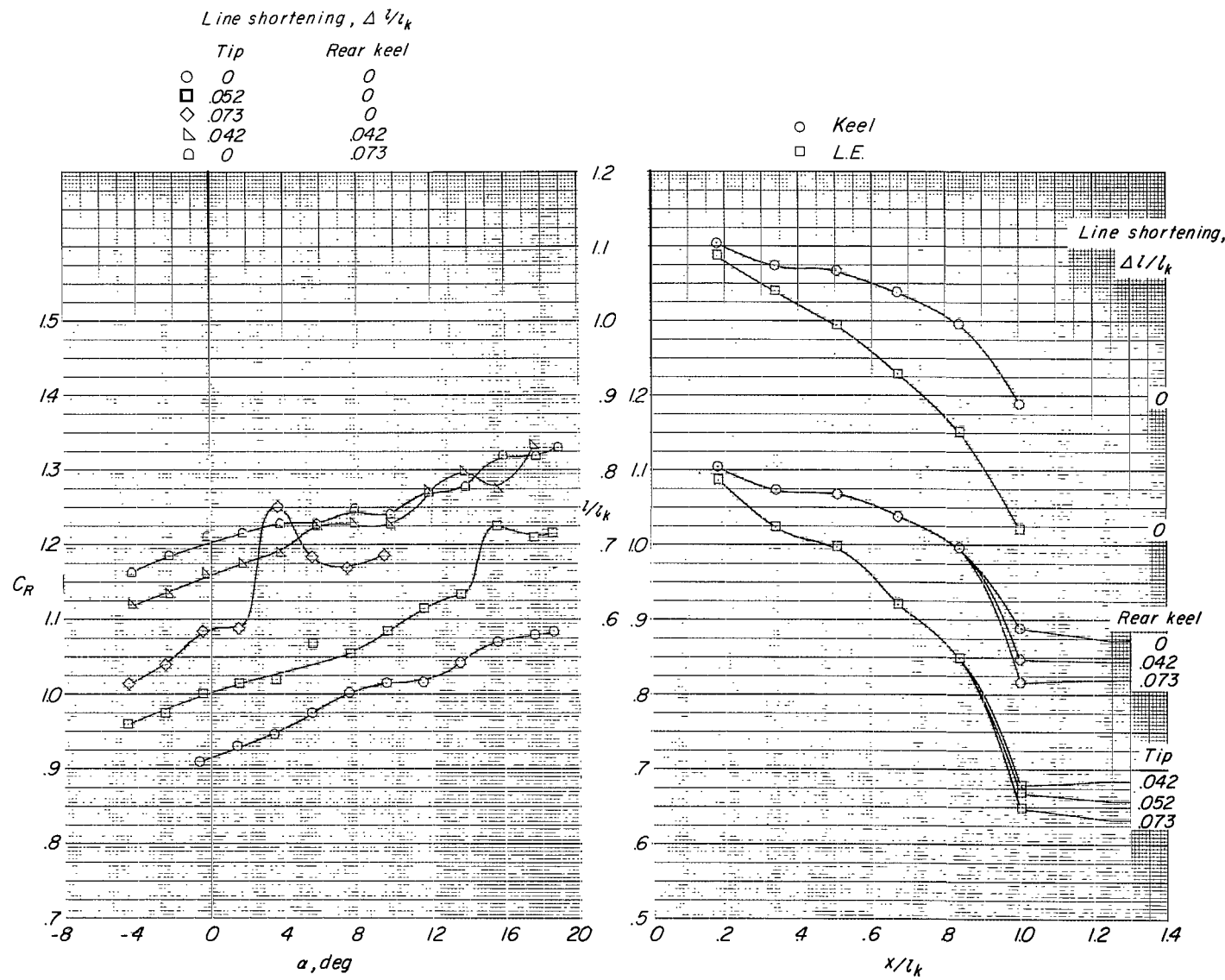
(a) Concluded.

Figure 30.- Continued.



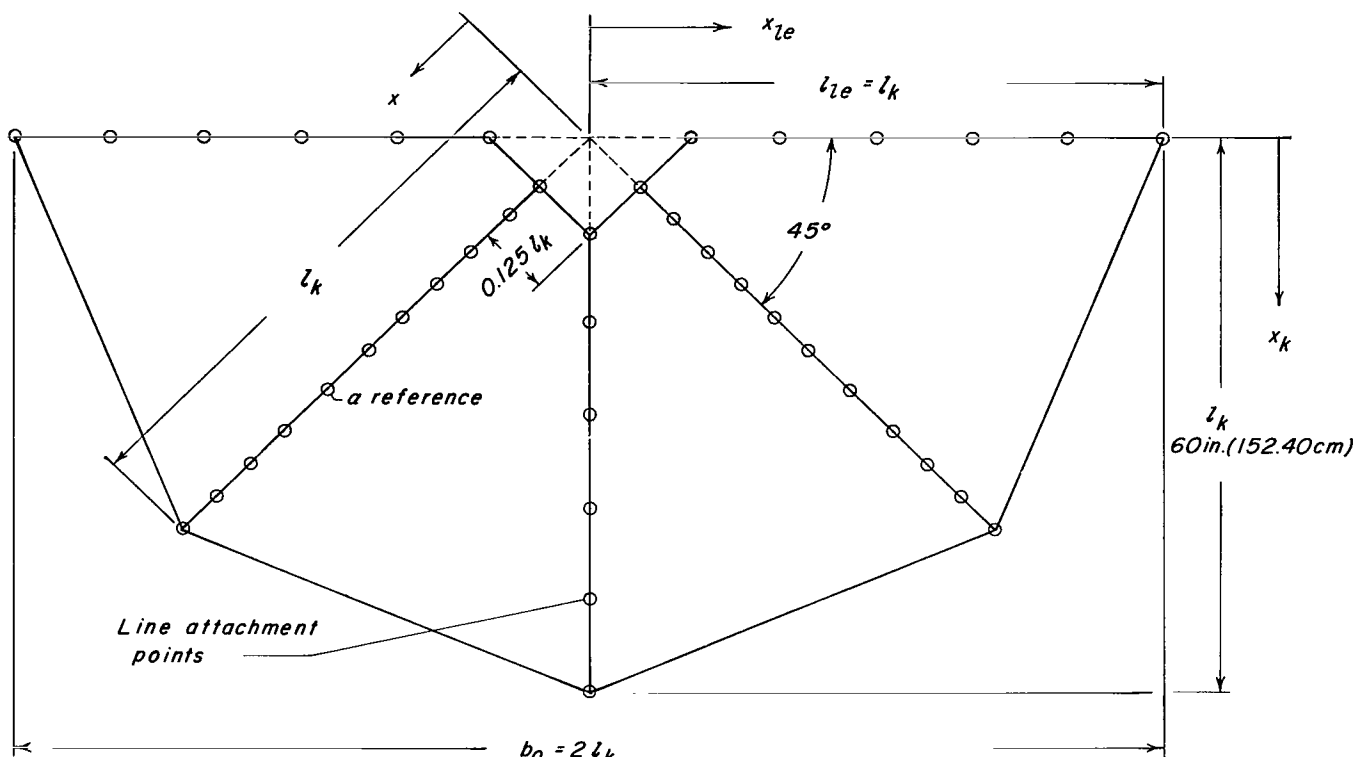
(b) Effect of control line shortening.  $q = 1.0 \text{ lb/ft}^2 (47.9 \text{ N/m}^2)$ .

Figure 30.- Continued.



(b) Concluded.

Figure 30.- Concluded.



$x/l_k$

Kee l and leading edge	Midspan
.177	.125
.333	.208
.500	.292
.667	.375
.833	.459
1.000	.542
	.645
	.750
	.833
	.917
	1.000

*Line attachment location*

Figure 31.- Planform of composite four-lobe parawing formed by joining two basic-planform parawings.

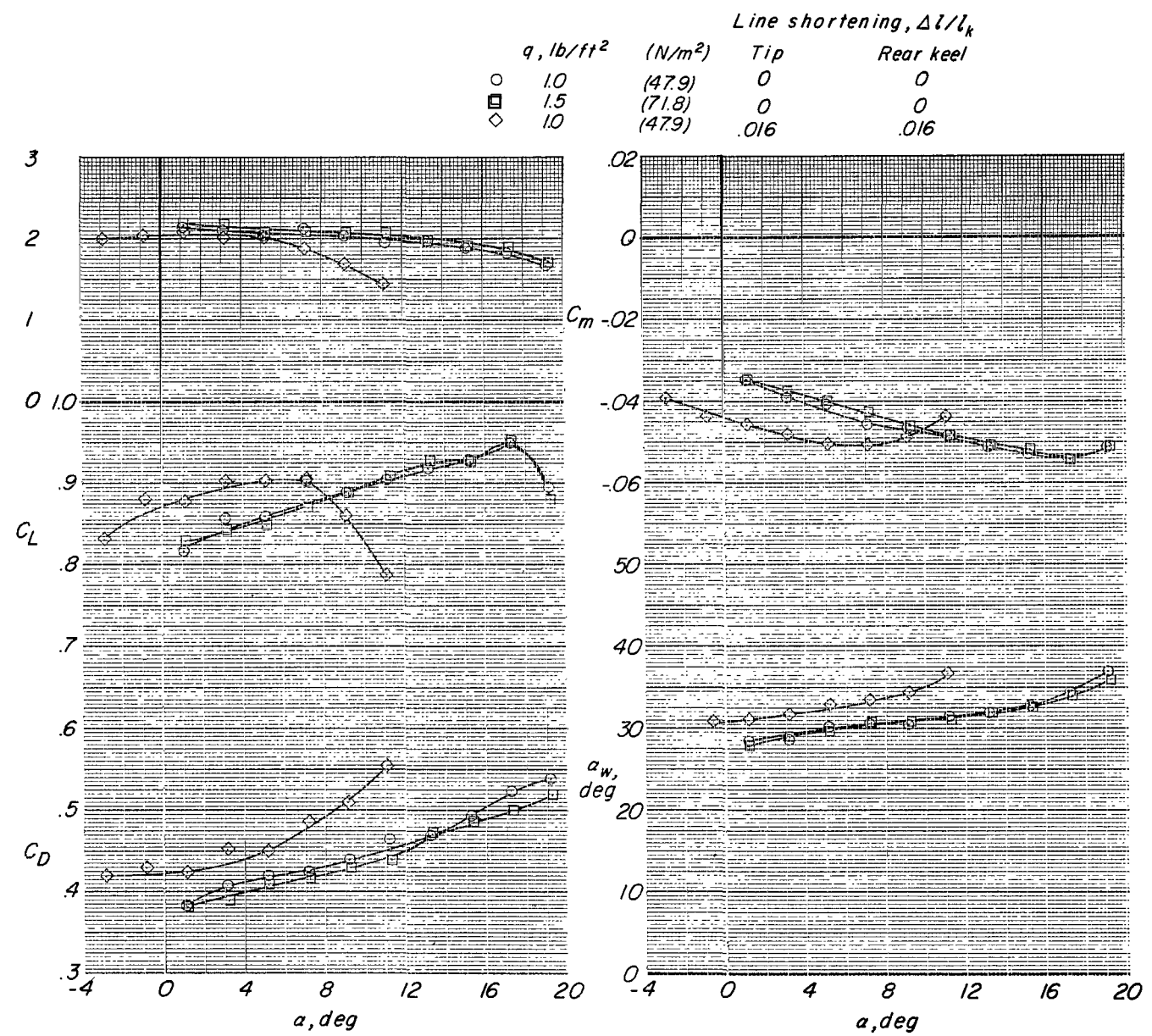


Figure 32.- Longitudinal aerodynamic characteristics of composite four-lobe parawing.

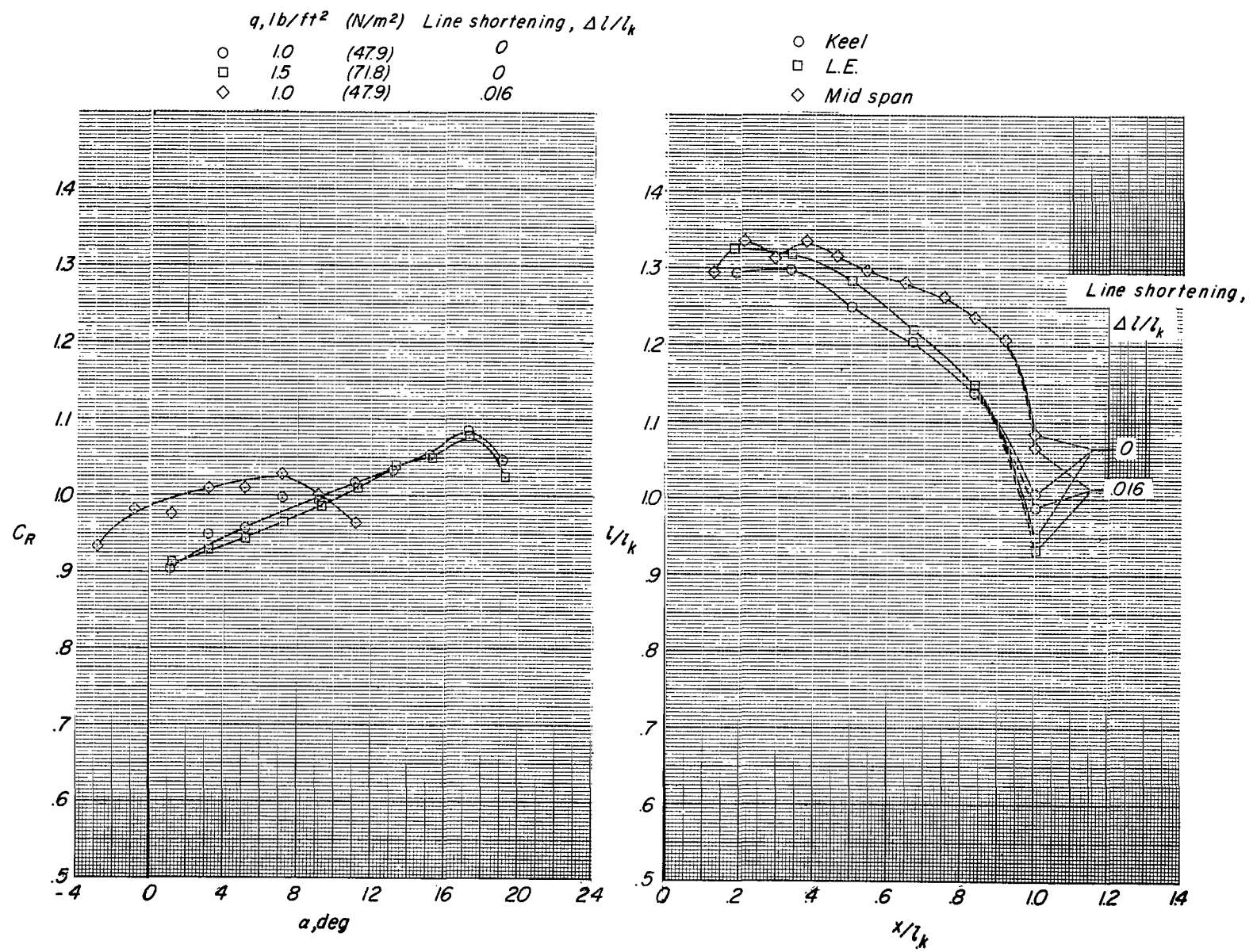
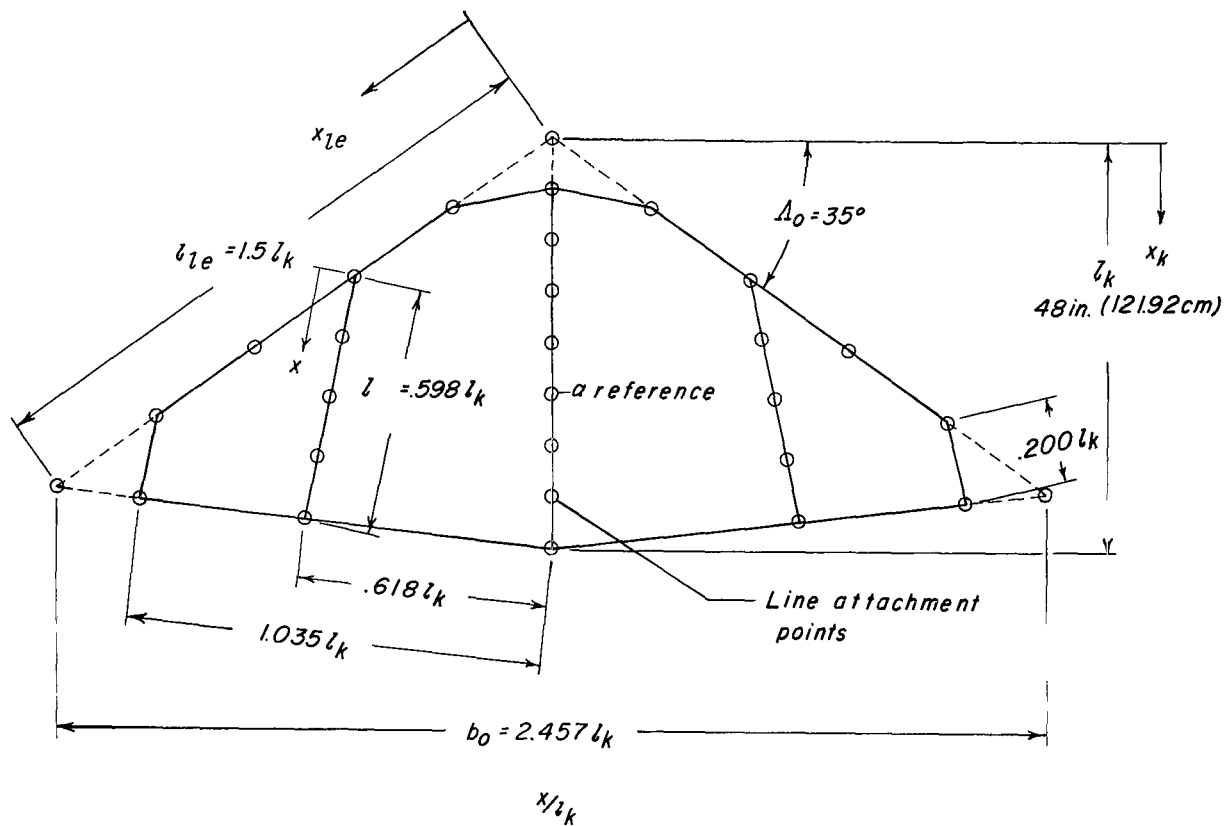


Figure 32.- Concluded.



Keel	Midspan	Leading edge
0	0	0
.125	.150	.300
.250	.299	.600
.375	.449	.900
.500	.598	1.200
.625		1.500
.750		
.875		
1.000		

Line attachment location

Figure 33.- Planform of four-lobe parawing with  $A_0 = 35^\circ$ .

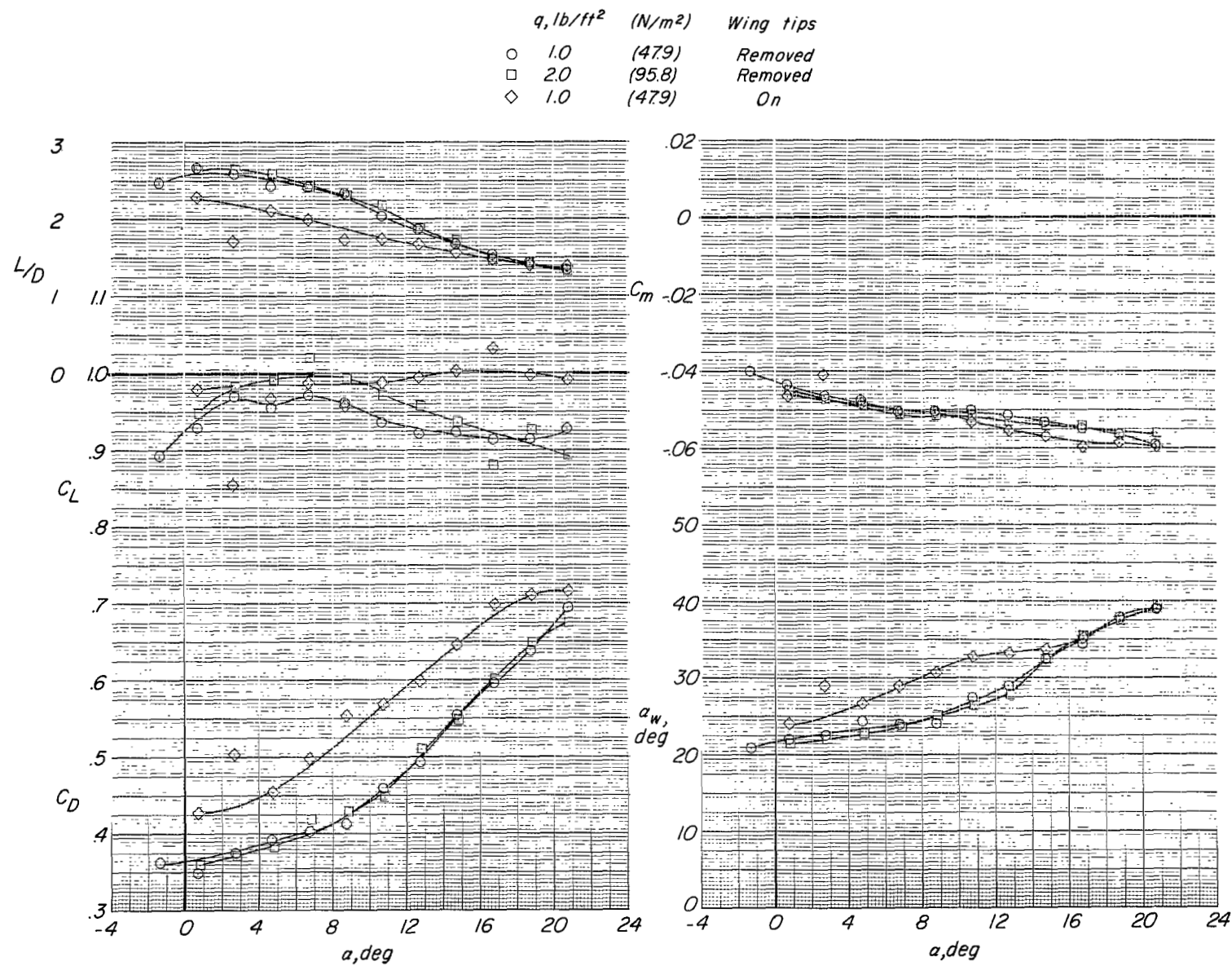


Figure 34.- Longitudinal aerodynamic characteristics of four-lobe parawing with  $\Lambda_0 = 35^\circ$ .

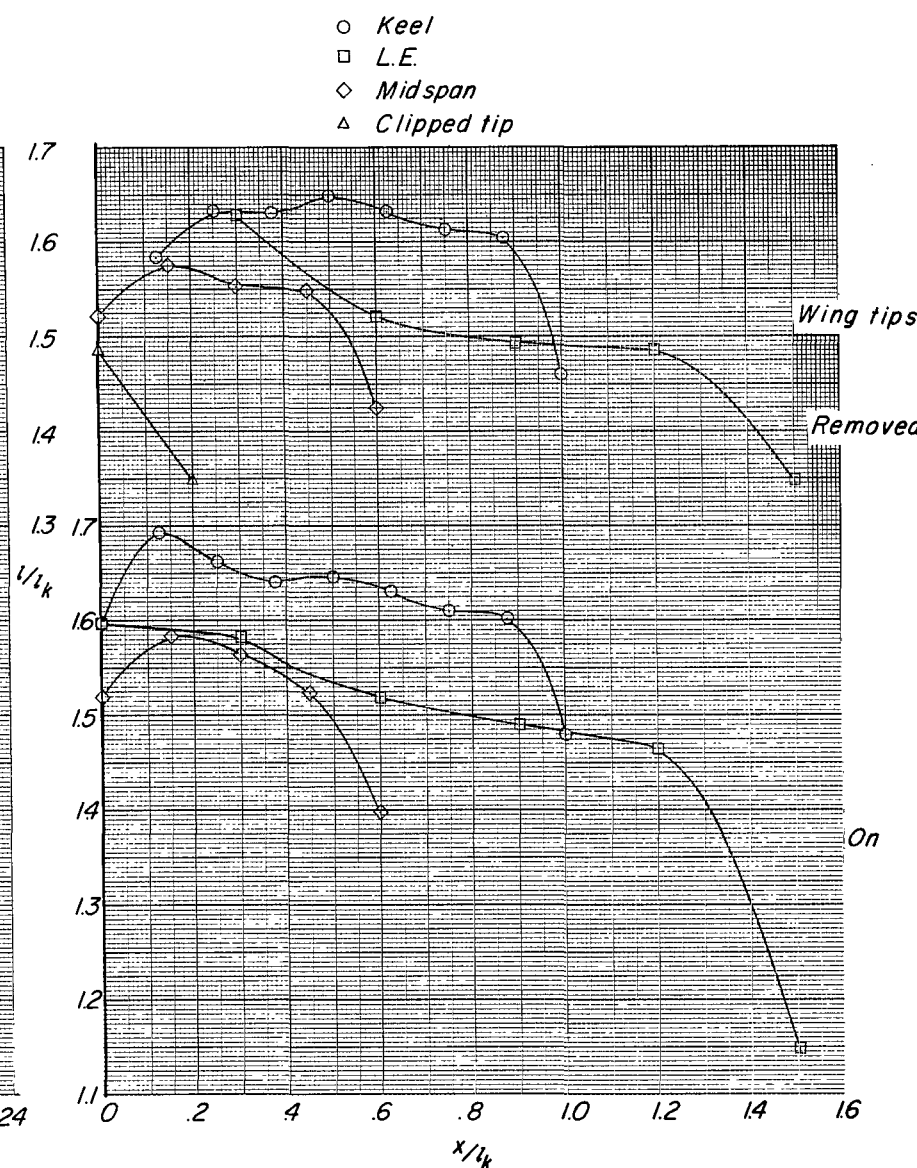
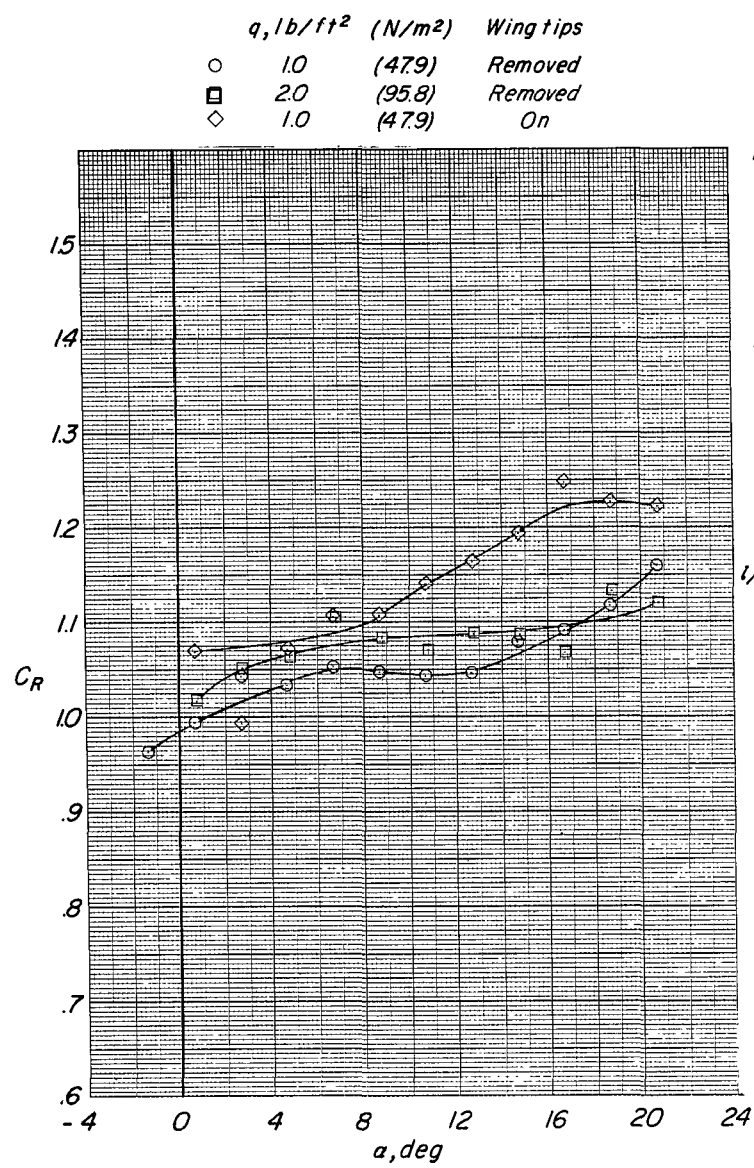
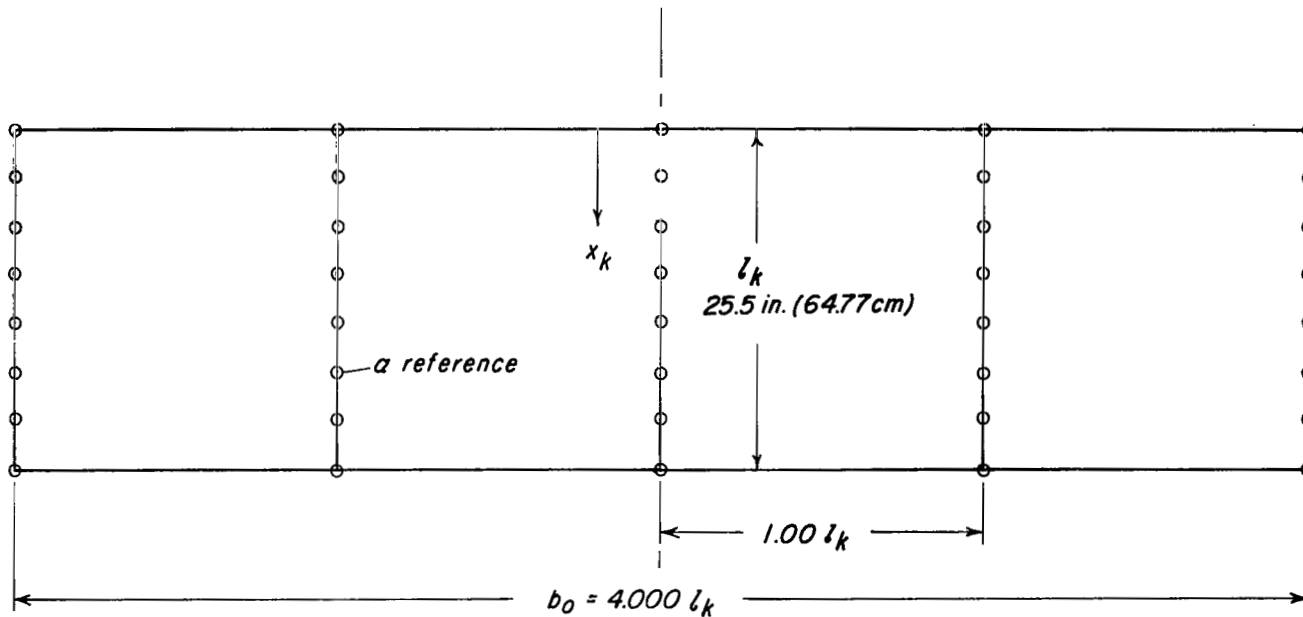


Figure 34.- Concluded.



$$x/l_k$$

*Keel, Midspan, and Tip*

.143  
.286  
.428  
.571  
.714  
.857  
1.000

*Line attachment location*

Figure 35.- Planform of rectangular, four-lobe parawing with aspect ratio of 4 and  $\Lambda_0 = 0^0$ .

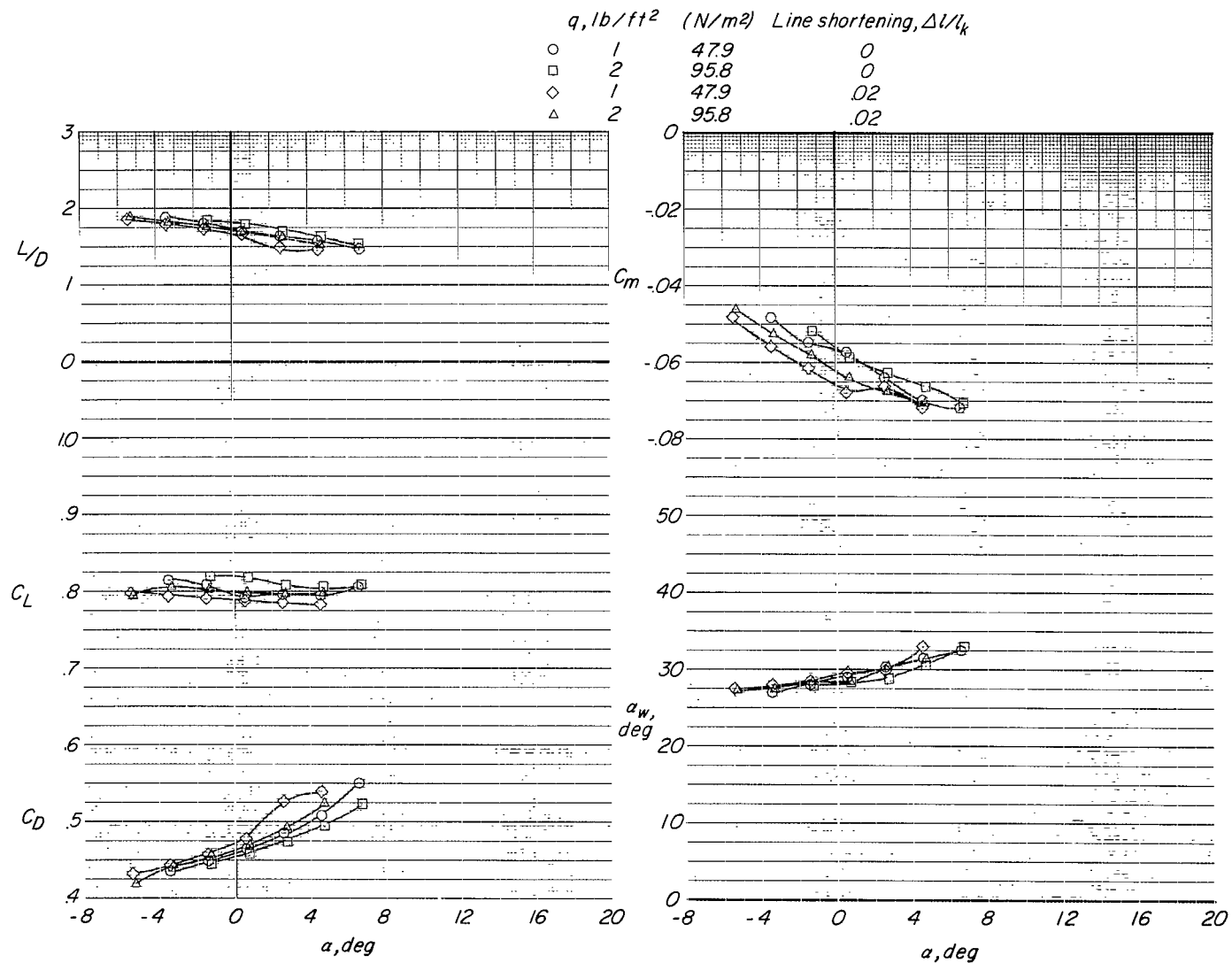


Figure 36.- Longitudinal aerodynamic characteristics of the rectangular, four-lobe parawing.

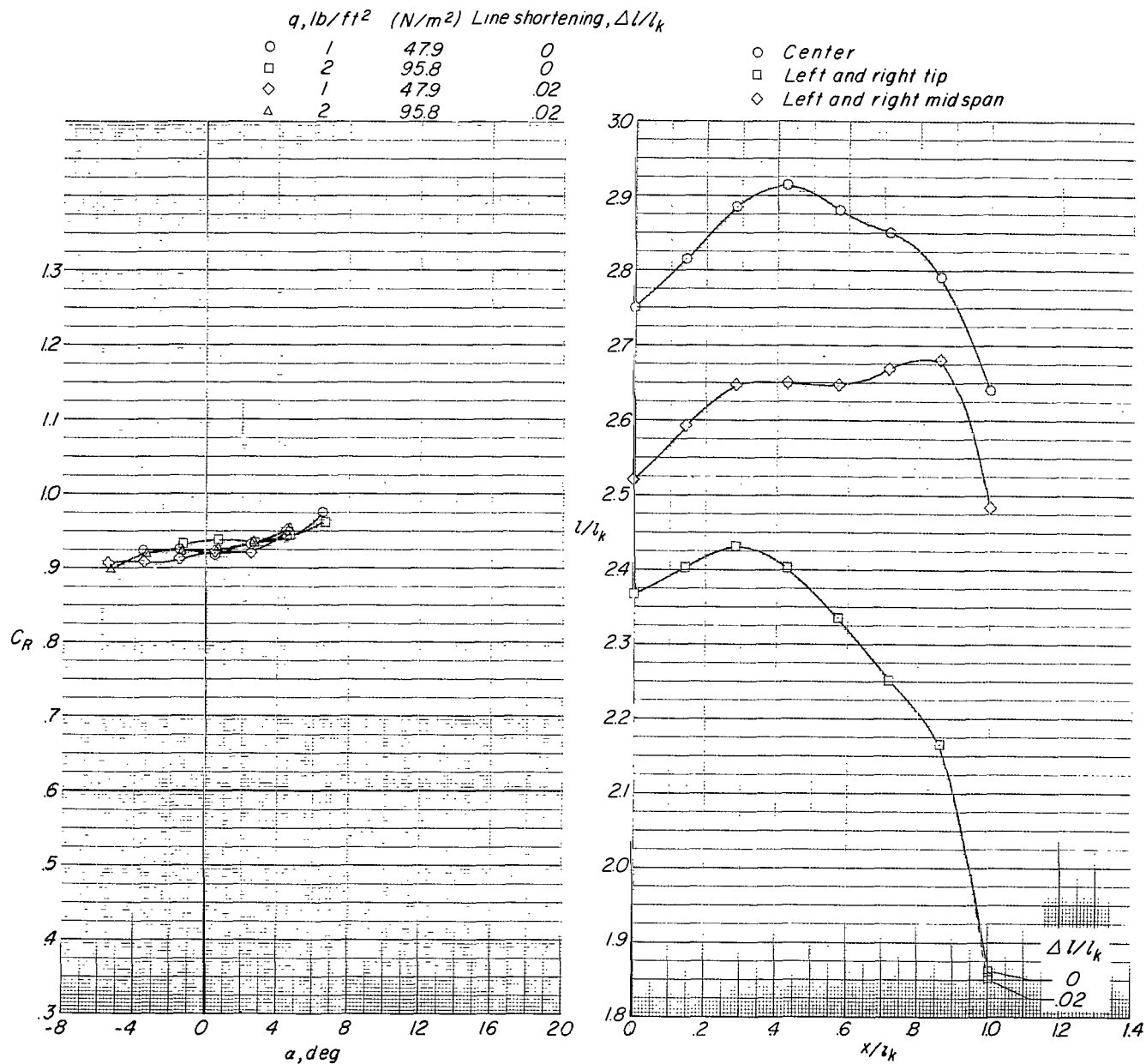


Figure 36.- Concluded.

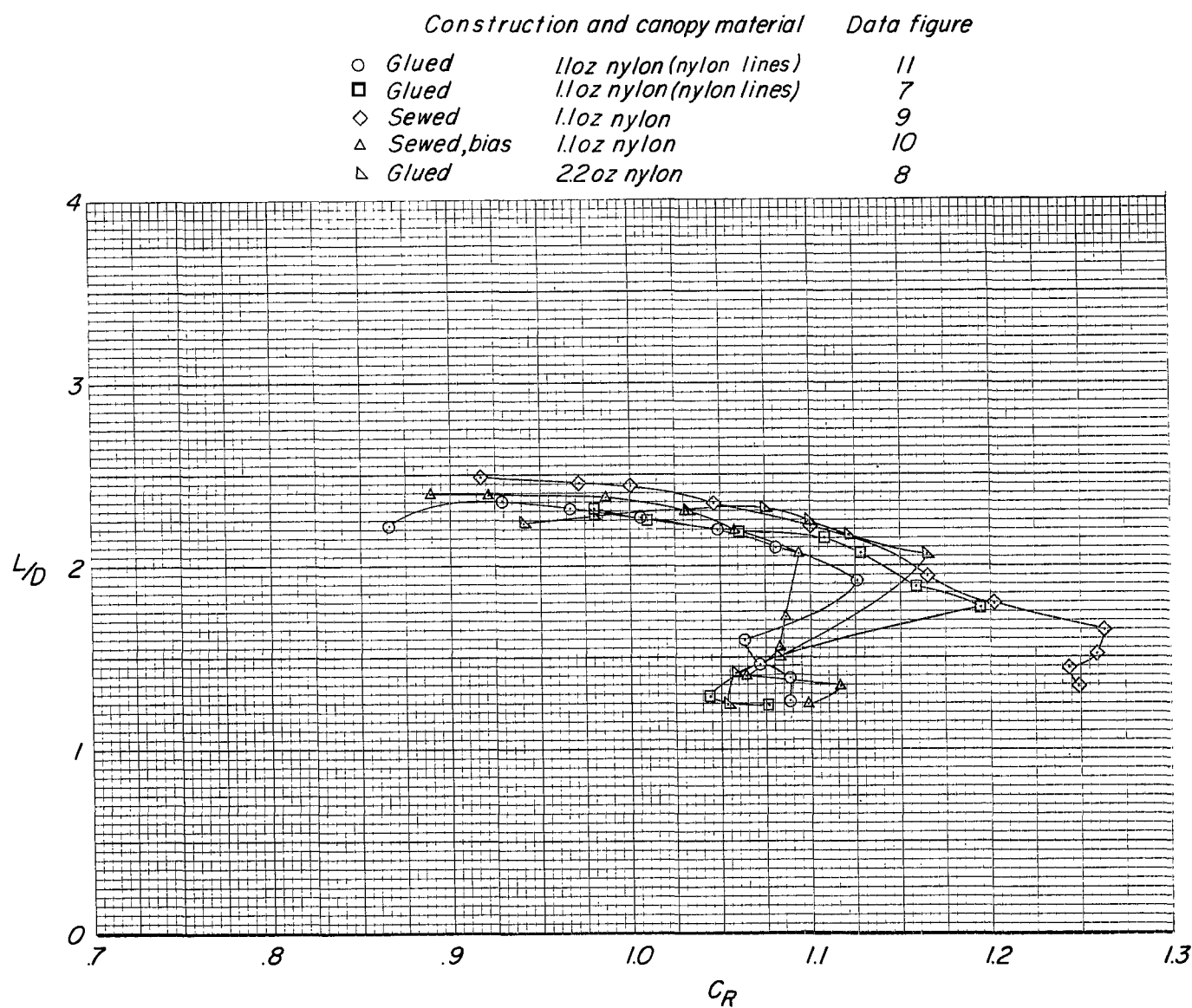


Figure 37.- Effect of construction method and canopy material on variation of lift-drag ratio with resultant-force coefficient for the basic wing.  
 $q = 2.0 \text{ lb/ft}^2 (95.8 \text{ N/m}^2)$ . ( $1.1 \text{ oz/yd}^2 = 37.3 \text{ g/m}^2$ ;  $2.2 \text{ oz/yd}^2 = 74.6 \text{ g/m}^2$ .)

*Configuration*

*Data figure*

○ <i>Basic</i>	9
□ <i>Curved leading edge</i>	21
◇ <i>8 keel and 7 leading-edge lines</i>	17
△ <i>Cambered keel</i>	19

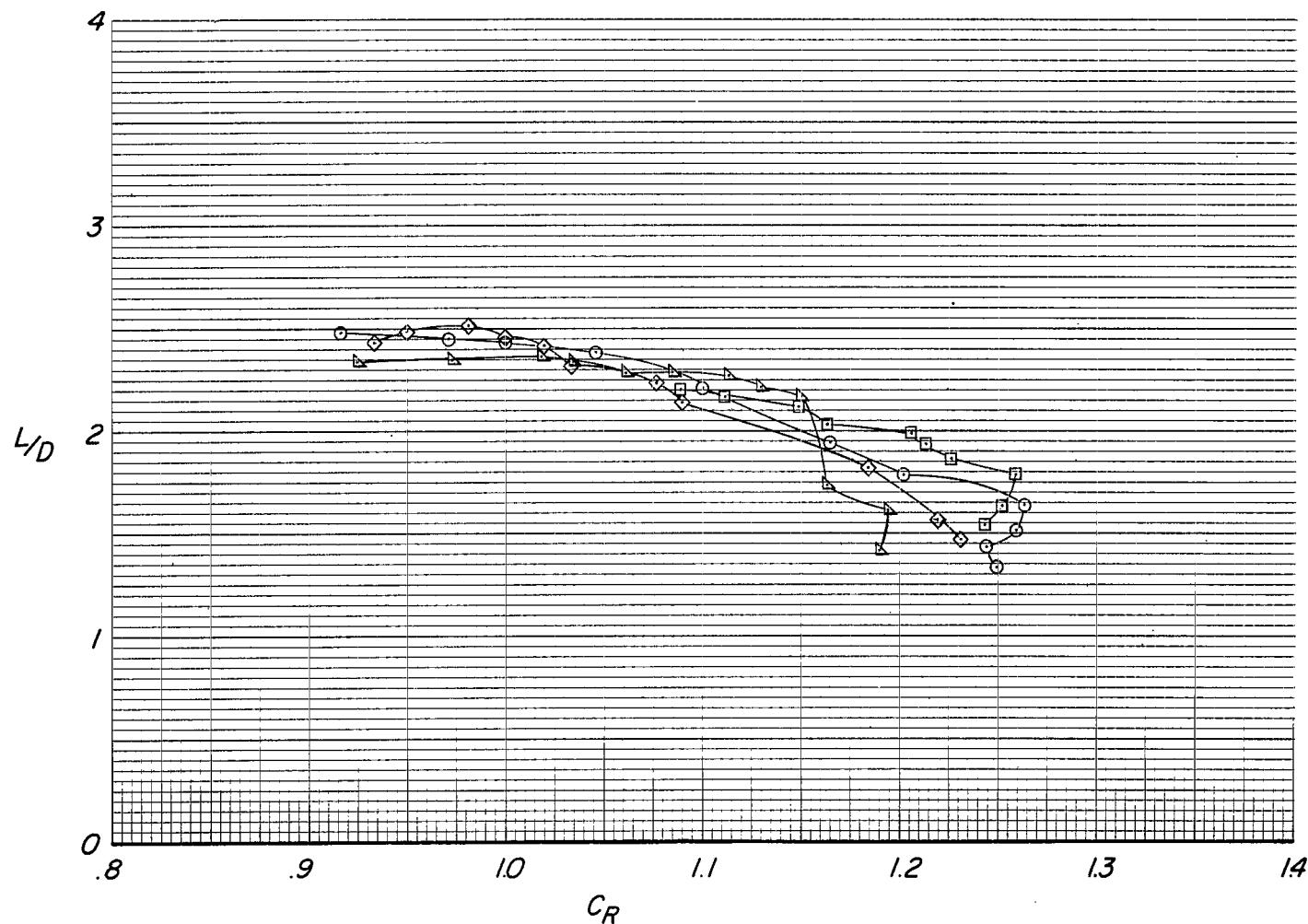


Figure 38.- Effect of modifications to basic configuration on variation of lift-drag ratio with resultant-force coefficient.  $q = 2.0 \text{ lb/ft}^2$  ( $95.8 \text{ N/m}^2$ ).

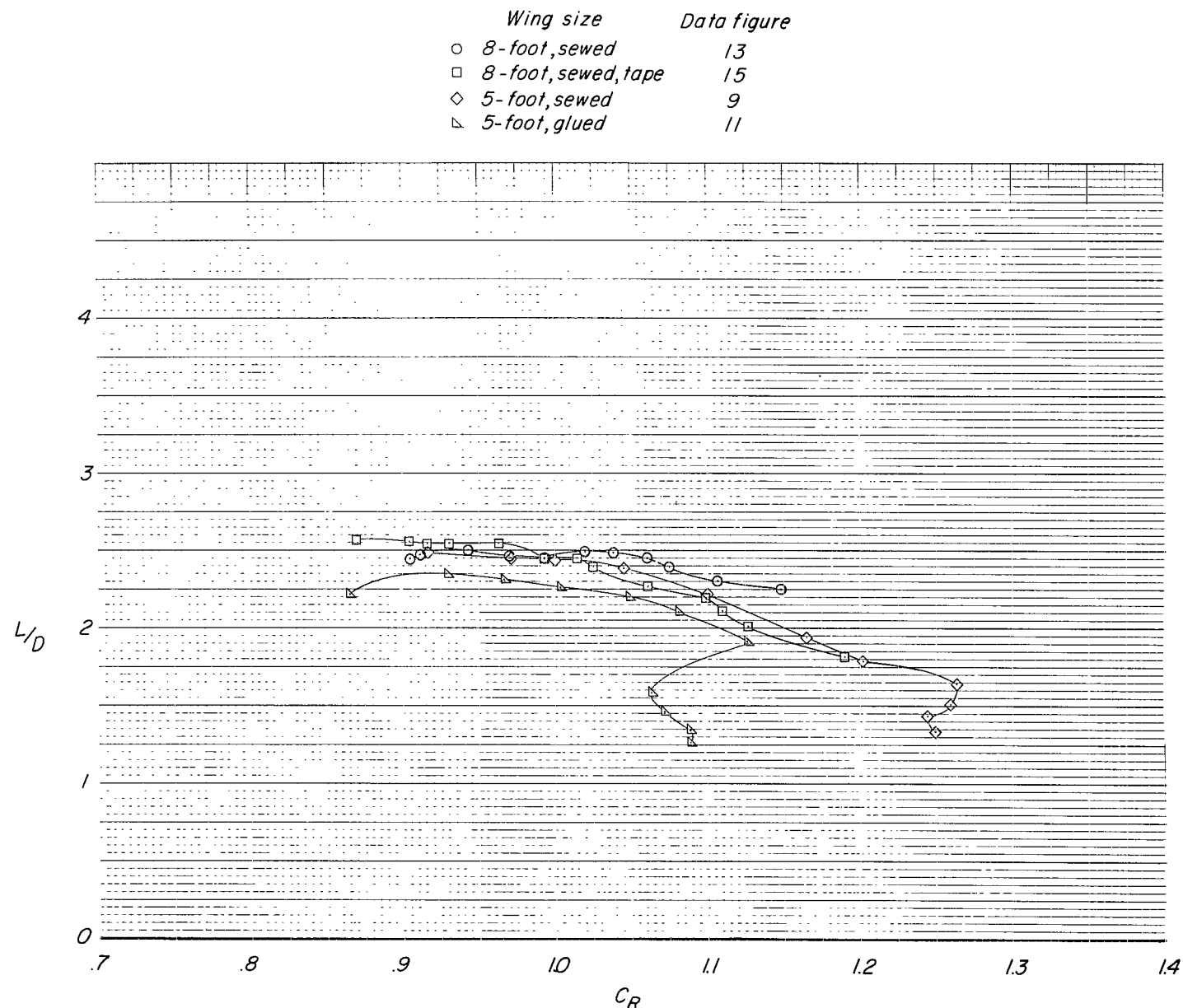


Figure 39.- Summary of aerodynamic characteristics of the 5-ft (1.524-m) and 8-ft (2.438-m) basic parawing configurations.

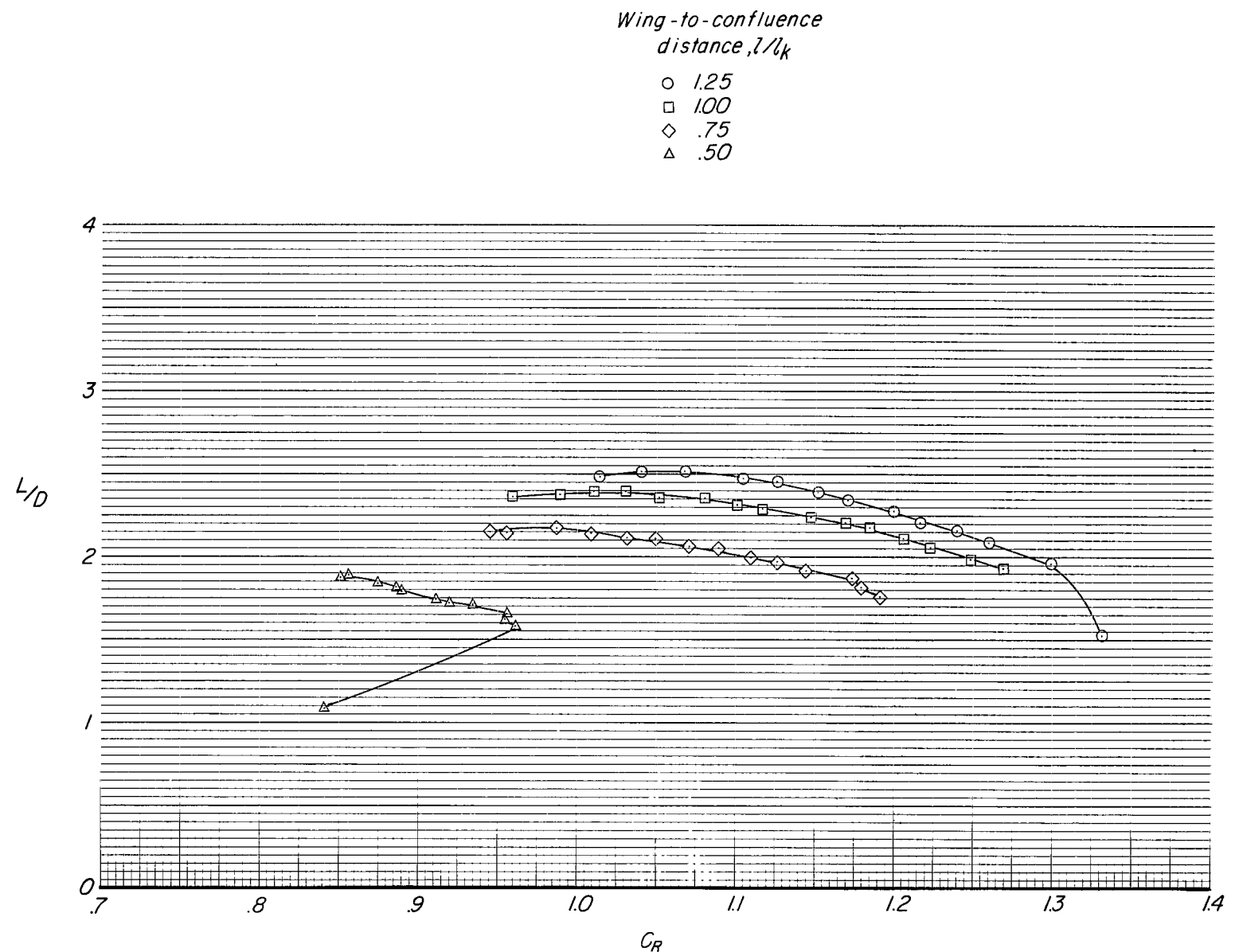


Figure 40.- Effect of decreasing wing-to-confluence separation distance for the basic parawing configuration. (Basic data presented in fig. 23.)

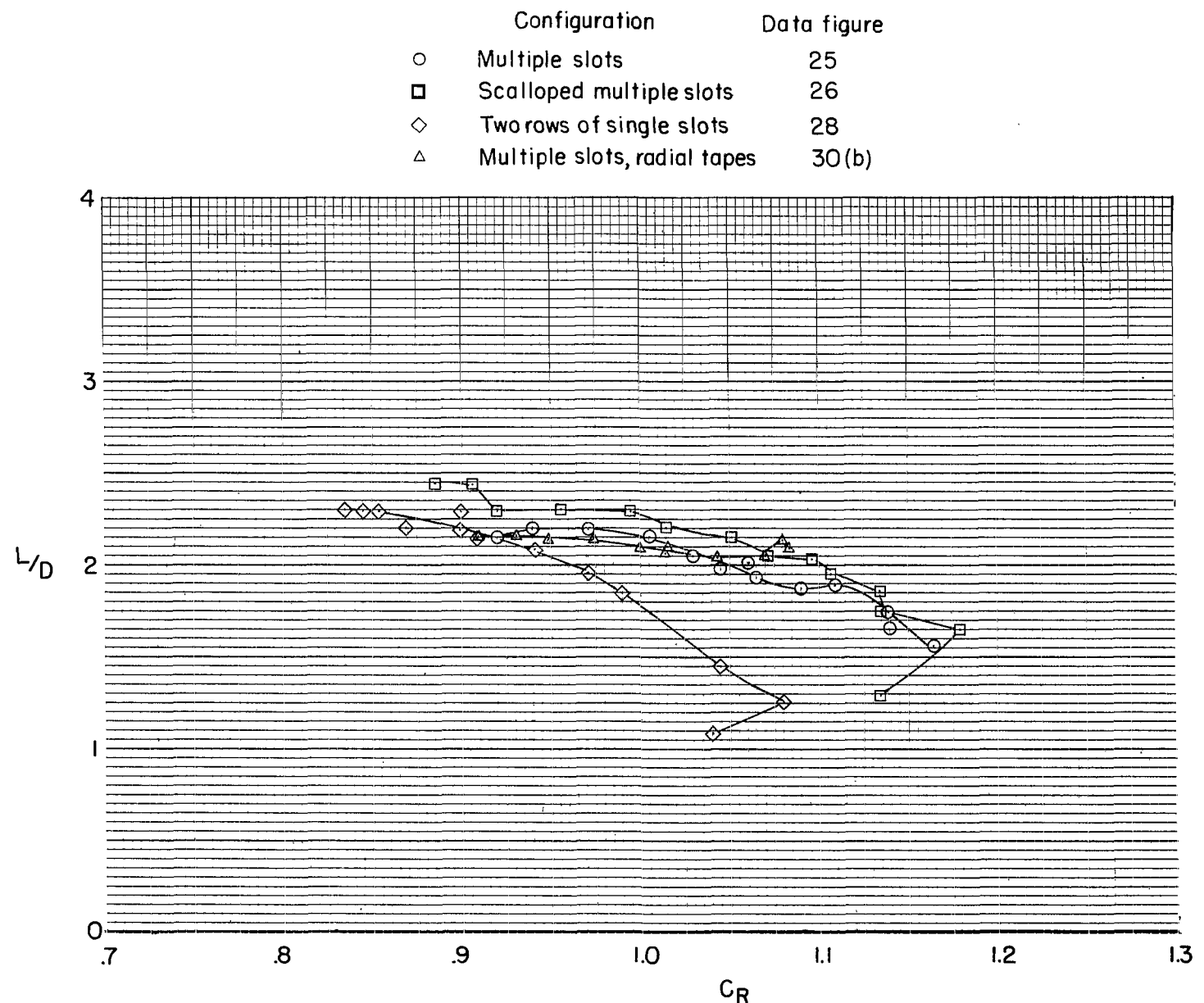
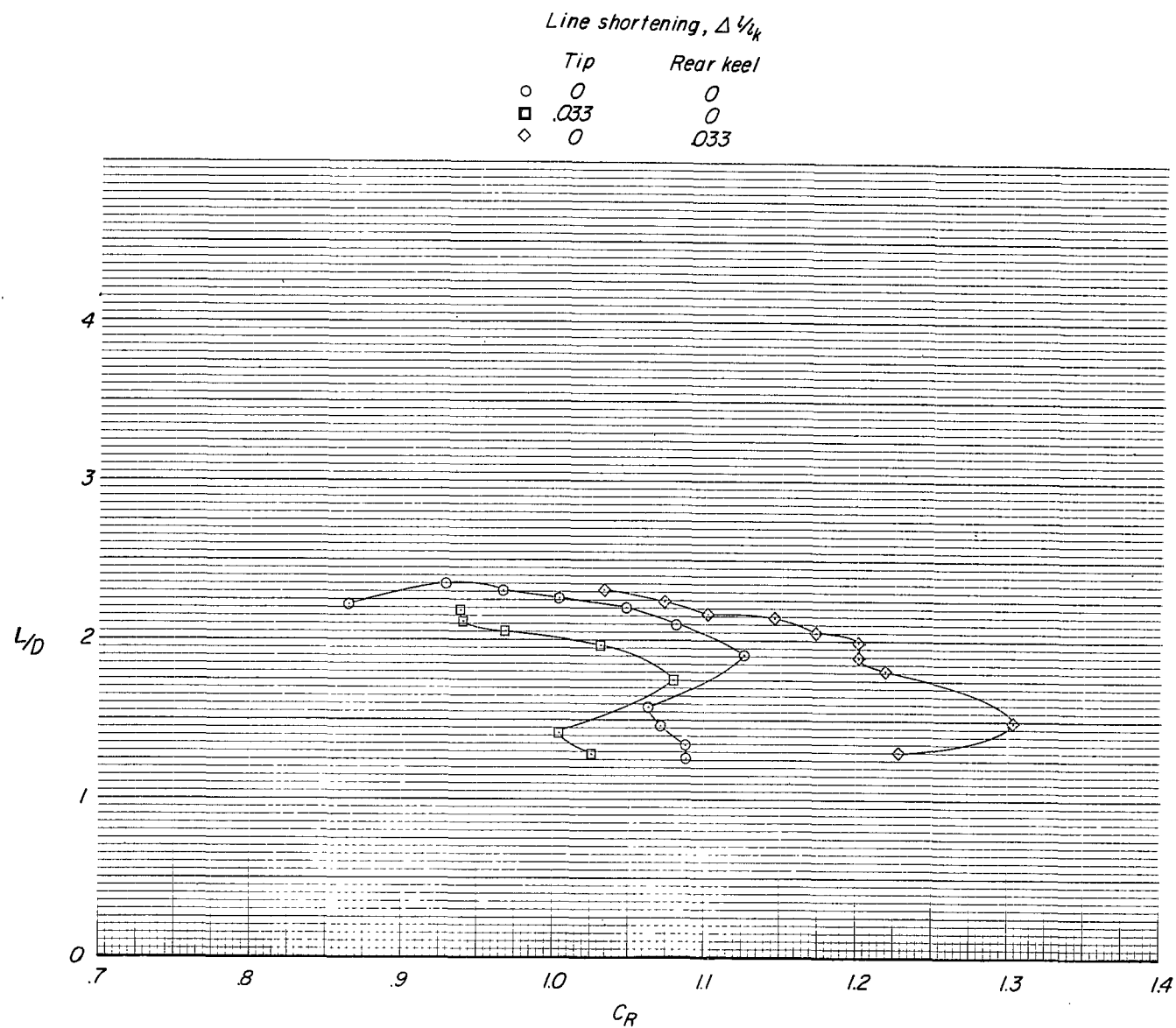
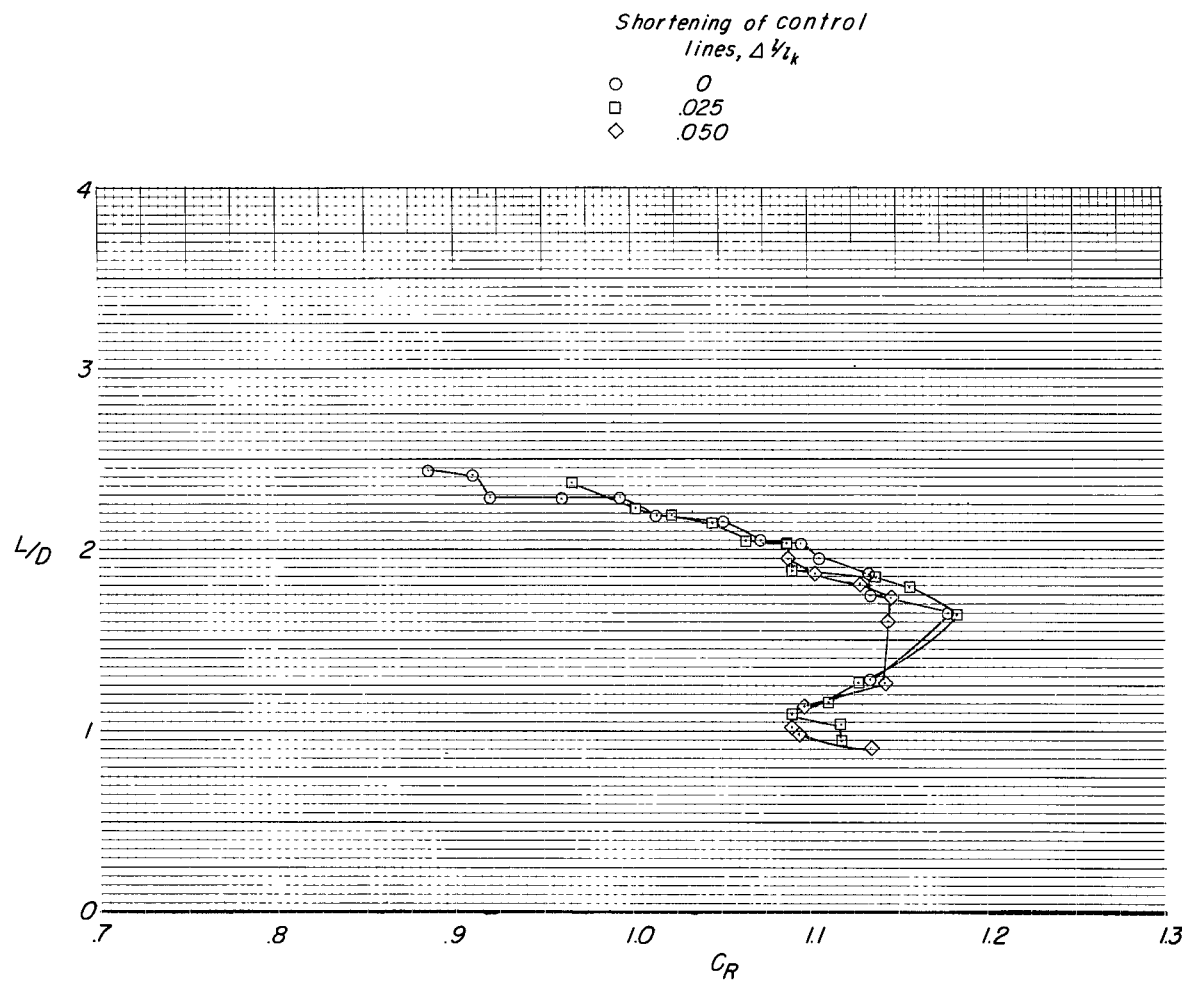


Figure 41.- Summary of aerodynamic characteristics of slotted parawings.



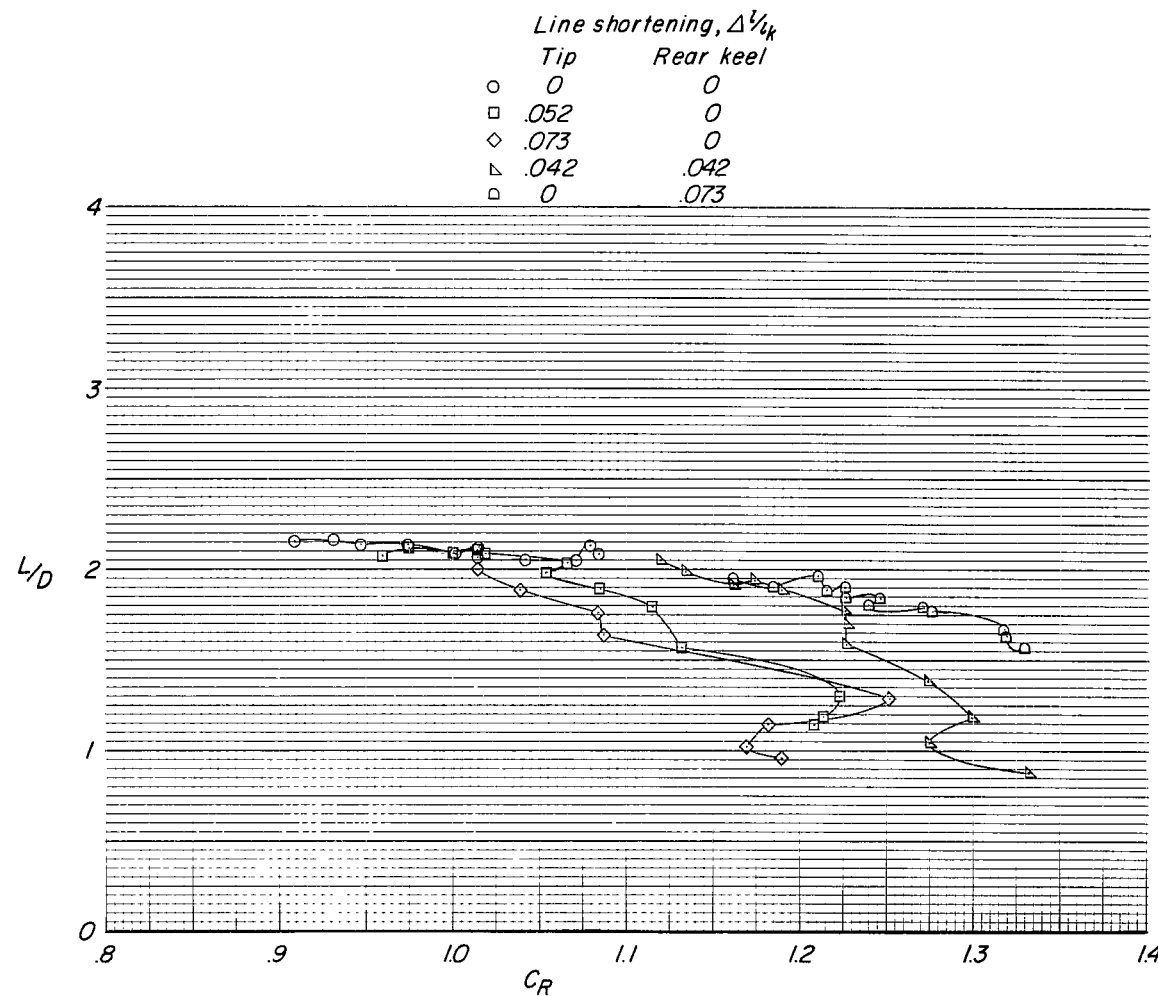
(a) Basic wing. (Basic data presented in fig. 11.)

Figure 42.- Effect of shortening rear lines on variation of lift-drag ratio with resultant-force coefficient.



(b) Wing with multiple slots and scalloped trailing edges on rear slots. (Basic data presented in fig. 26.)

Figure 42.- Continued.



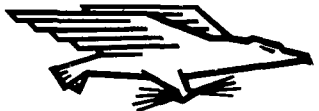
(c) Wing with multiple slots and radial tapes. (Basic data presented in fig. 30(b).)

Figure 42.- Concluded.

NATIONAL AERONAUTICS AND SPACE ADMINISTRATION  
WASHINGTON, D. C. 20546

OFFICIAL BUSINESS

FIRST CLASS MAIL



POSTAGE AND FEES PAID  
NATIONAL AERONAUTICS AND  
SPACE ADMINISTRATION

02U 001 26 51 3DS      70272 00903  
AIR FORCE WEAPONS LABORATORY /WLOL/  
KIRTLAND AFB, NEW MEXICO 87117

ATT E. LOU BOWMAN, CHIEF, TECH. LIBRARY

POSTMASTER: If Undeliverable (Section 158  
Postal Manual) Do Not Return

"The aeronautical and space activities of the United States shall be conducted so as to contribute . . . to the expansion of human knowledge of phenomena in the atmosphere and space. The Administration shall provide for the widest practicable and appropriate dissemination of information concerning its activities and the results thereof."

— NATIONAL AERONAUTICS AND SPACE ACT OF 1958

## NASA SCIENTIFIC AND TECHNICAL PUBLICATIONS

**TECHNICAL REPORTS:** Scientific and technical information considered important, complete, and a lasting contribution to existing knowledge.

**TECHNICAL NOTES:** Information less broad in scope but nevertheless of importance as a contribution to existing knowledge.

**TECHNICAL MEMORANDUMS:** Information receiving limited distribution because of preliminary data, security classification, or other reasons.

**CONTRACTOR REPORTS:** Scientific and technical information generated under a NASA contract or grant and considered an important contribution to existing knowledge.

**TECHNICAL TRANSLATIONS:** Information published in a foreign language considered to merit NASA distribution in English.

**SPECIAL PUBLICATIONS:** Information derived from or of value to NASA activities. Publications include conference proceedings, monographs, data compilations, handbooks, sourcebooks, and special bibliographies.

**TECHNOLOGY UTILIZATION PUBLICATIONS:** Information on technology used by NASA that may be of particular interest in commercial and other non-aerospace applications. Publications include Tech Briefs, Technology Utilization Reports and Notes, and Technology Surveys.

*Details on the availability of these publications may be obtained from:*

SCIENTIFIC AND TECHNICAL INFORMATION DIVISION  
NATIONAL AERONAUTICS AND SPACE ADMINISTRATION  
Washington, D.C. 20546